Electrochemical Analysis of CuCl/HCl Electrolyser

By

Reza Soltani

A Thesis Submitted in Partial Fulfillment

Of the Requirements for the Degree of

Master of Applied Science in Mechanical Engineering

Faculty of Engineering and Applied Science

University of Ontario Institute of Technology

October 2015

Abstract

This thesis presents an electrochemical study on a CuCl/HCl electrolyser which is the hydrogen generation step of the CuCl thermochemical hydrogen production cycle. The anode electrolyte is solution of 2 $\mathrm{mol.l^{-1}}$ $\mathrm{CuCl(aq)}$ in 10 $\mathrm{mol.l^{-1}}$ $\mathrm{HCl(aq)}$ and cathode electrolyte is considered as 11 $\mathrm{mol.l^{-1}}$ $\mathrm{HCl(aq)}$. Equilibrium and kinetic analyses are performed for the anode and cathode half-reactions as well as electrolysis full-cell reaction. Gibbs energy minimization method is used to determine equilibrium concentrations of stable anolyte ions. Determination of thermodynamic properties of ions in the solution is carried out via application of the Helgeson-Kirkham-Flowers equation of state and the Debye-Huckel theory. Activation and Ohmic overpotentials of electrolysis are used to determine the required voltage to trigger hydrogen evolution at cathode.

At 5% conversion of $\mathrm{Cu(I) \rightarrow Cu(II)}$ species in anolyte, decomposition potential of anode half-reaction is calculated to be -0.51V at room temperature. The cathode half-reaction is found to be spontaneous with an equilibrium potential of 0.11V at 25℃. Full-cell decomposition potentials at 25℃ and 80℃ are -0.40V and -0.44V, respectively, for the full conversion at anode. The cell potential is found to be -0.54V at 25℃ and it rises to -0.59V at 80℃. A higher working temperature results in more potential requirement for the cell while, it increases the overall electrochemical efficiency. Electrochemical efficiency of the cell is found to vary between 10% and 70% from low to high temperatures.

Keywords: Hydrogen production, CuCl, electrolysis, electrochemical analysis, equilibrium analysis, kinetic analysis, overpotential, efficiency.

Dedication

In dedication of my loving parents: Soheyla and Sadegh.

Acknowledgements

I would like to express my sincere gratitude to my supervisor, Professor Dr. Ibrahim Dincer and co-supervisor, Professor Dr. Marc A. Rosen for giving me this opportunity to be part of the Clean Energy Research Laboratory research group where I could fulfill most of my assigned goals for my Master's degree. I especially would like to thank Dr. Dincer who has been a life teacher for me. In many situations, his patience, guidance and support have helped me to cope with difficult problems. Financial support from the Ontario Research Excellence Fund is also gratefully acknowledged.

The data and information provided by Dr. Serguei Lvov and Derek M. Hall from the Pennsylvania State University regarding Gibbs energy minimization analysis are gratefully acknowledged. I would also like to register my appreciation of Dr.Victor Balashov, who assisted me in learning how to determine thermodynamic properties of aqueous ions. Dr. Calin Zamfirescu and Dr. Zhaolin Wang helped me to draw bright ideas at an early stage of the project. In addition, I would like to thank Farrukh Khalid, Kaveh Azarbayjani, and Forough Foroutan as well as Dr. Behnaz Rezaie and Dr. Peyman Shahi who have supported me since the beginning by their motivation. A special thanks go to Dr. Pouria Ahmadi, who gave me the incentive to work harder.

Last but not least, I sincerely thank my parents: My mother who taught me to believe that all the dots connect through my dreams under the leadership of almighty Allah and my father, who is my ultimate symbol of a hardworking and ambitious person. He taught me how to make a goal for myself and how to fight for it. He is the one who always came home late at nights to make it possible for me to go to school early in the morning.

Table of Contents

List of Figures

List of Tables

Nomenclature

A	Theoretical constant of Debye-Huckel parameter ($mol^{-0.5}kg^{0.5}$)
a	Activity of ion
ȧ	Common ion diameter (Å)
b	Input amount of element (mol)
B	Theoretical constant of Debye-Huckel parameter ($mol^{-0.5}kg^{0.5}$)
C	Empirical-extended parameter of third approximation of Debye-Huckel theory
c	Concentration of ions ($mol.l^{-1}$)
E	Potential (V)
Ex	Exergy (J)
$\overline{ex}$	Specific molar exergy ($J.mol^{-1}$)
F	Faraday constant ($C.mol^{-1}$)
$\bar{g}$	Specific molar Gibbs free energy ($mol.l^{-1}$)
$\bar{h}$	Specific molar enthalpy ($mol.l^{-1}$)
I	Ionic strength of electrolyte
k	Rate constant of reaction ($\mu mol.s^{-1}$)
L	Thickness of membrane (μm)
m	Number of existing phases
$\dot{N}$	Molar production rate ($mol.s^{-1}$)
P	Electric power (W)
Q	Heat (J)
z	Number of exchanged electrons

Greek Letters

α	Symmetry factor or transfer coefficient
γ	Activity coefficient of ion

ε	Gibbs conversion coefficient
η	Overpotential (V)
θ	Dielectric constant
Λ	Pre-exponential factor
ϕ	Lagrangian factor
$\bar{\mu}$	Molar chemical potential ($\mathrm{J.mol^{-1}}$)
σ	Membrane ionic conductivity ($\mathrm{S.cm^{-1}}$)
Φ	Stoichiometric number of element
Ψ	Efficiency

Subscripts

C	Current
Cell	Electrolyser full-cell
D	Decomposition
DH	Debye-Huckel
e	Electrolyte
en	Energy
ex	Exergy
et	Electron transfer
emt	electron-mass transfer
HER	Hydrogen evolution reaction
Heat	Heat
i	i^{th} ion

j	j^{th} phase
Mt	Mass transfer
Ox	Oxidant
P	Products
R	Reactants
r	Reaction
S	Setchenow coefficient
th	Thermodynamic
V	voltage
1	Reaction 1
2	Reaction 2
3	Reaction 3
4	Reaction 4

Superscripts

°	Standard condition
N	Stoichiometric number of species
Ch	Chemical
Ph	Physical

Acronyms

ATR	Autothermal reforming
aq	Aqueous
CCS	Carbon capture and sequestration
ECC	Energy conversion coefficient

E_xCC	Exergy conversion coefficient
eq	Equilibrium
GEM	Gibbs energy minimization
GHG	Greenhouse gas
HER	Hydrogen evolution reaction
HKF	Helgeson-Kirkham-Flowers
IEA	International Energy Agency
LHV	Lower heating value ($J.mol^{-1}$)
Mtoe	Million ton oil equivalent
OECD	Organization for Economic Co-operation and Development
PEM	Proton exchange membrane
POX	Partial oxidation
PPM	Part per million
SCWR	Supercritical water reactor
SMR	Steam methane reforming
TWh	Terawatt hour
WGS	water-gas shift

Chapter 1: Introduction

Global warming is a major concern for the environment. If no significant actions are taken, it will be cause of irreversible effects on the planet. Carbon dioxide (CO_2), methane and water vapor, known as so-called greenhouse gases, absorb solar irradiation from the Earth and do not let it pass through the atmosphere so they work as a blanket and cause continuous increase in temperature. A goal has been set to limit the long-term Earth's average temperature increase below 2℃ by controlling greenhouse effect [1]. One indicator of the scale of challenge is that CO_2 emissions in the past 27 years is equal to all the previous years as in the last decade emissions increased by almost 1.2% per day [2]. In 2012, the concentration of present carbon dioxide in the atmosphere was estimated about 435 parts per-million carbon dioxide equivalent (ppm CO_2eq) [2] and is predicted to increase by about 20% to around 550 ppm by 2050, leading to at least 2℃ global warming [3]. Human activities are the primary contributors to global warming. As technology is enhancing and more comfort is desired by people, the industry and other sectors, including the power sector have increasingly kept up with corresponding demands and the result is more severe damages to the environment. Overall, increasing global population and economic development as well as universal energy access as a goal, are drivers for energy system expansion [4]. The energy sector represents 66% of total anthropogenic GHG emission. World energy demand has been increasing, although OECD countries' consumption remains steady at approximately 5500 Mtoe, China is predicted to experience a slower pace in demand after 2015, while other countries have been demanding more energy since 1995. World energy demand is estimated to be around 14000 Mtoe in 2015, and is predicted to grow to 18500 Mtoe by 2040 [5]. Despite the clear negative effects, fossil fuels such as coal, oil, and natural gas continue to be the major fuels

for running and developing energy systems all over the world. Statistics released in 2014 by IEA [5] show that in 2012 fossil fuels contributed to meet 13500 Mtoe by 63% (oil 31.4%, coal 29.0%, natural gas 21.3%) while this number was 81.3% in 2010. To tackle the climate change problem, serious actions are necessary across the global energy sector. There are various ways to face global warming while meeting energy demands, such as: efficiency enhancement of current fossil fuel-based technologies; carbon capture and storage technologies (mainly coal-fired plants); development of smart grid systems; renewable energy storage; and innovations in clean energy systems [6]. Renewable power generation grew annually from 3.0% (2000-2006) to 5.5% in 2006-2013, and is likely to increase up to 40% annually from 2013-2018 to meet an international goal of 6900 terawatt hours (TWh) [6]. Renewable target share for 2025 is expected to be 35%, meaning activities in this area must be boosted to meet this level. Within all clean energy technologies, hydropower, onshore wind and solar photovoltaics have kept the expected pace to meet the target of preventing a global warming increase of 2℃ by 2050.

1.1: Hydrogen Applications

Hydrogen plays a crucial role in human life and will become even more important as population increases. Note that a main use of hydrogen is in production of fertilizers for food crops. Additionally, hydrogen may alleviate demands of some of commodities such as transportation fuels and other chemicals [7] as the population and the energy demand grow. Also, as renewable energy systems grow to contribute a larger share in energy and transportation sectors, storage systems become significantly more important. Energy storage is one of the key technologies to decarbonize power sector whereby temporal and geographical gaps between supply and consumption can be bridged [8]. In this regard,

hydrogen can play significant role as an energy carrier. To gain greater understanding of the roles of hydrogen within the energy and industrial sectors, Table 1.1 presents the various applications of hydrogen. Ramachandran and Menon [9] in 1998 categorized hydrogen consumption into four categories as:

1. Reactant for hydrogenation processes: where hydrogen is required to obtain compounds with lower molecular weight, having hydrocarbons cracked, saturation of compounds, and removal of nitrogen and sulphur compounds.
2. Coolant for electrical generators where rotating systems can benefit from unique physical properties of hydrogen to control friction.
3. Oxygen scavenger where hydrogen can chemically remove trace amounts of oxygen to prevent corrosion.
4. As a direct fuel.

Table 1.1: Hydrogen applications (Modified from [9]).

Category	Industries	Facts
Hydrogen as a Reactant	Petrochemical processing	Hydrogen is catalytically reacted with hydrocarbons in two ways: Hydrocracking and Hydroprocessiong; Hydrocracking is used to refine fuel to a lighter molecule with higher H/C ratio; Hydroprocessing is used to remove nitrogen and Sulphur compounds.
	Petrochemical production	Methanol is the major petrochemical product from hydrogen. Hydrogen and carbon monoxide at high pressure-high temperature react over a catalyst; Butyraldehyde from propylene; Acetic acid from syngas; Butanediol and tetrahydrofuran from maleic anhydride; Hexamethylene diamine

		from adiponitrile; Cyclohexane from benzene; Plastic recycling.
	Oil and fat hydrogenation	Hydrogen is used to decrease degree of unsaturation in fats and oils; Hydrogen is used to convert catalysts from oxide form to active metal form through reduction process.
	Fertilizers production	Ammonia as basis of fertilizers industry is produced by activation of nitrogen and hydrogen at high pressure; Ammonia consumes almost half of produced hydrogen in world.
	Metallurgical applications	Hydrogen is used in production of nickel in reduction stage.
	Electronics	Hydrogen is used to reduce silicon tetrachloride to silicon for growth of epitaxial silicon.
Hydrogen as oxygen remover	Metallurgical processes	Mixture of hydrogen and nitrogen is required to remove oxygen in heat treating applications.
	Nuclear industry	In Boiling Water Reactors (BWR) and Pressure Water Reactors (PWR) hydrogen is used to scavenge oxygen concentrations to below 100 ppb to prevent corrosion issues which lead to higher radiation levels from nuclear plant.
	Float glass manufacturing	Mixture of nitrogen and hydrogen is used to prevent oxidation of molten tin bath where glass floats on.
Hydrogen as fuel	Combustion fuel	In Aerospace industry, mixture of liquid hydrogen and oxygen produces highest amount of energy per unit weight of propellant; Hydrogen is also considered as fuel for car engines and gas turbines. Which has not gained marketability.
	Fuel cell fuel	Hydrogen and oxygen can generate electricity in a fuel cell for either transportation or power generation in buildings.
Hydrogen with unique physical properties	Benefiting from physical properties	Hydrogen has lowest viscosity among other fluids, therefore, it is used as lube for rotor of power generation systems; Hydrogen is also used in Weather Balloons.

1.2: Hydrogen Production Methods

Hydrogen production technologies can be categorized into two groups: 1) clean and 2) conventional hydrocarbon-based processes. In addition, other terms for clean technologies can be seen in the literature such as renewable, sustainable, and environmentally benign technologies, as well as green methods. Holladay et al. [10] state that the ability of hydrogen to be extracted from a wide variety of feedstock through different processes makes it possible for all regions of the world to produce their own hydrogen. This will consequently result in economy growth by preventing money and jobs from being exported. The main large-scale technologies that produce hydrogen are all fed by fossil fuels. For instance steam methane reforming technology accounted for almost 50% of the total world's hydrogen production in 2005 [11].

Hydrocarbons can produce hydrogen through two general methods: reforming and non-reforming techniques. Figure 1.1 presents the hydrocarbon-based hydrogen production processes. The three main reforming processes are steam reforming, partial oxidation (POX), and autothermal reforming (ATR). The following equations present the three main reforming processes:

Steam reforming: $C_xH_y + xH_2O = xCO + (x + 0.5y)H_2$ (1.1)

Partial oxidation: $C_xH_y + 0.5xO_2 = xCO + 0.5H_2$ (1.2)

Autothermal reforming: $C_xH_y + 0.5xH_2O + 0.25O_2 = xCO + (0.5x + 0.5y)H_2$ (1.3)

Steam reforming does not need oxygen and has a lower operating temperature than ATR and POX [10]. For instance, in the case of iso-octane (C_8H_{18}) reforming, the minimum

corresponding reaction temperatures are reported as 950℃, 1030℃, and 1200℃ via steam reforming, ATR, and POX, respectively, for oxygen-to-carbon ratio of unity [12].

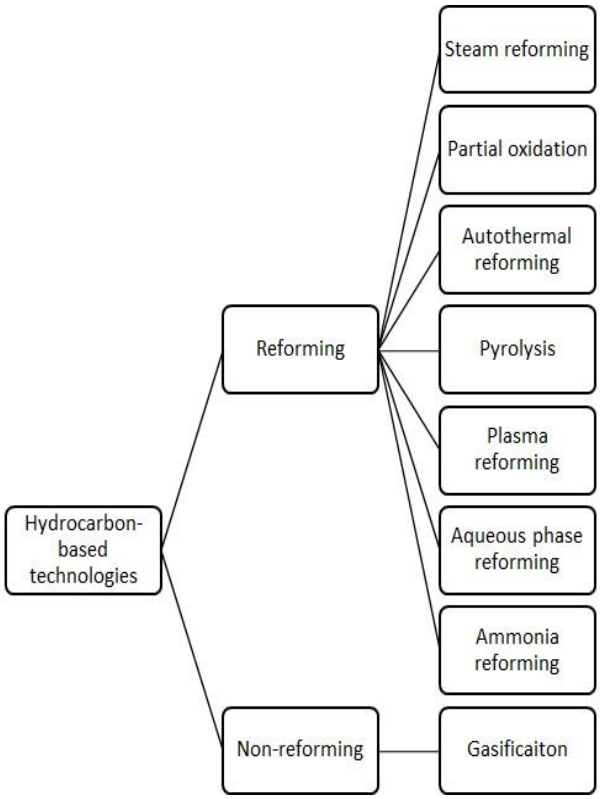

Figure 1.1: Hydrocarbon-based hydrogen production technologies (Modified from [10]).

Steam reforming is mainly used to extract hydrogen from methane that has been reported to have high energy efficiency of around 85% [13]. However, in another study, Zamfirescu and Dincer reported energy efficiency of 30%-40% and exergy efficiency of 27%-36% for all hydrocarbon reforming technologies. Usually, the SMR has a reaction temperature of 700℃-1000℃, pressure of 15bar-50bar and a steam-to-carbon ratio of 2-5[14]. Since the major reforming processes emit large amounts of carbon monoxide, one or a series of water-gas-shift reactors (WGS) are used to convert carbon monoxide to carbon dioxide:

Water-gas-shift reaction: $CO + H_2O = CO_2 + H_2$ (1.4)

Usually a series of high-temperature ($> 350℃$) and low-temperature (210℃-330℃) WGS reactors are used and the produced carbon dioxide can be captured though an appropriate carbon capture technique from an appropriate spot in the process. For instance Soltani et al. [11] studied a SMR process for the best carbon capture spot within the process and reported that there are some advantages and disadvantages for each of the three available points in the SMR process to capture carbon dioxide. Furthermore, each of ATR, POX and steam reforming has some advantages and disadvantages. SMR is the most common between the reforming technologies while it has the highest air emissions [15]. Therefore, in recent years studies have focused on improving performance of the process or development of carbon capture and sequestration systems [16, 17].

The main non-reforming technology for hydrocarbon-based hydrogen production is the gasification process. Gasification is described as conversion of a carbonaceous resource into a gaseous product with a tangible and useful heating value [18]. In other words, the thermochemical conversion of carbon-based liquid or solid fuel into a synthesis gas, which is composed of H_2 and CO, is named gasification [19] and requires a temperature between 800℃-1800℃, depending on the melting point of the used source [20]. Several simultaneous reactions occur in the gasification process. The most desired product of this process is hydrogen, which is produced through a WGS reaction. POX, water-gas, WGS reaction, and methanation reaction are presented as follows:

Partial oxidation: $C + O_2 = CO_2$ (1.5)

Water-gas: $C + H_2O = CO + H_2$ (1.6)

Water-gas-shift: $CO + H_2O = CO_2 + H_2$ (1.7)

Methanation: $C + 2H_2 = CH_4$ (1.8)

Gasification technology is commonly used for coal and biomass. However, biomass gasification is considered as a clean technology. Coal gasification, which is in a mature status and is commercially available, requires higher investment cost compared to other common hydrogen production systems [21].

1.2.1: Clean Hydrogen Production Technologies

Green and clean hydrogen production methods are expected to be the basis of the future hydrogen economy [22]. As stated earlier, the world's need of hydrogen will continue to grow significantly. Therefore, due to environmental issues of current mature hydrogen production technologies, clean methods should be developed and replaced. In the literature, there are various terms for new hydrogen production technologies, such as green, clean, sustainable, and renewable methods that all refer to a hydrogen production technology using resources other that fossil fuels and/or do not emit greenhouse gases. For instance, coal gasification with decarbonization technology (carbon capture and sequestration CCS) is considered a sustainable method. However coal is a fossil fuel [23]. Figure 1.2 presents various viable paths to produce four kinds of energies to run corresponding hydrogen production technologies from green resources.

Sustainable hydrogen production methods are: electrochemical, hybrid, biochemical, radiochemical, photochemical, and thermochemical [23]. Furthermore, sustainable hydrogen production methods from fossil fuel processes include integration of those systems to CCS or hydrocarbon-cracking via nuclear energy, solar energy, or plasma arch [23].

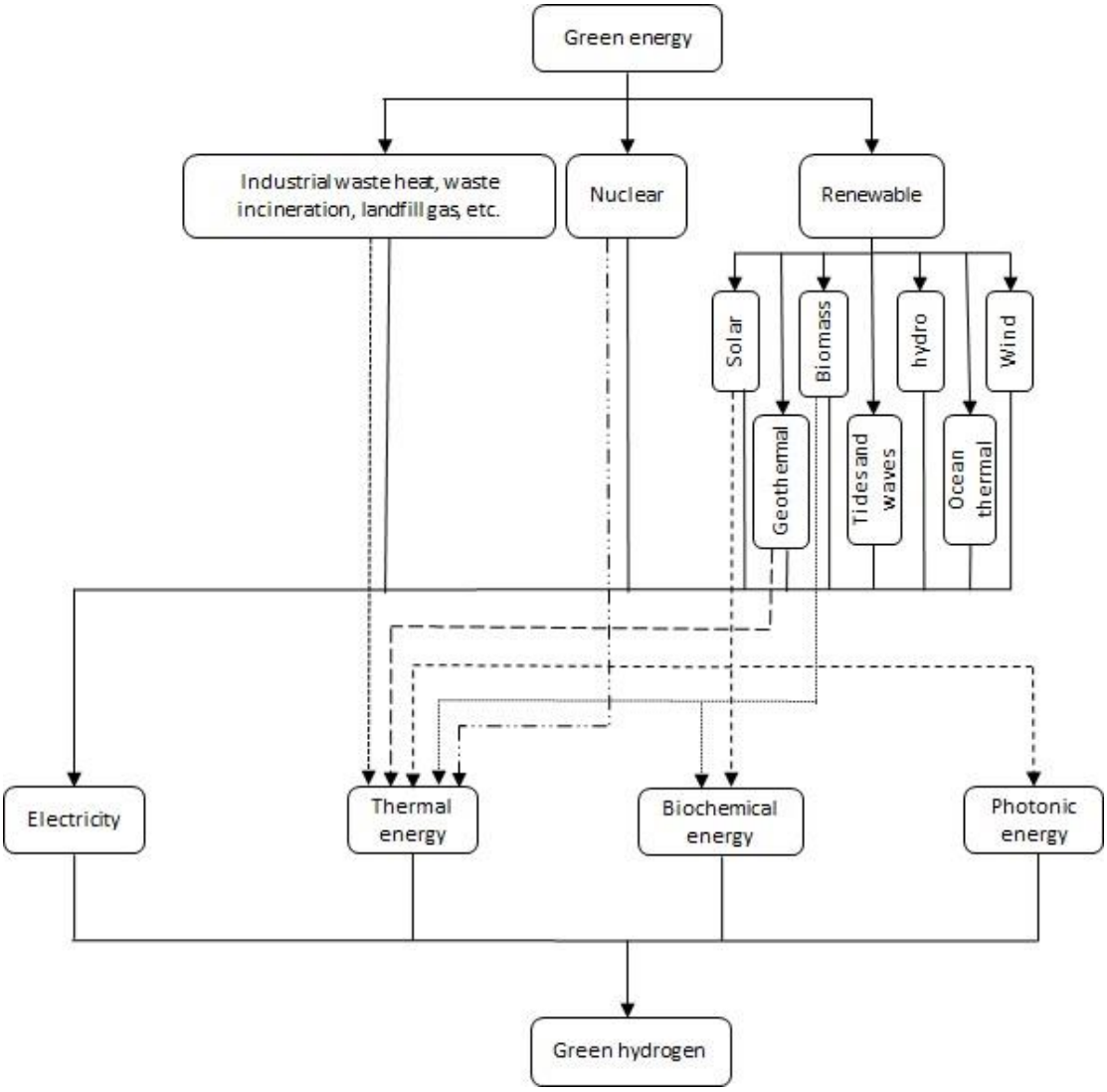

Figure 1.2: Green energy to green hydrogen path (Modified from [7]).

Thermochemical water splitting, which is a very clean and cost-effective method for hydrogen production relative to other methods [24], uses a series of heat-driven chemical reactions to generate oxygen and hydrogen. Over 200 thermochemical cycles have been proposed and are available in the open literature but only a few of them made it to experimental demonstrations [25]. After considering various criteria such as availability of materials, simplicity, chemical and thermodynamic feasibility, as well as safety aspects, eight

cycles with possible commercial importance are known: sulphur-iodine (S-I), copper-chlorine (Cu-Cl), magnesium-iodine (Mg-I), iron-chlorine (Fe-Cl), copper-sulfate (Cu-SO_4), cerium-chlorine (Ce-Cl), vanadium-chlorine (V-Cl), and hybrid chlorine. Cu-Cl cycle benefits from a lower temperature requirements, which is around 530℃ compared to at least 800℃ of other thermochemical cycles. There are also other advantages for Cu-Cl in terms of material requirements and maintenance costs [26]. Thermochemical cycles, which have been studied for more than 35 years, experienced extensive research between the 1970s and 1980s but, while there is no doubt about the technical feasibility of these cycles, in the last ten years, they have been of little interest [27].

1.3: Literature Review

Holladay et al. [10], Acar and Dincer [28], Garland et al. [29] and Dincer and Zamfirescu [23] are some of the available reviews and analysis studies in the literature on hydrogen production technologies. The following results can be summarized from their works:

- Electrolysis coupled with renewable sources is a near-term technology [10].
- Electrolysis for small-scale hydrogen production in distributed facilities would be more cost competitive than other technologies [10].
- Biomass gasification is a cheaper technology for hydrogen production ($/kg) while steam methane reforming and coal gasification are in second and third place, respectively [28].
- Bringing capital costs into effect, steam methane reforming is the cheapest technology [28].

- In term of process efficiency, biomass gasification has the best condition, followed by thermochemical water splitting (TWS) processes i.e. Cu-Cl and S-I [28].
- By 2020, distributed and centralized hydrogen production technologies are predicted to achieve the hydrogen cost target of 3 $/gas gallon equivalent [29].
- Steam methane reforming has the highest global warming potential among other technologies (12 kg CO_2 eq) [30].
- Renewable hydrogen production cycles provide the lowest environmental impact compared to fossil fuel based technologies (Solar: 0.37 kg CO_2 eq, Wind: 0.32 kg CO_2 eq) [30].
- Water splitting is considered as the most promising technology for hydrogen production because water is the most abundant resource containing hydrogen [23].
- Nuclear power plants integrated with the TWS process, especially the Cu-Cl, is the most promising large-scale environmentally benign hydrogen production method [23].

Regarding the efficiency enhancement of SMR as the most common technology, Song et al. [17] optimized a SMR system with a novel heat integration, therefore, total energy consumption of the process was reduced to almost 40% of current conventional SMR plants. Sadooghi and Rauch [16] conducted an experimental-analytical study and deduced that the presence of even small traces of sulphur in the gas feed for SMR drastically decreases the reformer efficiency. However, this effect can be reduced by increasing the reformer's temperature, but that would cause a higher fuel consumption rate in the furnace. A large amount of research focuses on developing the best catalyst for the steam reformer to gain a better efficiency with lower consumed energy. For instance, Arcotumapathy et al. [31]

reported that for a low steam-to-carbon ratio of 1-2 (S:C=1-2), a particular design of catalyst can increase methane conversion up to 99% at 1073 K compared to the current commonly used catalyst known as the Ni catalyst. Gholinezhad et al. [32] used a semi-clathrade formation for carbon capture purpose from syngas produced in the SMR process and they reported that using tetrabutylammonium significantly improves separation efficiency up to 96 mol% compared to the conventional separation method.

The abundance of coal resources on the Earth drives ongoing research for more efficient ways to extract hydrogen from it. Recent research focuses mainly on biomass high-temperature gasification as it is considered as one of the long-term solutions for central hydrogen production [29]. Abuadala et al. [33] conducted energy and exergy efficiency investigation of a biomass gasification system under the effect of temperature, and the amount of steam injection and hydrogen production. Another energy and exergy efficiency study shows that the gasifying medium changes the adiabatic temperature of the gasifier and the efficiency of air gasifying is higher than steam gasifying due to having higher temperatures [34]. A novel integration of a coal gasification process with an alkaline water electrolyser is proposed and thermodynamically modelled in a study by Herdem et al. [35], which claims that reductions in greenhouse gas emissions, and energy and exergy analyses, indicate efficiencies of 58% and 55%, respectively.

Carbon capture technologies are strongly considered for development and upgrading of coal gasification processes. In addition, underground coal gasification (UCG) has gained some attention as a clean coal technology [36]. The UCG involves gasification of deep underground coal seams that are inaccessible through conventional coal mining methods [36]. Surprisingly, the UCG is cheaper than a regular ground coal gasification process since it does

not involve mining, transportation, handling, or ash disposal costs [37, 38]. Olateju and Kumar [36] examined the techno-economic feasibility of hydrogen production via a UCG in Western Canada to support the oil sands bitumen upgrading industry. They reported that the cost of the UCG without and with carbon capture and sequestration technology would be 1.78 $/kg$H_2$ and 2.11-2.70 $/kg$H_2$, respectively. They also studied the costs of having a SMR plant in the same area and reported 1.73 $/kg$H_2$ and 2.14-2.41 $/kg$H_2$ without and with a CCS technology. Therefore, the UCG is highly cost competitive in Western Canada. Added to this, in Poland a group of researchers conducted an experimental simulation of a hard coal underground gasification process for hydrogen production [21]. They reported the feasibility of this technology by observing almost 60% of hydrogen concentration in the product stream.

Dincer and Zamfirescu [23] conducted a comprehensive investigation of sustainable hydrogen production methods and reported energy and exergy efficiencies of each method. Table 1.2 presents the selected technologies. Taking the production rate into account, it can be concluded that production methods linked to nuclear power plants, either thermally or electrically, are promising options. Kothari et al. [39] studied enviro-economic aspects of renewable and conventional hydrogen production cycles and claimed that electrolysis associated with solar energy, hydro power, wind power, and biomass are appropriate for significant hydrogen production. In an experimental study on reforming natural gas by concentrated solar power carried out by the aerospace center of Germany (DRL) [40], they reported 40% fuel saving for hydrogen production compared to conventional methods and the price was estimated about 2 ct€/kWh LHV of hydrogen, which is only 20% higher than conventional methods.

Table 1.2: Production rate, energy and exergy efficiency of selected sustainable hydrogen production methods (Data from [23]).

Method	Input energy	Production rate (MW)	Energy efficiency (%)	Exergy efficiency (%)
Electrolysis	Wind	0.01 – 400	22-40	21-39
	Tidal and Hydro	0.10 – 1000	60-65	58-63
	OTEC	30-300	4-5	45-50
	Solar PV	0.001-0.1	4-6	3-5
	Geothermal	10-300	10-15	20-30
	Nuclear	100-1000	19-32	17-29
	Waste heat	0.001-0.1	4-15	10-35
Thermochemical	Solar	75-400	36-40	33-37
	Nuclear	500-1500	40-43	35-37
Thermo-electrochemical	Solar	75-400	36-40	33-37
	Nuclear	500-1500	40-43	35-37

Furthermore, regarding hydrogen production from renewable resources, Levin and Chahine [22] stated that several clean technologies are emerging with excellent potential for on-site or distributed production, such as steam reforming of aqueous oxygenated hydrocarbons and gasification of biomass , while all renewable methods involve purification and storage issues.

Some water splitting technologies have gained more attention from researchers than others. For instance, the only available scientific paper in open literature for water thermolysis is from Baykara and Bilgen [41], who modelled the process thermodynamically and studied it, based on the first and second law of thermodynamics that reveal efficiencies about 4.11% and 3.39%, respectively. They deduced that separation of products by the solid diffusion method reveals the highest efficiencies. Rehman et al. [42] conducted an experimental study on water vapor plasmolysis for hydrogen production and reported energy efficiency of around 79% for the modelled process. Having low power consumption and a tangible production rate (20 g/kWh), they claimed this technology to be competitive with the electrolysis process.

Bockris and Gutmann [43] conducted a study on a genetically aided electrolyser and suggested the application of magnetically enhanced electrolysers as they have enhanced mass transport rates.

Wang et al. [44] conducted a comparative study on S-I and Cu-Cl cycles and reported that the two cycles do not differ significantly in term of heat requirement but temperature requirement of the Cu-Cl is 300 K lower than temperature requirement of the S-I cycle. Overall efficiencies of two cycles are found to be almost similar between 37% and 54% which depends on the amount of heat recovery within cycle. Cu-Cl compared to S-I involves fewer challenges regarding materials and product separation. Accordingly, the Cu-Cl project members have published reports [25, 45-49] that show tangible progress of Cu-Cl process. In the latest report [49] still some issues are mentioned to be targeted for future studies like development of a new appropriate membrane for electrolyser is required.

1.3.1: CuCl/HCl Electrolysis

Regarding the electrochemical step (electrolysis) of Cu-Cl cycle as well as other parts, many works have been carried out especially by UOIT, AECL, ANL, and PSU. Initially the AECL demonstrated feasibility of hydrogen production by Cu-Cl electrolyser continuously for several days [25, 46] and as a result two patents have been filed by AECL for Cu-Cl electrolyser development in 2010 [50] and 2015 [51]. They reported that electrolysis is feasible at considerably low potentials (0.6-0.7V) at a current density of 0.1 $\mathrm{A\,cm^{-2}}$ using inexpensive materials [45]. Also the AECL has done comprehensive studies about material selection for electrolyser cell through material degradation analysis [52]. In the US work has been focused on proper membrane development to reduce copper crossover from anode to

cathode which is considered as a poison for cell [47]. The intent is to identify a proper type of membrane with a same proton conductivity but with a lower copper crossover rate. Detail data on comparative study of considered membranes can be found in [48].

The Pennsylvania State University (PSU) has published tangible results through comprehensive experiments and also investigation of related theories. Gong et al. [53] performed CuCl/HCl electrolysis by applying potentials between 0.35 to 0.90V and used electrochemical impedance spectroscopy (EIS) and linear sweep voltammetry (LSV) methods to carry out conductivity measurements and determination of open circuit potentials. They observed virtual full conversion of $\mathrm{Cu(I)}$ species to $\mathrm{Cu(II)}$ species at 0.7V. However, Stolberg et al. [54] report this value around 0.9V. In addition, Gong et al. [53] tested seven different ion exchange membranes to perform electrolysis and they concluded that two membrane types i.e. AHT and AM-3 are highly resistive to copper crossover to catholyte. Moreover, increase in temperature was found to enhance electrolyser's efficiency by increasing transfer coefficients of half-reactions and correspondingly exchange current densities.

Balashov et al. [55] also performed experimental studies on CuCl/HCl electrolyser and reported that presence of $\mathrm{HCl(aq)}$ is not necessary for hydrogen evolution at the cathode. They developed a thermodynamic model of $\mathrm{CuCl - CuCl_2 - HCl - H_2O}$ solution based on the available data on solubility of $\mathrm{CuCl(s)}$ in $\mathrm{HCl - H_2O}$ solution with presence of $\mathrm{CuCl_2(aq)}$. Decomposition potential of electrolysis is reported around -0.4V for different anolyte concentrations. Voltage efficiency was 80% and current efficiency with good agreement to Faraday's law was determined to be 98%. Temperature increase was found to

increase required decomposition potential to run the electrolysis. In addition, increase in current density in their experiments resulted lower current efficiencies.

Khurana et al. [56] conducted experimental studies to determine that increase in temperature results into decreasing the membrane's Ohmic overpotential and also they reported that current density of cell under specific applied potential enhances by increase of temperature which almost contradicts results of Balashov et al. [55]. Schatz et al. [57] in their paper discussed steps of preparing membrane electrode assembly and running experiments and they reported that at 80℃ they could produce hydrogen with current density of 0.5 $A.\,cm^{-2}$ under 0.7V potential.

Hall et al. [58] conducted experimental investigations to determine activation overpotentials of anode and cathode half-reactions as well as full-cell overpotentials. It was concluded that magnitude of overpotential of cathode half-reaction is higher than anode half-reaction. The overall cell's overpotential to trigger hydrogen production was about 0.55V based on their reports. Also, by applying precise Pt loading on cathode, they could reduce catalyst amount by 68% maintaining same performance. In another study, Hall et al. [59] applied three available speciation models of CuCl/HCl electrolyser anolyte in conjunction with thermodynamics and experiments to perform an equilibrium and kinetic analysis on a CuCl/HCl electrolyser. They reported electrolysis efficiency of around 20% for current density of 0.5 $A.\,cm^{-2}$ while rising current density showed decreasing electrolyser efficiency. Accordingly, for temperatures around 25℃ they investigated effect of temperature on activity of active species to use it in development of clear thermodynamic model. Due to absence of data regarding kinetic parameters of the anode half-reaction. Hall et al. [60] in another study conducted electrochemical investigations and reported important data regarding kinetics of

the anode half-reaction such as transfer coefficient, exchange current density and symmetry factor of anode half-reaction. In addition, they concluded that no catalyst is needed on the anode because it has higher exchange current density than hydrogen evolution reaction on Pt of cathode. Kinetic analysis of hydrogen evolution reaction in detail was done by Hall et al. [61] to study and report kinetics of hydrogen evolution in concentrated $HCl(aq)$ as there is no other publicly available data about it. In another study the transport phenomenon through a Nafion 117 membrane in a CuCl/HCl electrolyser is studied by Hall et al. [62] and based on their claim presence of copper species affect hydronium flux from anode to cathode in highly reduced anolyte solutions. As another study at the PSU Khurana et al. [63] ran the electrolyser for 168 hours at 80℃ to produce hydrogen with $0.3\ A.\,cm^{-2}$ current density and studied the cell from a state-of-health point of view. For a fresh membrane 0.63V was reported as the required potential. Also, current density was observed to decline as time passed.

At the UOIT studies have been done regarding anode material improvements [64-66] as well as sensitivity analysis of various working parameters on hydrogen production from electrolyser via an experimental test bench of cell [67]. In this regard, through a fractional factorial design, cell potential predictive model is developed which predicts required applied potential as function of HCl-CuCl concentration, solution flow rates, current density, and temperature.

1.4: Motivation

As stated earlier, the Cu-Cl thermochemical hydrogen production cycle requires working temperatures around 530℃ and fortunately the Generation IV of super-critical water-cooled reactor (SCWR) has around same temperature as a waste heat stream. Therefore, these two

systems can be integrated to provide hydrogen production in large-scale with no emission. However, the Cu-Cl cycle can get the required energy at satisfying temperature from other sources for instance concentrated solar power technology. Generally, the two other ways of hydrogen generation as fossil-based and renewable source cycles, each have limiting barriers that for the former is GHGs emission and the later would be challenging for large-scale productions.

The Cu-Cl cycle has various equipment that hydrogen evolution takes place in an electrolyser. The applied electrolyser is PEM electrolyser. Anolyte is a concentrated solution of aqueous CuCl and HCl while catholyte can either be pure water or any concentration of aqueous HCl for hydrogen production purpose. More technical aspects will be discussed in further sections. Note that CuCl electrolyser requires half the amount of electricity potential for same hydrogen production rate by water electrolysis. Controlling copper crossover from anode to cathode and decreasing catalyst consumption for electrodes are main challenges for electrolyser. From integration point of view (electrolyser integrated with other component of Cu-Cl cycle), main challenge is having less $CuCl_2(aq)$ products in exit stream of anode for required hydrogen production. Furthermore, using the best and cost-effective membrane and electrodes have been titles for various research conducted by project members.

1.5: Objectives

The objective of this thesis is to provide an electrochemical model for the CuCl/HCl electrolyser and subsequently studying the performance and efficiency of electrolyser. In this regard, the specific objectives are listed as follows:

Objective 1: By Equilibrium thermodynamic analysis of electrolysis the cell is studied in hypothetical equilibrium state to identify the ideal performance condition and also limitations of system. The first objective consists of the following steps:

- Determination of thermodynamic properties of ions, considering ion-ion interactions.
- Calculation of decomposition potentials of anode and cathode half-reactions, as well as full-cell reaction.
- Identification of the main electrolysis reaction for the studied case.
- Investigation of effects of conversion degree and temperature on Gibbs conversion coefficient of half-reactions and full-cell reaction.
- Investigation of effects of conversion degree and temperature on decomposition potential of cell.

Objective 2: By Kinetic analysis the cell is studied in a non-equilibrium state and present imperfections regarding electrolysis can be determined. The second objective consists of the following steps:

- Determination of activation overpotentials of anode and cathode half-reactions.
- Determination of current-overpotential curves for anode and cathode half-reactions.
- Determination of Ohmic overpotential of proton exchange membrane of cell.
- Calculation of the overall required voltage for electrolysis at various current densities.
- Determination of voltage efficiency and electrochemical overall efficiency.
- Investigation of the effect of temperature on activation and Ohmic overpotentials.
- Calculation of energy and exergy conversion coefficients.

Chapter 2: Background

2.1: Water Splitting Hydrogen Production Technologies

Clean hydrogen production technologies can be classified in various ways based on different criteria, while, taking primary resources into account they can be categorized into three groups: water based, fossil fuel based, and biomass based. Due to this fact that water is the most abundant hydrogen carrier, water splitting technologies are considered one of the promising ways to satisfy hydrogen needs of future. Figure 2.1 shows the water splitting technologies.

A brief description of each mentioned technology is provided as follows:

1. Electrolysis is decomposition of water into $H_2(g)$ and $O_2(g)$ by direct electricity current.
2. Thermochemical process is decomposition of water into $H_2(g)$ and $O_2(g)$ by cyclic closed-loop chemical reactions.
3. In a thermo-electrochemical process thermal and electrical energy are used to run cyclic chemical and electrochemical reactions to split water into $H_2(g)$ and $O_2(g)$.
4. Photo-electrochemical process uses a hybrid cell to generate photovoltaic power to run electrolysis process.
5. Thermolysis is thermal decomposition of water into its molecules at over 2500 K.
6. In a photocatalysis system, complex homogenous catalysts or molecular devices are applied to generate $H_2(g)$ by photo-initiated electrons.
7. Through biophotolysis, biological systems which are based on cyanobacteria are used to produce $H_2(g)$ in a controlled manner.

8. An enzymatic process uses polysaccharides to produce required energy to split water.
9. Plasmolysis involves process of water splitting by electrical discharges.
10. Magnetolysis is electrolysis of water when the required voltage is generated inside the cell by magnetic induction.
11. Radiolysis is use of radioactive materials or highly energetic particles in order to decompose water into its molecules.

Among all water splitting methods thermochemical processes have been more of interest due to this fact that over 200 thermochemical cycles have been proposed. However just few of them have been studied experimentally due economic issues [45]. Eight cycles (S-I, Cu-Cl, Ce-Cl, Fe-Cl, Mg-I, V-Cl, Cu-SO_4, and hybrid chlorine) are considered as possible commercial cycles taking some criteria into account like abundance of materials, chemical viability, and safety issues. Major interests in thermochemical processes are: 1) normally catalyst is not used for chemical reactions; 2) Only water is consumed; 3) Hydrogen and Oxygen are the only products and are separated streams (no separation needed); and 4) all other chemicals are recycled [23]. The overall process is written as:

$$H_2O(l) + \text{Heat}\ (600\ \text{K} - 1200\ \text{K}) \rightarrow \text{Closed loop chemical reactions} \rightarrow$$

$$H_2(g) + O_2(g) \qquad (2.1)$$

There are some thermochemical cycles that are called hybrid cycles. They require small amounts of electricity to run some oxidation-reduction (redox) reactions:

$$H_2O(l) + \text{Electricity}(0.50 - 1.0\text{V}) + \text{Heat}(600\ \text{K} - 1200\ \text{K}) \rightarrow$$

$$\text{closed loop chemical reactions} \rightarrow H_2(g) + O_2(g) \qquad (2.2)$$

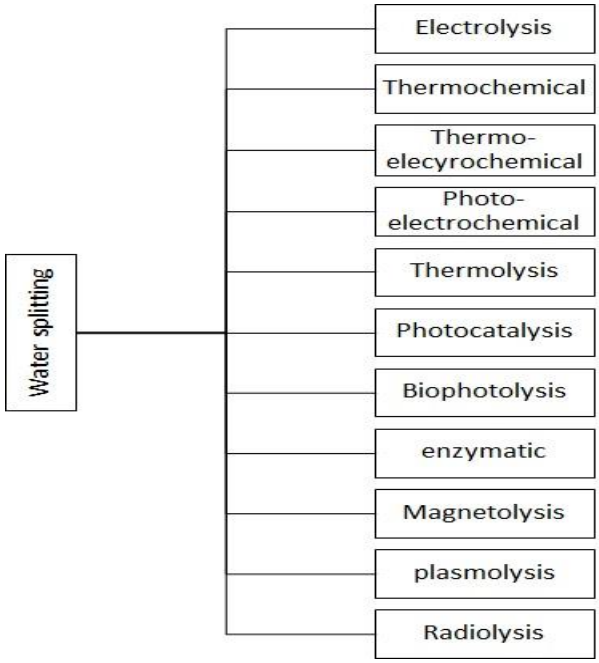

Figure 2.1: Water splitting technologies (Modified from [7] and [68]).

From equation 2.2 it can be seen that the required voltage and temperature are reasonable. The sulfur-iodine process takes place through a multi-step process (there are several types of S-I processes). The following reactions present a three-step S-I cycle for water decomposition as most common cycle [68, 69]:

$$\text{Hydrolysis at 393 K: } I_2(l+g) + SO_2(g) + 2H_2O(g) \rightarrow 2HI(g) + H_2SO_4(l) \quad (2.3)$$

$$O_2 \text{ generation at 1123 K: } H_2SO_4(g) \rightarrow SO_2(g) + H_2O(g) + 5O_2(g) \quad (2.4)$$

$$H_2 \text{ generation at 723 K: } 2HI(g) \rightarrow I_2(g) + H_2(g) \quad (2.5)$$

The hydrolysis step is exothermic while both hydrogen and oxygen generation steps are endothermic. Some institutions have been active to develop S-I processes such as the Japan Atomic Energy Agency (JAEA) [70], General Atomics (GA) [71], CEA of France [72], and

Sandia National Laboratory (SNL) [73]. The GA have demonstrated a pilot plant with production rate of 2kgH_2/day.

2.2: Cu-Cl process

Moderate temperature requirement of the Cu-Cl process (550℃) compared to 800℃ or higher for other thermochemical cycles as well as lower complexity, inexpensive chemicals and high efficiency [74] make the Cu-Cl cycle interesting especially for next generation of super-critical water-cooled reactors (SCWR) known as Generation IV SCWR.

Canada as leader of Cu-Cl cycle project has put effort to develop an integrated large lab-scale demonstration equipment [48] through the generation IV international forum (GIF) [75]. The Canadian-led team consists of University of Ontario Institute of Technology (UOIT), University of Toronto, University of Guelph, University of Western Ontario, University of Waterloo, University Network of Excellence in Nuclear Engineering (UNENE), and Atomic Energy of Canada Limited (AECL) as Canadian collaborators and Argonne National Laboratory (ANL), and Pennsylvania State University (PSU) as the U.S. members. Each of named members focus on some particular aspects of project with UOIT as the place to demonstrate and develop unit operations. In future, all unit operations will be integrated to a whole cycle at UOIT which will be the final step of large-scale pilot cycle development project.

There are various types of Cu-Cl processes (2-5 steps); Table 2.1 presents four-step cycle. The four-step Cu-Cl cycle has two low-temperature and two high-temperature steps. The electrolysis and drying steps can take place at temperatures lower than 100℃, while hydrolysis and thermolysis require energy sources with temperature of around 400℃ and

500℃, respectively. Step one, is where hydrogen is generated. To obtain this goal, other three steps provide required materials for step one, and step one closes the cycle by providing required material of step two. Overall, through a closed cyclic process, the only outputs of system are hydrogen and oxygen.

Table 2.2: Steps of a four-step copper-chlorine cycle for hydrogen production.

Step	Name	Reaction	Temperature
1	Electrolysis	$2CuCl(aq) + 2HCl(aq) \rightarrow 2CuCl_2(aq) + H_2(g)$	<100℃
2	Drying	$CuCl_2(aq) \rightarrow CuCl_2(s)$	<100℃
3	Hydrolysis	$2CuCl_2(s) + H_2O(g) \rightarrow Cu_2OCl_2(s) + 2HCl(g)$	400℃
4	Thermolysis	$Cu_2OCl_2(s) \rightarrow 2CuCl(l) + 0.5O_2(g)$	500℃

2.3: Electrolysis

The simplest way to split water into its molecules is electrolysis. Electrolysis as the name implies is decomposition of water into hydrogen and oxygen by electrical potential. Water electrolyser is the most common electrolysis process. There are three types of water electrolysers: alkaline electrolyser, proton exchange membrane electrolyser (PEME), and solid oxide electrolyser (SOE) that the most common electrolysis cell is alkaline ones. However, researches on the other two types have been growing faster [76]. The overall electrolysis reaction regardless of the process can be written as follows:

$$H_2O(\text{l or g}) + \text{Electriciy} \rightarrow H_2(g) + 0.5O_2(g) \quad (2.6)$$

A general layout of an electrolytic cell is depicted by Figure 2.2. A direct current is applied between anode electrode and cathode electrode to maintain electrical balance while electrons leave negative charged ions from anode to cathode in order to generate hydrogen molecules.

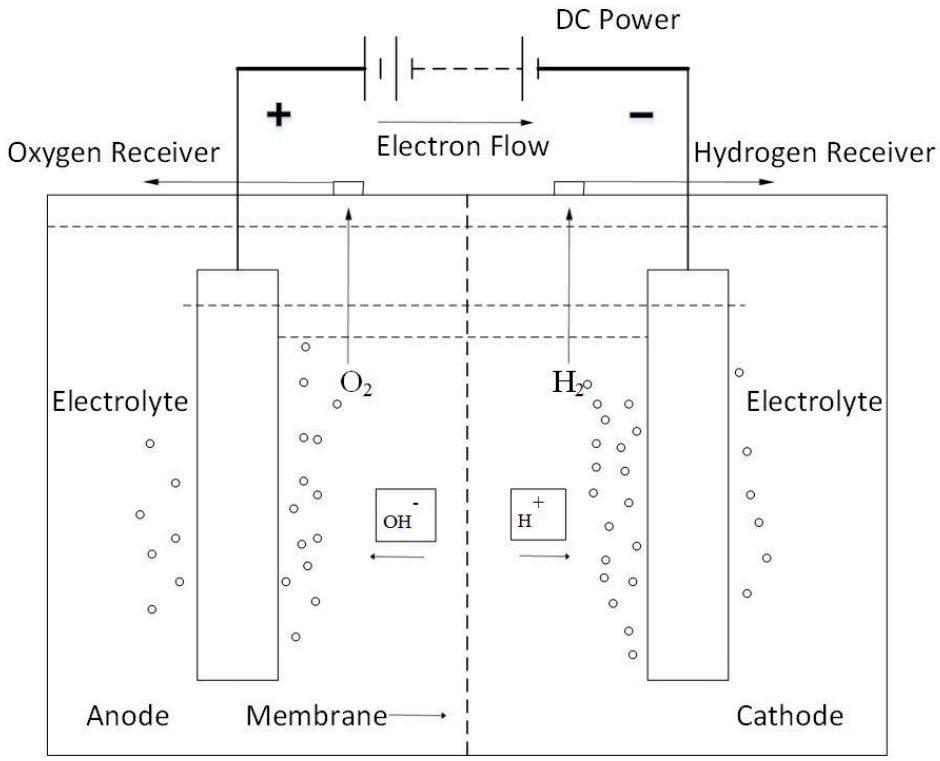

Figure 2.2: General schematic of water electrolysis (Modified from Zeng et al. [77]).

2.4: Electrolysis Step in Cu-Cl Cycle

As stated earlier, Cu-Cl thermochemical cycle which is a hybrid thermochemical cycle requires electricity potential to run its electrochemical step. Intake streams to PEM CuCl/HCl electrolyser are HCl(aq) and CuCl(aq) that are generated from hydrolysis and thermolysis steps, respectively. And the outlet streams are hydrogen gas and $CuCl_2$(aq). The hydrogen gas is stored while $CuCl_2$(aq) is sent to dryer to produce $CuCl_2$(s) granules for hydrolysis step. Figure 2.3 shows a CuCl/HCl electrolyser cell. Cu(I) ions oxidize to Cu(II) ions (Cu(I)→Cu(II)) on the anode surface and hydrogen ions are carried by water molecules (hydronium) through the membrane to cathode side. Next, on the cathode surface hydrogen

ions grab electrons and generate hydrogen gas molecules. Overall oxidation-reduction (redox) process is shown as follows:

$$2CuCl(aq) + 2HCl(aq) \longrightarrow 2CuCl_2(aq) + H_2(g) \quad (2.7)$$

In the anode, based on concentrations of CuCl(aq) and HCl(aq) several Cu(I) and Cu(II) species can form:

$$Cu^{+}(aq) + nCl^{-}(aq) \leftrightarrow CuCl_n^{1-n}(aq) \quad (2.8)$$

$$Cu^{2+}(aq) + nCl^{-}(aq) \leftrightarrow CuCl_n^{2-n}(aq) \quad (2.9)$$

The anode and cathode half-reactions are presented as equations 2.10 and 2.11, respectively. The anode half-reaction takes place on a graphite electrode and does not need any metal catalyst while, cathode half-reaction requires a catalyst. A graphite electrode coated with Pt catalyst is found to be appropriate [25].

$$\text{Anode half} - \text{reaction: } CuCl(aq) + HCl(aq) \longrightarrow CuCl_2(aq) + H^{+}(aq) + e^{-} \quad (2.10)$$

$$\text{Cathode half} - \text{reaction: } H^{+}(aq) + e^{-} \longrightarrow 0.5H_2(g) \quad (2.11)$$

Since there are more than one Cu(I)→Cu(II) processes, based on temperature, pressure and concentrations, one should investigate the series of available anode half-reactions on anode surface which is one of targets of this study. The overall cell efficiency from electrochemistry point of view can be defined as multiplication of equilibrium Gibbs conversion coefficient, current efficiency and voltage efficiency as follows:

$$\varepsilon_{EC} = \varepsilon_{th} \times \varepsilon_v \times \varepsilon_c = \frac{\overline{\Delta_r h}}{\overline{\Delta_r g}} \times \frac{E_D}{E_{EC}} \times \varepsilon_c \quad (2.12)$$

where $\Delta_r h$ denotes overall energy required by the full-cell reaction, $\Delta_r g$ is related to amount of only electrical charge required by full-cell reaction, E_D is decomposition potential of cell in equilibrium mode, E_{EC} is applied potential to cell considering all cell imperfections, and ε_c is division of hydrogen production rate by theoretical production rate. However, from input-output (control volume analysis) point of view, energy and exergy efficiencies or energy conversion coefficient and exergy conversion coefficients of an electrolyser can be defined as follows:

$$\psi_{en} \text{or ECC} = \frac{LHV_{H_2} \times \dot{N}_{H_2}}{Q_{electric} + Q_{heat}} \tag{2.13}$$

$$\psi_{en} \text{ or } E_x CC = \frac{Ex_{H_2} \times \dot{N}_{H_2}}{Ex_{electric} + Ex_{heat}} \tag{2.14}$$

where LHV_{H_2} denotes lower heating value of hydrogen, $\dot{N}_{H_2}$ is molar outlet flow rate of hydrogen, $Q_{electric}$ and Q_{heat} are rate of input electric charge and input heat to the cell, respectively; Ex_{H_2} is exergy content of hydrogen, while Ex is corresponding exergy input rate of variables. Therefore, through an electrochemical analysis of the cell as well as control volume analysis, one can compare different efficiency definitions (Gibbs conversion coefficient, electrochemical efficiency, energy conversion coefficient, and exergy conversion coefficient) which is part of this study.

The CuCl/HCl electrolysis involves couple of issues that the most important one is copper crossover through membrane from anode to cathode which is considered as poison for cell as degradation factor. In this regard, some studies have been carried out to tackle this problem [55, 56]. Apart from membrane, finding the best material for electrodes is another issue.

2.5: Electrochemical Analysis

Electrochemical analysis can be categorized into equilibrium and kinetic analyses. An equilibrium study applies thermodynamics to investigate the ideality of the system. In other words, this answers to the question that what are the limitations of the system. A kinetic analysis shows the behavior of the studied system under potential so there is no equilibrium. However, in order to carry out this study details of electrochemistry had to be studies, discussing all founding electrochemical aspects would be time consuming and out of scope of this study as there are many reference books [78, 79] with different conventions. Therefore, in this section, only some important applied aspects of electrochemistry and terms are explained as follows and one can refer to mentioned reference books for more details. In approach and methodology section required details on the applied equations are explained.

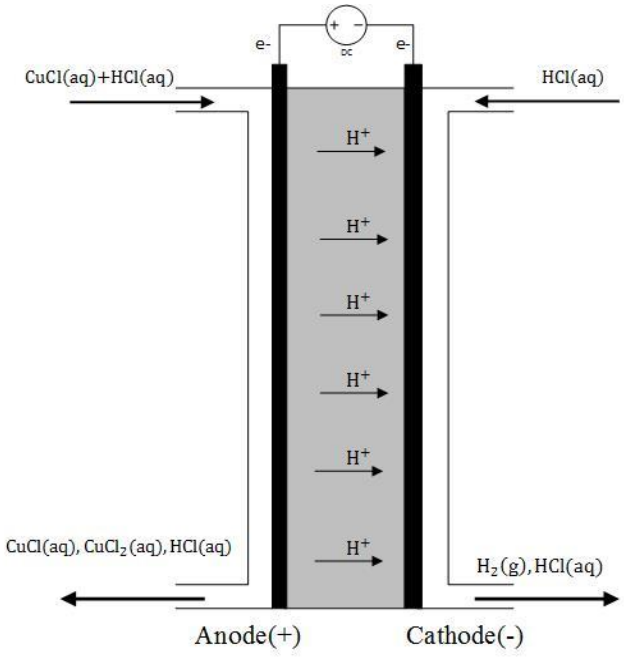

Figure 2.3: Schematic of a CuCl/HCl electrolyser; $CuCl(aq)$ refers to all $Cu(I)$ species and $CuCl_2(aq)$ refers to $Cu(II)$ species.

1. Equilibrium: Equilibrium state is the situation where reactions (forward and backward) are adequately fast therefore the reaction can be considered reversible. At equilibrium no current flow can be established i.e. anode does not send electron to cathode and hydrogen ions (hydronium) do not pass membrane.
2. Standard state: Standard state in electrochemistry refers to pressure of 1 bar, temperature of 25℃ and molarity (or molality) of 1. However, in this study standard values of thermodynamic properties are determined for different temperatures.
3. Electrolyte solution: Electrolyte solution consists various charged or neutral ion species as result of dissociation and association of molecules of solute and solvent.
4. Molarity and molality: Molarity is a solution concentration scale. 1 molar is 1 mole of an aqueous specie in 1 liter of a solution ($\mathrm{mol.\,l^{-1}}$) while molality denotes mole of a specie present in one kilogram of solution ($\mathrm{mol.\,kg^{-1}}$). If density of solvent is close to 1 $\mathrm{g.\,cm^{-3}}$ molarity and molality are close in value but at a higher temperature they will be different since density is function of temperature [80].
5. Chemical potential: Chemical potential is the most important property of a specie in solution and can be written as follows:

   $\mu_i = \mu_i^{\circ} + \mathrm{RTln}a_i$

   where μ_i° denotes chemical potential of the specie at standard condition and a_i designates activity of the specie.
6. Activity and activity coefficient: Activity is the value that should be used instead of concentration in all thermodynamic equations [80]. Activity coefficient denotes the difference between chemical potential values of a specie in ideal and real solution at same concentration.

7. Decomposition potential: Decomposition potential is the required potential to trigger a redox reaction in an electrolytic cell at equilibrium. For a fuel cell the equilibrium potential is called open circuit potential.
8. Standard decomposition potential: When the electrolyte of an electrolyser is extra dilute i.e. close to 1 molar concentration, the corresponding equilibrium potential is named standard decomposition potential instead of decomposition potential.
9. Anode half-reaction: The reaction that takes place on anode electrode of a cell which is dominantly oxidation and losing electron.
10. Cathode half-reaction: The reaction that takes place on cathode electrode of a cell and is dominantly reduction which is gaining electron.
11. Anodic and cathodic half-reactions: Each oxidation-reduction (redox) reaction has a forward reaction which is anodic and backward which is cathodic. This defection is based on the following convention:

$$\mathrm{ion}^{\mathrm{charge}} \leftrightarrow \mathrm{ion}^{\mathrm{charge-n}} + \mathrm{ne} \qquad (2.15)$$

12. Overpotential: There are overpotentials or irreversibilities within an electrolytic cell that result into higher potential demand to trigger product generation compared to equilibrium potential.
13. Activity overpotential: Activity overpotential corresponds to electrode where oxidation-reduction reactions occur. It can be combination of mass transfer and charge (electron) transfer or only electron transfer.
14. Ohmic overpotential: One sort of irreversibility in cell which stems from resistivity of membrane against ion transfer is called Ohmic overpotential.

Chapter 3: Electrochemical Analysis

3.1: Approach and Methodology

Two main steps lead to electrochemical model of the CuCl/HCl cell: Equilibrium analysis and kinetic analysis. In every electrochemical study, the first step to go through is the equilibrium condition study to determine limits and borders of cell performance from thermodynamics viewpoint. Then, kinetic study is carried out to investigate present overpotentials within cell during electron transfer and hydrogen evolution process. At the end, control volume analysis can also be carried out to determine energy and exergy efficiency or energy and exergy conversion coefficients of electrolysis cell considering inputs and outputs. Targets of two main steps can be outlined as follows:

- Equilibrium analysis: To determine half-cell decomposition potentials, full-cell decomposition potential, standard decomposition potentials for half-cells and full-cell, equilibrium Gibbs conversion coefficient, temperature dependence of decomposition potentials, Gibbs conversion coefficient, and heat transfer of the cell.
- Kinetic analysis: To determine activation overpotentials of electron transfer and mass transfer for half-cell redox reactions, membrane Ohmic overpotential for cell, overall efficiency of cell from electrochemical point of view, and temperature dependency of overpotentials.

Since the CuCl/HCl electrolyser works with concentrated electrolytes, to gain the above mentioned goals, study should be initiated by hiring a speciation model for anolyte (anode electrolyte), because it's not simply mixture of Cu^{+}, Cl^{-}, H^{+}. There are limited speciation models for anolyte of the CuCl/HCl electrolyser in literature [55,81, 82]. After identifying an

appropriate speciation model, it should be investigated that in what concentration for each of species equilibrium can be maintained, in other words, what is the equilibrium concentration of species in the solution. It should be stated that due to lack of approach to a speciation software at the UOIT, the PSU was asked to help this study by GEM analysis via the Hch software. I provided PSU with corresponding required inputs (Table 3.1) and they provided me with results of GEM analysis (Table 4.1). Presented species in Table 3.1 are selected by PSU. Obtained results from PSU are used and analyzed from various aspects in this study. In addition, the PSU provided this study with this notion that various conversion degrees of anolyte species affect equilibrium of anolyte. Next, last step prior to start the equilibrium study is to determine thermodynamic properties of considered species in the solution for various temperatures and pressures. Due to the fact that aqueous ions thermodynamic properties are not available in the literature, one should use programs to determine properties. Having enough data to start (ion species, concentrations and properties) equilibrium analysis can be started, followed by kinetic and energy/exergy conversion coefficient analyses. Figure 3.1 presents the analysis steps and arrows show which step uses data from other steps.

Some parametric studies are carried out for all obtained results to determine effect of temperature. At the end, obtained results are compared to available published reports, if applicable.

3.2: Speciation Analysis

In an electrolyte solution there are forms of reactions that occur: dissociation (partial or complete), precipitation, and association of present ions through equilibrium reactions [83]. Moreover, initial substances of electrolyte dissociate and new formed ions associate to form

complexes. Therefore, anolyte of CuCl/HCl electrolyser is not $Cu^+ - Cl^- - H^+ - CuCl - CuCl_2 - H_2O$, there are other complexes to take into account. The speciation of CuCl-$CuCl_2$-HCl-H2O, regardless of internal equilibrium reactions for each specie, can be given as equation 3.21.

$$CuCl(aq) + CuCl_2(aq) + HCl(aq) + H_2O \leftrightarrow H^+(aq) + Cu^+(aq) + Cu^{2+}(aq) + Cl^-(aq) + HCl^0(aq) + CuCl^0(aq) + CuCl^{2-}(aq) + CuCl_3^{2-}(aq) + CuCl^+(aq) + CuCl_2^0(aq) + CuCl_3^-(aq) + CuCl_4^{2-}(aq) + CuOH^0(aq) + CuOH_2^-(aq) + CuOH^+(aq) + CuO^0(aq) + HCuO_2^-(aq) + CuO_2^{2-}(aq) + HCuCl_2(aq) + Cu_2Cl_3(aq) \quad (3.1)$$

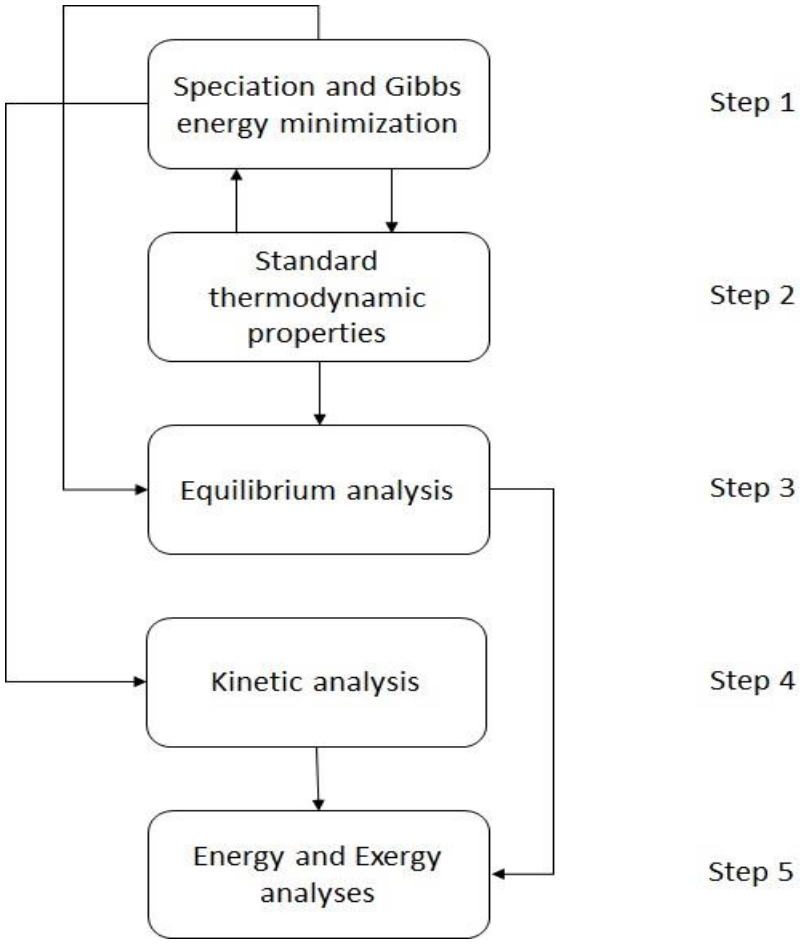

Figure 3.1: Analysis steps and their interactions; GEM is considered as part of speciation analysis.

Overall, anolyte species are complex of oxides, hydroxides and chlorides or copper. The following reaction presents general equilibrium reaction of chloride species formation:

$$Cu^{+}(aq) + nCl^{-}(aq) \leftrightarrow CuCl_n^{1-n}(aq) \quad (3.2)$$

$$Cu^{2+}(aq) + nCl^{-}(aq) \leftrightarrow CuCl_n^{2-n}(aq) \quad (3.3)$$

No precipitation reaction is assumed for anolyte and the only phase to be considered is aqueous phase. After identifying complex species and remained dissociated ions, the chemical equilibrium status should be determined, which means concentration of each of species should be determined. Basically, this part is the most important part of electrolyte study and provides useful data for the other steps.

3.2.1: Gibbs Energy Minimization

The approach to determine equilibrium concentrations for species is Gibbs Energy Minimization (GEM) method. For multicomponent systems, the Gibbs energy is written in term of chemical potential that is sum of product of chemical potential and molar content of each species (i) in each phase (j) [84]:

$$G = \sum_j \sum_i \mu_i^j . n_i^j \quad (3.4)$$

Basically, a global minimum G of solution with certain thermodynamic variables (Temperature and Pressure) is criterion of equilibrium. On top of temperature and pressure, mass constraints and also especially for electrolyte systems, charge constraints have to be taken into account. Therefore, for electrolyte systems, other than a global minimum G criterion, electrical neutrality constraint should be met and it is when net charge of the system

is zero [84]. Bringing both Gibbs energy and electrical neutrality criterion into consideration, a Lagrangian function builds up [84] as:

$$L = \sum_j \sum_i \mu_i^j . n_i^j - \sum_{k=1}^{l} \left[\lambda_k \left[b_k - \sum_{j=1}^{m} \sum_{i=1}^{p} \phi_{ik}^j . n_i^j \right] \right] \quad (3.5)$$

where the second right-hand side term is combination of mass balance equation and charge constraint. Also, λ_k is lagrangian factor, b_k is k^{th} element's input amount, and m is number of existing phases; p is number of species in j^{th} phase, and ϕ_{ik}^j is the stoichiometric number of k^{th} element in i^{th} specie

Partial derivatives of the above function with respect to concentrations and phases will result into extreme points for minimum Gibbs energy. Then, corresponding concentrations and phases of defined species will be identified [59, 84].

There are some program packages that have been developed to carry out GEM procedure, such as HCh [85], ChemSage [86], FactSage [87], and GEMS-PSI [88]. All of them are developed to model dynamic geochemical processes thermodynamically to investigate equilibrium compositions [89]. This study uses the HCh package in this regard as it has been the only package used for CuCl/HCl electrolyser thermodynamic modelling [55, 59].

The HCh package was developed by Shavrov in 1999 to model natural and chemical technological processes that take place in aqueous solutions, non-aqueous (solid or liquid), gas mixtures, or pure phases in open and closed chemical systems. Briefly explained, the proposed algorithm to solve GEM method by Shavrov is composed of three main parts that make up the package [85]:

- UNITHERM: User can define and call the required substances for study like aqueous solutions or pure substances.
- MAIN: the program MAIN is responsible for maintaining calculations of thermodynamic properties from thermodynamic database.
- GIBBS: the program GIBBS does the GEM procedure and calculates equilibrium composition in the system.

Figure 3.2 depicts full interactions between components of HCh package, one can see that thermodynamic database provides initial data. HCh uses Helgeson-Kirkham-Flowers (HKF) model [90] to calculate thermodynamic properties of aqueous species. Determination of standard thermodynamic properties of aqueous ions is discussed in the following section. Note that standard refers to 1 $\mathrm{mol.\,kg^{-1}}$ and 1 bar condition. In order to obtain thermodynamic properties of ion species from standard values activity of ions should be determined using activity coefficient models. The HCh uses the HKF model to find standard properties, then calculated thermodynamic properties for solution based on concentration of ions. Overall, the final result from GEM step is concentration values of all thermodynamically stable species in the anolyte of the electrolyser at equilibrium condition. Table 3.1 presents inputs parameters and selected ions for GEM.

As stated earlier, due to unavailability of the HCh software was not available at UOIT, the GEM analysis was performed at PSU. Moreover, the results are presented elsewhere by collaboration of the PSU and the UOIT for various $\mathrm{Cu(I)} \rightarrow \mathrm{Cu(II)}$ degree of conversion from 0% to 5% [91].

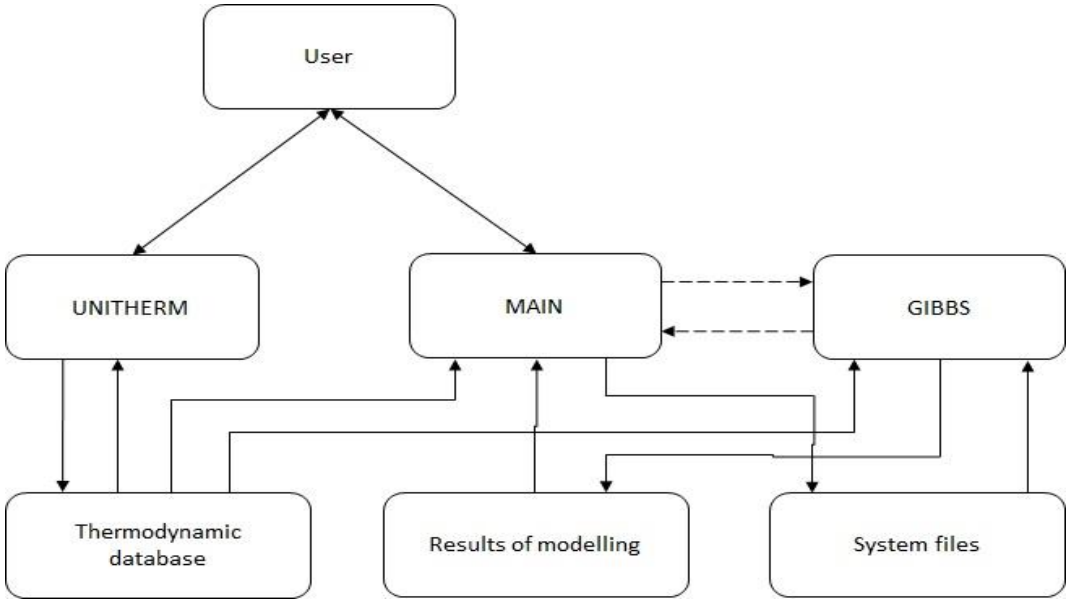

Figure 3.2: Structure of HCh package based on interactions of components; solid-line arrows show information transmission directions, and dashed-line arrows show control transmission (Modified from [89]).

The following assumptions are invoked by PSU to run the GEM analysis:

- Mean activity coefficients are assumed to be the same as a pure HCl(aq) solution.
- As density information for 2 $\mathrm{mol.l^{-1}}$ CuCl(aq) and 10 $\mathrm{mol.l^{-1}}$ HCl(aq) is not available, therefore density of solution is assumed to be $1302\ \mathrm{g.l^{-1}}$ (based on pure HCl(aq) density trends), which is slightly larger than previous studies [59] that were on 2 $\mathrm{mol.l^{-1}}$ CuCl(aq) and 7 $\mathrm{mol.l^{-1}}$ HCl(aq) solution.

Note that the 5% is reported as the maximum conversion degree in experimental studies by PSU [92] which is known as virtual complete conversion degree. Moreover, without doing GEM calculations and investigation equilibrium condition in electrolyte, no electrochemical study is possible to perform. In other words, concentration of species should be a result, not assumption for parametric studies.

Table 3.1: Input parameters and defined species for Gibbs energy minimization of anolyte.

Input parameters	$HCl(aq)$: 10 $mol.l^{-1}$
	$CuCl(aq)$: 2 $mol.l^{-1}$
	Temperature: 25℃
	Pressure: 1 bar
Selected species	$H^+(aq)$
	$Cu^+(aq)$
	$Cu^{2+}(aq)$
	$Cl^-(aq)$
	$HCl^0(aq)$
	$CuCl^0(aq)$
	$CuCl^{2-}(aq)$
	$CuCl_3^{2-}(aq)$
	$CuCl^+(aq)$
	$CuCl_2^0(aq)$
	$CuCl_3^-(aq)$
	$CuCl_4^{2-}(aq)$
	$CuOH^0(aq)$
	$CuOH_2^-(aq)$
	$CuOH^+(aq)$
	$CuO^0(aq)$
	$HCuO_2^-(aq)$
	$CuO_2^{2-}(aq)$
	$HCuCl_2(aq)$
	$Cu_2Cl_3(aq)$

3.3: Standard Thermodynamic Properties

Standard thermodynamic properties of aqueous ions cannot be found in literature for various temperatures and pressures. Standard partial molal thermodynamic properties of aqueous ion species can be predicted for various temperatures and pressures by using HKF equations of states [93]. Helgeson and Kirkham started publishing their results through developing thermodynamic equations of states for electrolyte solutions since 1974 [94], and in 1981 they revised their previous model with cooperation of Flowers [90] into the HKF model. The

general concept of the HKF model is that ions properties are regarded as sum of an intrinsic property and an electrostriction contribution [93]:

$$X_i = X_{intrinsic,i} + \Delta X_{electrostriciton,i} \quad (3.6)$$

Intrinsic properties correspond only to the ion, while electrostriction contributions stem from ion-solvent interactions. The electrostriction contribution is made up of structural collapse and solvation contributions:

$$\Delta X_{electrostriciton,i} = \Delta X_{collapse,i} + \Delta X_{solvation,i} \quad (3.7)$$

And consequently, equations of states are developed for ion's standard thermodynamic properties through a complicated semi-empirical approach [90, 93, 94] that for sake of brevity details are not stated here.

In this study in order to employ the HKF model, the SUCRT92 program [95] is used to carry out calculations of standard specific molar thermodynamic properties (standard Gibbs energy, standard entropy, standard enthalpy) for all anolyte and catholyte species at temperatures between 15℃ and 80℃, pressure of 1bar and concentration of 1 molal. Basically, the SUCRT92 is interaction of three FORTRAN77 programs (SUPCRT92, MPRONS92, CPRONS92) that were developed in 1992 by Johnson et al. [95] to benefit from advances in theoretical geochemistry. The SUPCRT92 makes it possible to determine values of standard thermodynamic properties of wide variety of aqueous species, gases and minerals for elevated temperatures and pressures [95] using data from [81, 82, 96, 97]. Data for $H^+(aq), H_2(g), Cu^+(aq), Cu^{2+}(aq)$, and $Cl^-(aq)$ were already available in the SUCRT92 database, but for the rest of anolyte species the MPRONS92 module of program was used to define new species by importing the HKF parameters and standard values available from [81].

Table 3.2: Standard specific molar thermodynamic properties and HKF model parameters at 25℃.

Ion species	$\overline{\Delta_f g^{\circ}}^{(a)}$	$\overline{\Delta_f h^{\circ}}^{(a)}$	$\bar{s}^{\circ(b)}$	$a_1^{(c)} \times 10$	$a_2^{(s)} \times 10^{-2}$	$a_3^{(d)}$	$a_4^{(e)} \times 10^{-4}$	$c_1^{(b)}$	$c_2^{(e)} \times 10^{-4}$	$\omega^{(a)} \times 10^{-2}$
$Cu^+(aq)$	11950	17132.0	9.70	0.783	-5.868	8.05	-2.53	17.2	-0.24	0.33
$Cu^{2+}(aq)$	15675	15700.0	-23.2	-1.102	-10.47	9.86	-2.34	20.3	-4.39	1.47
$Cl^-(aq)$	-31379	-39933.0	13.5	4.032	4.801	5.56	-2.84	-4.40	-5.71	1.45
$H^+(aq)$	0.0000	0.000000	0.00	0.000	0.000	0.00	0.00	0.00	0.00	0.00
$CuCl_2^0(aq)$	-46142	-64160.0	0.80	5.080	4.626	3.92	-2.97	37.5	8.01	-0.03
$CuCl^0(aq)$	-22608	-26338.0	22.1	4.108	2.253	4.85	-2.87	17.3	0.96	-0.03
$HCl^0(aq)$	-22873	-103805	35.8	9.975	16.57	-0.76	-3.46	4.05	5.04	-0.41
$CuCl^+(aq)$	-16520	-23847.0	-6.50	1.748	-3.510	7.12	-2.63	29.3	2.95	0.64
$CuCl_3^-(aq)$	-75338	-106846	-2.20	9.625	15.72	-0.43	-3.42	63.8	11.7	1.66
$CuCl_3^{2-}(aq)$	-88675	-107537	55.8	13.25	24.57	-3.91	-3.79	63.9	7.90	2.85
$CuCl_4^{2-}(aq)$	-103579	-152534	-18.5	14.67	28.04	-5.27	-3.93	87.5	14.0	3.49

(a) cal.mol^{-1}; (b) cal.mol^{-1}.K^{-1}; (c) cal.mol^{-1}.bar^{-1}; (d) cal.K.mol^{-1}.bar^{-1}; (e) cal.K.mol^{-1}

There are three available speciation models in literature for aqueous CuCl/HCl solution. Developers of these models considered some ions in solution and used the HKF model, compared it to experimental data and determined the HKF parameters for that specific ion. Furthermore, reference [88] is used for $HCl^{\circ}(aq)$. Table 3.2 presents standard specific molar thermodynamic properties and HKF parameters used by SUPCRT92 and imported manually from [81, 88]. Note that the term standard refers to temperature of 25℃, pressure of 1bar and molality of unity. However, properties can be calculated for various temperatures

and pressures for 1 molal of ions and still using standard term for them. Therefore, in this study as different temperatures are studied, standard refers to 1bar and 1 molal.

3.4: Equilibrium Thermodynamics

Conducting the equilibrium thermodynamics is necessary to investigate the ideal performance of system. Decomposition potential of anode and cathode half-cell redox reactions are modelled in this section and then full-cell decomposition potential can be found. Gibbs conversion coefficient is also determined. Parametric study is carried out for different $\mathrm{Cu(I)} \rightarrow \mathrm{Cu(II)}$ conversion degrees and temperatures. The Engineering Equation Solver (EES) program is used to carry out the electrochemical study. Lookup tables are made to import the standard specific molar thermodynamic properties of ions at 15℃ -80℃ obtained from the SUPCRT92.

Initially, half-cell redox reactions should be identified for anode and cathode. In previous studies on CuCl/HCl electrolysis, various probable anode half-reactions are stated which all depend on what concentration of CuCl(aq) and HCl(aq) is used. For instance, for a solution of 1 $\mathrm{mol.l^{-1}}$ of $\mathrm{CuCl(aq)}$ and 6 $\mathrm{mol.l^{-1}}$ of $\mathrm{HCl(aq)}$ the following reactions are reported as possible anodic half-reactions [25]:

$$\mathrm{CuCl_2^-(aq) \longrightarrow CuCl_2^0(aq) + e^-} \quad (3.8)$$

$$\mathrm{CuCl_2^-(aq) + Cl^-(aq) \longrightarrow CuCl_3^-(aq) + e^-} \quad (3.9)$$

$$\mathrm{CuCl_3^{2-}(aq) \longrightarrow CuCl_3^-(aq) + e^-} \quad (3.10)$$

For 0.5 $\mathrm{mol.l^{-1}}$ of $\mathrm{CuCl(aq)}$ and 6 $\mathrm{mol.l^{-1}}$ of $\mathrm{HCl(aq)}$ the following reaction takes place [47]:

$$CuCl_4^{3-}(aq) \rightarrow CuCl^{+}(aq) + 3Cl^{-}(aq) + e^{-} \quad (3.11)$$

And for 2.5 mol CuCl (s) in 8.71 mol. kg^{-1} of HCl(aq) the following half-reaction are reported to be probable at anode [59]:

$$Cu^{+}(aq) \rightarrow Cu^{2+}(aq) + e^{-} \quad (3.12)$$

$$CuCl_3^{2-}(aq) \longrightarrow CuCl_3^{-}(aq) + e^{-} \quad (3.13)$$

$$CuCl_3^{2-}(aq) + Cl^{-}(aq) \longrightarrow CuCl_4^{2-}(aq) + e^{-} \quad (3.14)$$

In this study, based on the structure of an oxidation-reduction reaction and also knowing which species are present at anolyte (Table 3.1), four reactions are considered for equilibrium study as probable anodic half-reactions:

$$Cu^{+}(aq) \longrightarrow Cu^{2+}(aq) + e^{-} \quad (3.15)$$

$$CuCl_3^{2-}(aq) \longrightarrow CuCl_3^{-}(aq) + e^{-} \quad (3.16)$$

$$CuCl^{0}(aq) \longrightarrow CuCl^{+}(aq) + e^{-} \quad (3.17)$$

$$CuCl_3^{2-}(aq) + Cl^{-}(aq) \longrightarrow CuCl_4^{2-}(aq) + e^{-} \quad (3.18)$$

Above stated reactions are mentioned as Reaction1 to Reaction4 all through this text. The cathode half-reaction is hydrogen evolution reaction with invoking this assumption that no copper species are present in catholyte which is not far from reality. In this regard, previous studies show that with high concentration of HCl(aq) around 11 molar at cathode no copper crossover is observed [55]. However, it should be pointed out that concentration of HCl(aq) at cathode does not affect hydrogen evolution reaction [57]. The only effect it has is stopping copper species to migrate into catholyte from anolyte. Hydrogen evolution reaction (HER) is:

$$H^+(aq) + e^- \rightarrow 0.5H_2(g) \quad (3.19)$$

Hydrogen evolution reaction is mentioned as HER in this text. Therefore candidates for full-cell reaction can be written as follows:

$$Cu^+(aq) + H^+(aq) \longrightarrow Cu^{2+}(aq) + 0.5H_2(g) \quad (3.20)$$

$$CuCl_3^{2-}(aq) + H^+(aq) \longrightarrow CuCl_3^-(aq) + 0.5H_2(g) \quad (3.21)$$

$$CuCl_3^{2-}(aq) + H^+(aq) + Cl^-(aq) \longrightarrow CuCl_4^{2-} + 0.5H_2(g) \quad (3.22)$$

$$CuCl^0(aq) + H^+(aq) \longrightarrow CuCl^+(aq) + 0.5H_2(g) \quad (3.23)$$

Note that water electrolysis can also be considered as one of the present reactions in the cell but it's not applicable in this study because the minimum required voltage to generate hydrogen form water electrolysis is around 1.5V [27]. This is already evident that the working voltage for a CuCl/HCl electrolyser is almost half of potential of water electrolysis [45-49]. Therefore, water electrolysis does not occur in CuCl/HCl cell.

3.4.1: Standard Decomposition Potential

There is a corresponding standard decomposition potential (E_D°) for Reaction1-Reaction4 and the HER. This decomposition potential shows which reaction takes place easier by applying external potential in standard molarity with assumption of extra lean electrolyte. Standard decomposition potential can be formulated as follows:

$$E_{D,r}^\circ = -\frac{\overline{\Delta_r g^\circ}}{z_r.F} \quad (3.24)$$

where subscript r designates each reaction and F denotes Faraday constant which is 96485 $C.mol^{-1}$ of electron. z denotes number of electrons in each half-reaction. Actually, $\overline{\Delta_r g^\circ}$

varies by temperature and reveals informative data about probability of a half-reaction. However, concentrations of species have to be implemented into calculations as it arises non-ideality for electrolyte. After getting half-reaction standard decomposition potentials, full-cell standard decomposition potential can be determined as follows:

$$E^{\circ}_{D,cell} = E^{\circ}_{D,cathode} - (-E^{\circ}_{D,anode}) \quad (3.25)$$

3.4.2: Standard Gibbs Conversion Coefficient

Standard Gibbs conversion coefficient is division of overall required energy for reaction by only electrical charge:

$$\varepsilon^{\circ}_{th} = \frac{\overline{\Delta_r h^{\circ}}}{\overline{\Delta_r g^{\circ}}} \quad (3.26)$$

The overall energy required by a redox reaction consists of two parts: electrical demand ($\overline{\Delta_r g^{\circ}}$) and heat demand ($T\overline{\Delta_r s^{\circ}}$):

$$\overline{\Delta_r h^{\circ}} = \overline{\Delta_r g^{\circ}} + T\overline{\Delta_r s^{\circ}} \quad (3.27)$$

The entropy change ($\Delta_r s^{\circ}$) through a reaction can either be negative ($\Delta_r s^{\circ} < 0$) or positive ($\Delta_r s^{\circ} > 0$), which means the reaction is heat-releasing or heat-demanding, respectively. Heat-releasing reactions have Gibbs conversion coefficient of less than 1, while heat-demanding reactions result into Gibbs conversion coefficient of higher than 1.

3.4.3: Decomposition Potential

Decomposition potential of half-cell reactions and also full-cell reaction can be determined through equation 3.28 taking this fact into account that instead of $\overline{\Delta_r g^{\circ}}$, $\overline{\Delta_r g}$ should be used, which means that non-idealities within electrolyte have to be considered. By non-ideality I

mean ion-ion interactions in a concentrated electrolyte. The ideal electrolyte is dilute. Overall, in order to bring non-idealities into consideration, Debye-Hückel theory is used, which helps to determine the thermodynamic properties of species from their corresponding standard thermodynamic properties. Standard thermodynamic properties are only appropriate for dilute electrolytes. The following sequential equations show how to determine decomposing potential:

$$E_{D,r} = -\frac{\overline{\Delta_r g}}{z_r.F} \tag{3.28}$$

$$\overline{\Delta_r g} = \overline{\Delta_r g^{\circ}} + RT \ln\left(\frac{\prod a_R}{\prod a_P}\right) \tag{3.29}$$

where subscripts R and P refer to all ions in reactant and product side, respectively.

$$a_i = c_i^{\nu}.\gamma_i^{\nu} \tag{3.30}$$

where a_i is activity of i^{th} ion as product of molar concentration of that ion (c_i) and activity coefficient. Molar concentration is provided from GEM and ν denotes stoichiometric coefficient. $\frac{\prod a_R}{\prod a_P}$ is also known as quotient (Q) of reaction.

$$\ln\gamma_i = -\frac{A_{DH} z_i^2 \sqrt{I_e}}{1+B_{DH}\dot{a}\sqrt{I_e}} \tag{3.31}$$

Here, I_e is the molar scale ionic strength of electrolyte:

$$I_e = 0.5 \sum c_i.z_i^2 \tag{3.32}$$

A_{DH} and B_{DH} are the theoretical constants of Debye-Hückel theory:

$$A_{DH} = A(\theta T^{-3/2}) \tag{3.33}$$

$$B_{DH} = B(\theta T^{-1/2}) \tag{3.34}$$

where θ designates dielectric constant. $A = 1.8248 \times 10^6 \sqrt{\rho/1000}\,(\text{mol}^{-0.5}\text{kg}^{0.5})$; $B = 50.291 \times 10^{10} \sqrt{\rho/1000}\,(\text{mol}^{-0.5}\text{kg}^{0.5})\text{m}^{-1}$. However, A_{DH} and B_{DH} can be calculated using properties of water [80]; $A_{DH} = 1.172(\text{kg.mol}^{-1})^{0.5}$ and $B_{DH} = 0.328(\text{kg.mol}^{-1})^{0.5}$. ȧ denotes common diameter of an aqueous ion is usually chosen somewhere between 3 and 5 Å [80].

Note that the Debye-Hückel theory is developed for ionic strength of below 0.001 molal, which corresponds to a dilute solution [80]. For a highly concentrated electrolyte, researches are ongoing to develop an appropriate theory because the processes of ion association/dissociation and hydration complicate achieving this goal. In this study, third approximation of the Debye-Hückel theory [98] is used:

$$\log\gamma_i = CI_e - \log\left(1 + \frac{\sum c_i}{55.34}\right) - \frac{A_{DH} z_i^2 \sqrt{I_e}}{1 + B_{DH} \dot{a} \sqrt{I_e}} \tag{3.35}$$

where CI_e is empirical-extended parameter for the electrolyte. Parameter C can be found through sets of experiments and calculations that, due to relevance of work in references [55] and [59] to this study, $C = 0.1438$. The second term in equation 3.35 is mole fraction to molarity conversion that 55.34 is numbers of moles of water molecules in one liter of water. For a neutral specie for instance $CuCl^0(aq)$, the third right-hand term of equation 3.35 is zero because charge number is zero. In addition, instead of C, C_s is used which is Setchenow coefficient and is function of temperature, pressure and identity of supporting electrolyte [55]. For temperatures 20℃-30℃ this coefficient is calculated to be 0.21 by Balashov et al. [55], therefore, for neutral species:

$$\log\gamma_i = C_s I_e - \log(1 + \frac{\sum c_i}{55.34}) \quad (3.36)$$

Note that in a multicomponent solution like anolyte of this study, this approximation of Debye-Hückel theory can only be used when one of the electrolytes in dominating [80]. In this study the HCl(aq) is dominating electrolyte in anolyte and catholyte. Finally, the following equation which is the Nernst equation can be obtained to determine decomposition potential for half-cell and full-cell reactions:

$$E_D = E_D^0 + \frac{RT}{z_r.F} \ln\left(\frac{\prod a_R}{\prod a_P}\right) \quad (3.37)$$

In this study full-cell decomposition potential can be calculated through the following equation:

$$E_{D,cell} = E_{D,cathode} - (-E_{D,anode}) \quad (3.38)$$

3.4.4: Gibbs Conversion Coefficient

Same as for standard Gibbs conversion coefficient, the following equation determines the Gibbs conversion coefficient for half-cell and full-cell reactions.

$$\varepsilon_{th} = \frac{\overline{\Delta_r h}}{\overline{\Delta_r g}} \quad (3.39)$$

Previous section showed how to calculate $\Delta_r g$, while the following equation calculates enthalpy of species by taking activity of ions into account:

$$\overline{\Delta_r h} = \overline{\Delta_r h^\circ} - RT^2 \frac{\partial \ln Q}{\partial T} \quad (3.40)$$

where $\frac{\partial \ln Q}{\partial T}$ denotes differential variation of activity of reactant and product species with regard to each other. To obtain this value, $\Delta_r h$ data provided in [59] for 25℃ and 1bar are

used to estimate $\frac{\partial \ln Q}{\partial T}$ of half-cell reactions. Having enthalpy and Gibbs energy data of reactions, entropy through reaction can also be determined:

$$\overline{\Delta_r s} = \frac{\overline{\Delta_r h} - \overline{\Delta_r g}}{T} \tag{3.41}$$

Note that the data in [59] correspond to full-cell reactions, but estimated data used in this study are for half-cell reactions, for sake of simplicity. Table 3.3 presents applied parameters and invoked assumptions for equilibrium thermodynamics analysis.

Table 3.3: The parameters and assumptions are applied for equilibrium thermodynamic analysis.

Parameters	Value	Reference
å (Angstrom)	5	[80]
C	0.1438	[59]
C_s	0.21	[59]
$A_{DH}(kg.mol^{-1})^{0.5}$	1.172	[80]
$B_{DH}(kg.mol^{-1})^{0.5}$	0.328	[80]
$\frac{\partial \ln Q}{\partial T}$ of Reaction1	-0.03393	[59]
$\frac{\partial \ln Q}{\partial T}$ of Reaction2	-0.01008	[59]
$\frac{\partial \ln Q}{\partial T}$ of Reaction3	-0.04270	[59]

3.5: Kinetic Analysis

Kinetic analysis is carried out in this study to develop polarization curves for half-cell and full-cell reactions. In other words, activation and Ohmic overpotentials within the cell are calculated. Then, required potential for running the electrolysis can be determined:

$$E_{cell} = -\left(\left|E_{D,cell}\right| + \left|\eta_{anode}\right| + \left|\eta_{cathode}\right| + \left|\eta_{ohmic}\right|\right) \tag{3.42}$$

Total activation overpotential of a single electrode is contribution of charge transfer overpotential and mass transfer overpotential:

$$\eta_{electrode} = \eta_{et} + \eta_{mt} = \eta_{emt} \tag{3.43}$$

From the other hand for each electrode, there are two reactions: anodic and cathodic. For anode electrode, forward reaction is anodic and backward reaction is cathodic, while for cathode electrode, forward reaction is cathodic and backward reaction is anodic. Net current of an electrode can be shown as follows:

$$i_{electrode} = i_{anodic} + i_{cathodic} \tag{3.44}$$

Since the general format of Butler-Volmer equation is employed to bring diffusion mass transfer into consideration, anodic and cathodic currents of each electrode can be determined as following:

$$i_{anodic} = i_{\circ,electrode} \left[1 - \frac{i_{electrode}}{i_{lim,anodic}}\right] \exp\left\{\frac{(1-\alpha)z_r F \eta_{electrode}}{RT}\right\} \tag{3.45}$$

$$i_{cathodic} = -i_{\circ,electrode} \left[1 - \frac{i_{electrode}}{i_{lim,cathodic}}\right] \exp\left\{\frac{-\alpha z_r F \eta_{electrode}}{RT}\right\} \tag{3.46}$$

where $i_{\circ,electrode}$ is exchange current density of electrode which can be named as dynamic equilibrium current of electrode. Each electrode, depending on the prime redox reaction occurring on it, has a particular limiting current value for forward and backward reactions. α denotes symmetry factor or transfer coefficient of an electrode. Note that for single-step redox reactions like anode half-reactions of this study the symmetry factor and transfer coefficient are the same, while for the hydrogen evolution reaction (HER) which is a double-step reaction, the transfer coefficient is used. For the anode, assuming one-step reaction, exchange current density can be determined as follows [61]:

$$i_{\circ,anode} = F k_{\circ,anode} (c_{ox}^{1-\alpha} c_{red}^{\alpha}) \tag{3.47}$$

where c_{ox} and c_{red} designate molar concentrations of oxidant and reductant of a half-cell reaction on the anode. For instance, considering Reaction1 the oxidant is $Cu^{2+}(aq)$ and the reductant is $Cu^{+}(aq)$. $k_{\circ,anode}$ is the average rate constant of anode half-reaction. For cathode, equation 3.47 cannot be used because there is no data regarding k_0 value of the HER in concentrated acidic solution in the literature. Therefore, $i_{\circ,cathode}$ value available from [61] is directly used. Hall et al. [61] applied the Koutecky-Levich method [99] to use experimental results in order to determine the $i_{\circ,anode}$ and α on a glassy carbon and platinum (Pt) electrode and they then reported the $k_{\circ,anode}$ values resulting from equation 3.47. However, the $i_{\circ,anode}$ is not used directly in this study; the $k_{\circ,anode}$value is applied to obtain the $i_{\circ,anode}$ from equation 3.47. In this way, a parametric study of temperature dependency for exchange current density can be carried out through the temperature dependency of the oxidant and reductant concentrations, and the $k_{\circ,anode}$. The Tafel equation is employed to study the effect of temperature on the transfer coefficient of the anode:

$$k_{\circ,anode} = \Lambda \exp\left(\frac{-\eta_{anode}}{RT}\right) \tag{3.48}$$

where Λ designates a pre-exponential factor which is a constant value. Therefore, if available data for the $k_{\circ,anode}$ from [61] and the η_{anode} resulting from equation 3.45 at 25℃ are used, Λ can be determined. Then, by varying the temperature at constant η_{anode} or by varying the η_{anode} at constant temperature, the behavior of the $k_{\circ,anode}$ can be studied. On the other hand, the oxidant and reductant concentrations vary by temperature. Hall et al. published important kinetic parameters of the Butler-Volmer equation for the CuCl/HCl electrolyser [60, 61]. While their experiments correspond to other values of solution concentrations, in this study a linear approximation is used to apply the effect of the specific anolyte concentrations on the

original data. Due to the importance of these results and applying them in this study, the following points have to be emphasized regarding Hall et al.'s work:

- One-step reaction for anode half-reaction
- Two-step reaction for HER
- Anode electrode is Glassy Carbon (GC)
- Cathode electrode is Platinum (Pt)
- Rotating Disk Electrode is used for both anode and cathode half-cell studies
- Anode kinetic study is conducted for 1, 5, and 10 $\mathrm{mmol.\,kg^{-1}}$ of $\mathrm{CuCl(aq)/CuCl_2(aq)}$ in 8 $\mathrm{mol.\,kg^{-1}}$ of $\mathrm{HCl(aq)}$
- Cathode kinetic study is conducted for 8 $\mathrm{mol.\,kg^{-1}}$ of $\mathrm{HCl(aq)}$

Since the kinetic data is used from [60, 61] the provided results in this study correspond to the above mentioned considerations. A 8 $\mathrm{mol.\,kg^{-1}}$ (7.71 $\mathrm{mol.\,l^{-1}}$) of $\mathrm{HCl(aq)}$ is the commonly used concentration in CuCl/HCl electrolyser studies, but as stated earlier, using a 11 $\mathrm{mol.\,l^{-1}}$ $\mathrm{HCl(aq)}$ solution in the cathode provided better results for stopping copper crossover in the cell. Therefore, for this study, 11 $\mathrm{mol.\,l^{-1}}$ is used at the catholyte. Table 3.4 presents applied kinetic parameters for anode and cathode half-reaction kinetic analyses:

Table 3.4: Applied parameters for kinetic analysis of anode and cathode half-reactions (Data used from [60, 61]).

Parameter	Value	
	Anode	cathode
k_0 ($\mu\mathrm{mol.\,s^{-1}}$)	210	NA
$i_{\circ,\mathrm{electrode}}$ ($\mathrm{A.\,cm^{-2}}$)	387e-3	1.018e-3
A	0.43	2.00
$i_{\mathrm{lim,anodic}}$($\mathrm{A.\,cm^{-2}}$)	1.2	1.0913-3
$i_{\mathrm{lim,cathodic}}$($\mathrm{A.\,cm^{-2}}$)	-1.2	-1.128

The assumption of zero current leakage in the studied cell is invoked, therefore the cathode receives the same amount of current as the anode provides:

$$i_{cathode} = -i_{anode} \tag{3.49}$$

In order to determine the resistance of the proton exchange membrane (PEM) to hydrogen ions transportation, which is named as the Ohmic overpotential of the cell, the same procedure is selected as it is used for a water electrolyser membrane [100, 101]. Overall, Ohmic overpotential is a function of the humidification, thickness and temperature of a membrane which is assumed to be the same as the temperature of the anolyte and catholyte. Considering Figure 3.3, the sequential equations result in cell Ohmic overpotential.

$$\eta_{ohmic} = R_{PEM} \times i_{cell} \tag{3.50}$$

where R_{PEM} denotes Ohmic resistance of PEM. i_{cell} presents the overall cell current:

$$|i_{cell}| = |i_{anode}| \tag{3.51}$$

$$R_{PEM} = \int_0^L \frac{dx}{\sigma[\lambda(x)]} \tag{3.52}$$

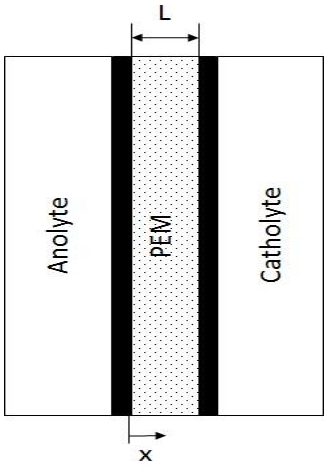

Figure 3.3: Schematic of membrane-electrode assembly for Ohmic overpotential analysis.

where L denotes the thickness of the membrane from the anode-membrane interface to the membrane-cathode interface. Membrane ionic conductivity (σ) can be determined from the empirical expression developed for Nafion 117 PEM [102]:

$$\sigma[\lambda(x)] = [0.5139\,\lambda(x) - 0.326]\exp\left[1268\left(\frac{1}{303} - \frac{1}{T}\right)\right] \quad (3.53)$$

Also, the water content through Nafion 117 PEM can be calculated as follows [103]:

$$\lambda(x) = \frac{\lambda_{anode} - \lambda_{cathode}}{L}x + \lambda_{cathode} \quad (3.54)$$

where the λ_{anode} and $\lambda_{cathode}$ are water content values at the anode-membrane and membrane-cathode interfaces, respectively. Fortunately, Nafion 117 has been investigated as one of the appropriate membrane candidates for the CuCl/HCl electrolyser [56]. Therefore, in this study the developed method can be employed to study Ohmic overpotential. However, as empirical equations are for a water electrolyser, for aqueous electrolytes the same procedure is used by invoking the assumption that ions do not affect the hydration of the membrane. λ is reported to go as high as 22 for a membrane in contact with liquid water at almost 100℃ [102]. Table 3.5 presents used data for this study. The membrane thickness in one of the relevant studies on a CuCl/HCl electrolyser is reported to be 115μm. However, it should be studied as a parametric study value.

Table 3.5: Water content and thickness of membrane.

parameter	Value	Reference
λ_{anode}	14	[103]
$\lambda_{cathode}$	10	[103]
L(μm)	100-150	[55]

3.5.1: Voltage and Current Efficiency

Determination of the voltage and current efficiency values is needed to study the total electrochemical efficiency of the cell. The term electrochemical is used because two more efficiency definitions can also be defined for the cell that are from control volume point of view. Total electrochemical efficiency of cell can be achieved as follows through multiplication of thermodynamic, voltage and current efficiency:

$$\varepsilon_{EC} = \varepsilon_{th} \times \varepsilon_{v} \times \varepsilon_{c} \tag{3.55}$$

$$\varepsilon_{v} = \frac{E_{D,cell}}{E_{Cell}} \tag{3.56}$$

$$\varepsilon_{c} = \frac{\dot{N}_{H_{2,experiment}}}{\dot{N}_{H_{2,theory}}} \tag{3.57}$$

$$\dot{N}_{H_{2,theory}} = \frac{i_{cell}}{z_{HER}F} \tag{3.58}$$

where subscripts v and c denote voltage and current, respectively. Determination of ε_c is only available through an experimental study. Since running an experiment is beyond the scope of this project, the corresponding value of ε_c is obtained from relevant experimental projects on CuCl/HCl electrolyser such as [55]. The value is reported somehow between 95% and 99%. In addition, number of involved electrons in the HER of one mole of hydrogen gas is 2 (z_{HER}). It should be clarified that in electrochemistry studies it's frequent to use the misleading term of thermodynamic efficiency (ε_{th}), while from thermodynamics viewpoint, thermodynamic efficiency can either be energy or exergy efficiency based on first and second laws of thermodynamics, respectively. It's why a new term for ε_{th} as Gibbs conversion coefficient is defined.

3.5.2: Heat Transfer

After conducting equilibrium and kinetic analyses, it has to be determined whether the cell's process, taking into account the full-cell reactions and also overpotentials, is heat-demanding or heat-releasing. Overall, heat transfer equation of cell can be written this way:

$$\dot{Q}_{heat} = Q_{heat} \times \dot{N}_{H_2} \tag{3.59}$$

$$Q_{heat} = (Q_{internal} - Q_{reaction}) \tag{3.60}$$

$$Q_{reaction} = T\,\Delta_r s \tag{3.61}$$

$$Q_{internal} = z_{HER} F(|\eta_{anode}| + |\eta_{cathode}| + |\eta_{ohmic}|) \tag{3.62}$$

where $Q_{reaction}$ as it implies, determines whether the redox reaction to produce hydrogen is heat-releasing or heat-demanding. Thermodynamical explanation of a $Q_{reaction} < 0$ is that the reaction does not need any heat while it releases heat. On the other hand, internal irreversibilities (overpotentials) generate heat (equation 3.62), therefore this adds to the heat generation from reactions, and heat release can be calculated.

For a thermodynamically heat-demanding reaction ($Q_{reaction} > 0$), to see if the cell requires heat or releases heat, the $Q_{internal}$ should be compared to $Q_{reaction}$. If $Q_{internal} \geq Q_{reaction}$ then no external heat is needed and electrolyser can either be known as heat-releasing ($Q_{internal} > Q_{reaction}$) or heat-neutral ($Q_{internal} = Q_{reaction}$). But, If $Q_{internal} < Q_{reaction}$, then consequently Q_{heat} amount of heat should be provided by an external heat source. Figure 3.4 depicts the flowchart which is used in this study to determine whether the cell is heat-demanding or heat-releasing.

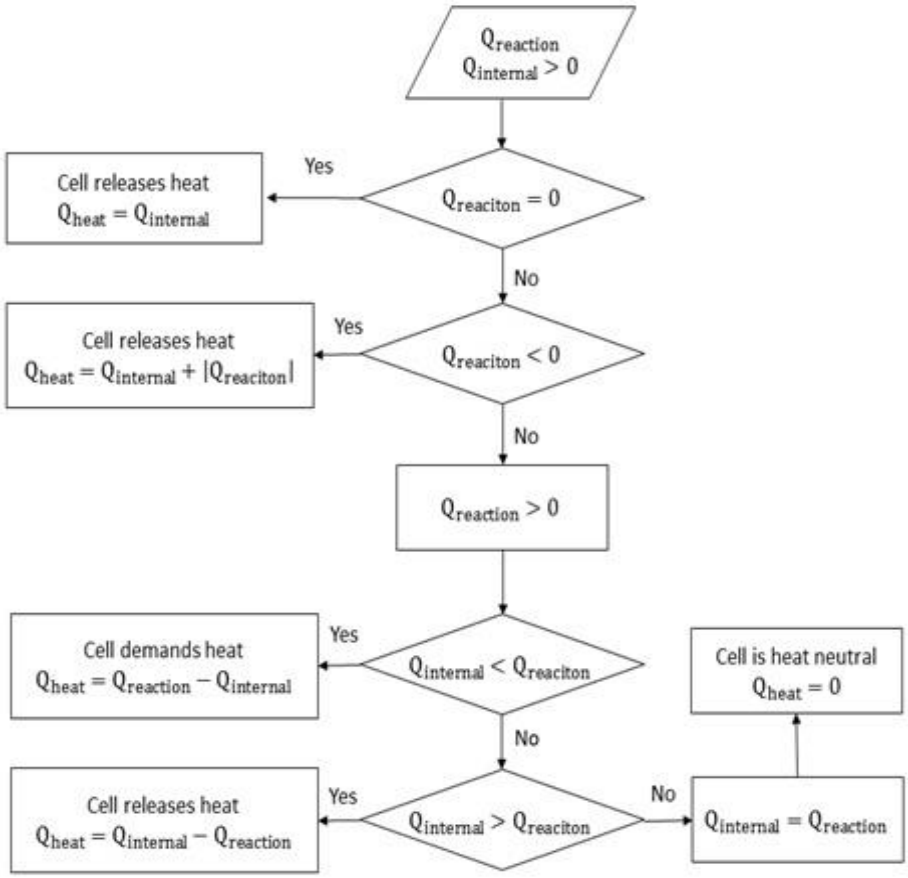

Figure 3.4: Process to determine whether cell is heat-demanding or heat-releasing.

3.6: Energy and Exergy Conversion Coefficients

The target of control volume analysis in this study is to determine energy and exergy conversion coefficients of electrolyser to compare them to electrochemical efficiency. Thereby, both approaches can be discussed and compared. The assumed control volume for the studied cell is depicted in Figure 3.5; inputs and outputs are shown. The only outputs of a Cu-Cl cycle is $H_2(g)$ and $O_2(g)$ while only $H_2(g)$ corresponds to the electrolyser and all other materials are recycled through internal processes. Therefore, the only output of studied control volume is considered $H_2(g)$ and other interactions are electricity and heat.

The following energy and exergy conversion coefficient expressions can be defined for a heat-demanding cell:

$$\mathrm{ECC} = \frac{\mathrm{LHV}_{H_2} \times \dot{N}_{H_2}}{P_{\mathrm{electrical}} + \dot{Q}_{\mathrm{heat}}} \tag{3.63}$$

$$E_x\mathrm{CC} = \frac{\mathrm{Ex}_{H_2} \times \dot{N}_{H_2}}{\dot{E}x_{\mathrm{electrical}} + \dot{E}x_{\mathrm{heat}}} \tag{3.64}$$

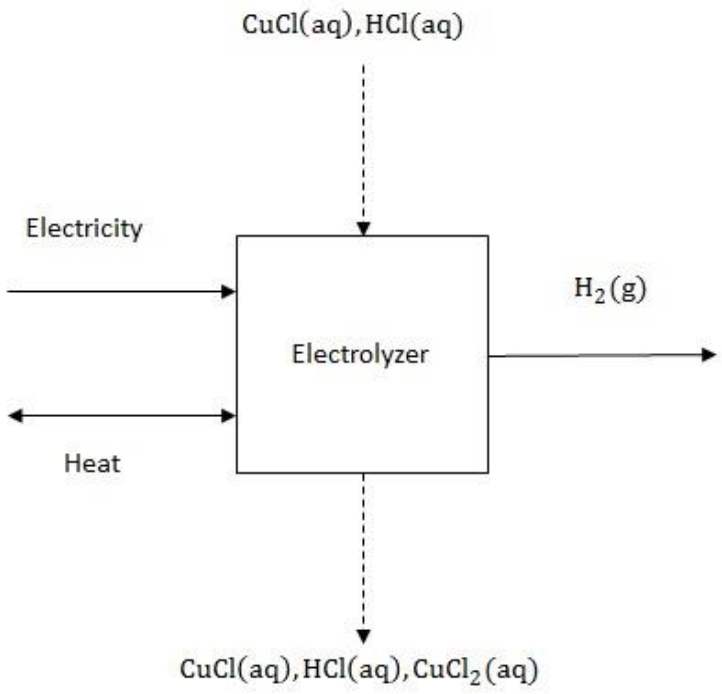

Figure 3.3: Electrolyser control volume for energy and exergy analyses.

And for a heat-releasing cell the energy and exergy conversion coefficient expressions can be written as:

$$\mathrm{ECC} = \frac{\mathrm{LHV}_{H_2} \times \dot{N}_{H_2}}{P_{\mathrm{electrical}}} \tag{3.65}$$

$$E_xCC = \frac{Ex_{H_2} \times \dot{N}_{H_2}}{\dot{E}x_{electrical}} \quad (3.66)$$

However, if applying above equations result value of higher than 100% then conversion coefficient should be used instead of efficiency to name the equation. Note that the amount of heat release from the electrolyser (for a heat-releasing situation) would not be of valuable extent, because the working temperature is low. Due to not possibility of heat recovery from the cell in a heat-releasing mode, the heat interaction term is omitted. Exergy of outlet hydrogen consists of two parts as chemical and physical exergy:

$$Ex_{H_2} = Ex^{ph}{}_{H_2} + Ex^{ch}{}_{H_2} \quad (3.67)$$

where superscripts ph and ch denote physical exergy and chemical exergy, respectively. Physical exergy is calculated as below:

$$Ex^{ph}{}_{H_2} = (h - h_0) - T(s - s_0) \quad (3.68)$$

The product hydrogen is assumed to be at atmospheric temperature and pressure (25℃ and 1bar) which is reference environment condition, therefore, $Ex^{ph}{}_{H_2} = 0$. The molar exergy content of hydrogen gas is used from [104] as 236.09 $kJ.mol^{-1}$ considering atmospheric water as reference state of hydrogen. Adding to this, lower heating value (LHV) of hydrogen is 239.92$kJ.mol^{-1}$. The electrical power (energy) can be determined as follows:

$$P_{electrical} = E_{cell} \times i_{cell} \quad (3.69)$$

And exergy rate of input electricity is exactly the same as energy input rate:

$$\dot{E}x_{electrical} = P_{electrical} \quad (3.70)$$

While heat transfer accompanied exergy input rate is given as follows:

$$\dot{E}x_{heat} = \dot{Q}_{heat} \times \left(1 - \frac{T_0}{T_{source}}\right) \tag{3.71}$$

$$T_0 = T_{cell}$$

where T_0 denotes dead state temperature which can be defined as working temperature of the cell, and T_{source} is temperature of heat source used to provide required heat for cell which should be higher than cell's temperature.

Chapter 4: Results and Discussion

This section is dedicated to presenting results of this study and comparing them with relevant results provided by experimental works conducted on the CuCl/HCl electrolyser, if applicable. First, speciation and equilibrium condition is discussed for anolyte. Then, probability of occurrence for four possible reactions on the anode electrode will be discussed. After, thermodynamic properties of electrochemically active species are presented. The core part is presenting and discussing equilibrium thermodynamics, kinetics, and energy and exergy conversion coefficients analyses results for the anode and cathode half-cell reactions as well as the full-cell reaction.

4.1. Speciation and Gibbs Energy Minimization of Anolyte

Table 4.1 presents Gibbs energy minimization results of this study which was first published by Soltani et.al. [91]. Presented results are equilibrium concentrations of present stable species in the anolyte for various $\mathrm{Cu(I)} \rightarrow \mathrm{Cu(II)}$ conversion degrees. Stated earlier, maximum observed conversion degree in experiments by Hall et al. [60] was reported 5% at 0.7V. Note that concentration amounts of considered oxide and hydroxide species of copper, and also $\mathrm{Cu_2Cl_3(aq)}$, were found nonstable and neglecting them did not change the predicted decomposition potentials [105]. Therefore, those species are omitted from results discussion.

First point of interest is that the concentration of $\mathrm{CuCl_3^{2-}(aq)}$ is significantly higher than other $\mathrm{Cu(I)}$ species. As a result, it can be predicted that this ion will be the dominating redox contributor on the anode as Reaction2. Note that more conversion degree can be achieved by applying more potential between anode and cathode electrodes in reality. As the conversion degree rises, obviously $\mathrm{Cu(II)}$ species increase in concentration dominantly for $\mathrm{CuCl_3^-(aq)}$.

It is observed that concentration of $H^+(aq)$ drops marginally for higher conversion degrees. Figures 4.1-4.3 depict concentration change of three important species using data from Table 4.1. In order to obtain the trend of concentration change by temperature, more conversion degree levels have to be taken into account between 1% and 5% conversion degree. However, 5% conversion degree has been reported as maximum conversion degree available in anode [92], therefore this can satisfy needs of this study as well as no-conversion and small degrees of conversion that are available from Table 4.1. 5% conversion degree is used as working condition for overpotentials analysis in this study.

Table 4.1: Equilibrium concentrations of anolyte species for zero to maximum $Cu(I) \rightarrow Cu(II)$ conversion degrees; results are obtained from GEM by Hch software (Data provided by the PSU).

$Cu(I) \rightarrow Cu(II)$	0.0%	0.01%	0.50%	1.0%	5.0%
$CuCl(aq)\ mol.l^{-1}$	2.0000	1.9998	1.9900	1.9800	1.9000
$CuCl_2(aq)\ mol.l^{-1}$	0.0000	0.0002	0.0098	0.0100	0.0800
$HCl(aq)\ mol.l^{-1}$	10.0000	9.9998	9.9902	9.9900	9.9200
$H^+(aq) mol.l^{-1}$	9.999763	9.999563	9.989963	9.989763	9.91977
$Cu^+(aq)\ mol.l^{-1}$	5.58e-14	5.58e-14	5.58e-14	5.57e-14	5.49e-14
$Cu^{2+}(aq)\ mol.l^{-1}$	2.1e-12	3.19e-9	1.57e-7	1.61e-7	1.33e-6
$Cl^-(aq)\ mol.l^{-1}$	6.000273	6.000098	5.991633	5.98875	5.924741
$HCl^0(aq)\ mol.l^{-1}$	0.000235	0.000235	0.000235	0.000234	0.000231
$CuCl^0(aq)\ mol.l^{-1}$	4.74e-10	4.74e-10	4.73e-10	4.72e-10	4.61e-10
$CuCl^{2-}(aq)\ mol.l^{-1}$	0.000509	0.000509	0.000507	0.000505	0.000489
$CuCl_3^{2-}(aq)\ mol.l^{-1}$	1.99949	1.999291	1.989493	1.979495	1.89951
$CuCl^+(aq)\ mol.l^{-1}$	1.57e-10	2.37e-7	1.17e-5	1.20e-5	9.82e-5
$CuCl_2^0(aq)\ mol.l^{-1}$	5.14e-10	7.80e-7	3.83e-5	3.92e-5	0.000319
$CuCl_3^-(aq)\ mol.l^{-1}$	1.48e-8	2.25e-5	0.001104	0.001127	0.009092
$CuCl_4^{2-}(aq)\ mol.l^{-1}$	1.16e-7	0.000176	0.008646	0.008821	0.07049

As stated earlier, based on defined species and structure of redox reactions, four reactions are predicted to take place on the anode (equations 3.15-3.18). After obtaining equilibrium concentration values via GEM analysis, Reaction2 looks to be the dominating

anodic half-reaction, as concentration of $CuCl_3^{2-}(aq)$ is significantly dominant. However, decomposition potentials of half-reactions have to be calculated to determine the dominant reaction. For instance, it should be investigated which reaction has the lowest or highest decomposition potential. Basically, a reaction with a lower decomposition potential level can take place by applying less voltage compared to a reaction with a higher decomposition potential; in addition to this, another fact to be considered is that for two half-cell reactions with same amount of decomposition potential the one with a higher oxidant concentration dominates the other reaction.

For the catholyte, no speciation and GEM analysis is carried out as the solution is assumed to be only HCl(aq). Therefore, having $11 mol.l^{-1}$ of HCl(aq), concentraiotn of $H^+(aq)$ and $Cl^-(aq)$ are simply assumed to be $11 mol.l^{-1}$.

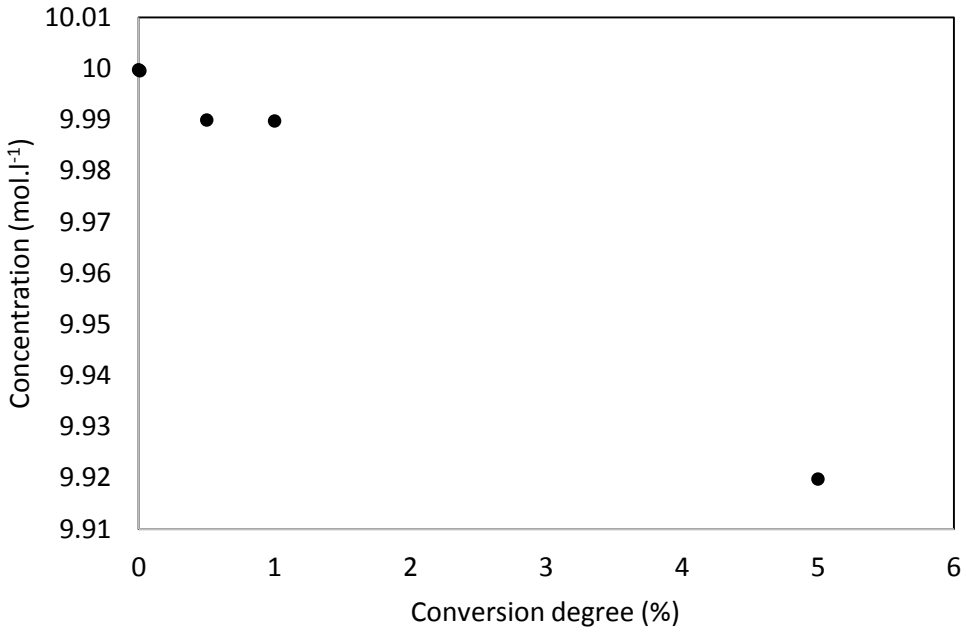

Figure 4.1: Effect of low and high Cu(I) → Cu(II) conversion degree on equilibrium concentration of $H^+(aq)$ in anolyte.

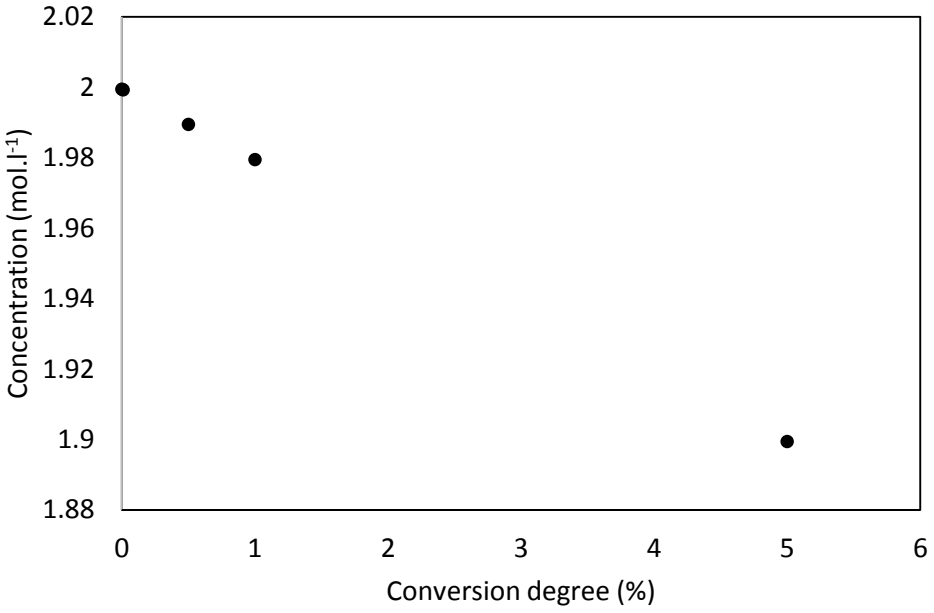

Figure 4.2: Effect of zero to maximum Cu(I) → Cu(II) conversion degree on equilibrium concentration of $CuCl_3^{2-}$(aq) in anolyte.

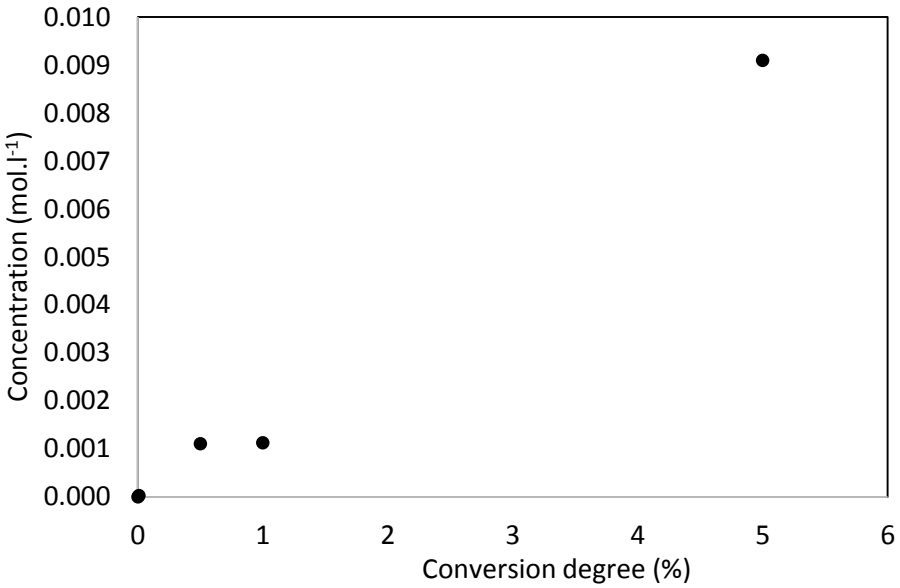

Figure 4.3: Effect of zero to maximum Cu(I) → Cu(II) conversion degree on equilibrium concentration of $CuCl_3^{-}$(aq) in anolyte.

Note that in this project, no parametric study can be done to analyze effect of the inert $CuCl(aq)$ and $HCl(aq)$ on species equilibrium concentration unless through running a comprehensive GEM for various $CuCl(aq)$ and $HCl(aq)$ concentration combinations. Therefore, since no data are available in open literature in this regard, no discussion is provided here.

4.2: Standard Thermodynamic Properties

Standard thermodynamic properties of all present species are extracted from SUPCRT92 database program. Tables 4.2 and 4.3 for instance present corresponding results for the dominant anolyte specie and hydrogen ion, respectively.

Table 4.2: Standard thermodynamic properties of $CuCl_3^{2-}(aq)$ for different temperatures; standard state is temperature of 25℃, pressure of 1bar and concentration of 1 molar.

T (℃)	$\bar{h}^{\circ}$ J. mol^{-1}	$\bar{s}^{\circ}$ J. mol^{-1}. K^{-1}	$\bar{g}^{\circ}$ J. mol^{-1}
15	-446324.016	246.019	-368622.952
20	-448202.632	239.325	-369832.128
25	-449934.808	233.467	-371016.200
30	-451558.200	228.028	-372170.984
35	-453089.544	223.007	-373296.480
40	-454558.128	218.405	-374401.056
45	-455972.320	213.802	-375480.528
50	-457344.672	209.618	-376539.080
55	-458683.552	205.434	-377576.712
60	-459997.328	201.669	-378597.608
65	-461298.552	197.485	-379593.400
70	-462583.040	193.719	-380572.456
75	-463863.344	190.372	-381534.776
80	-465139.464	186.606	-382476.176

Since standard properties are defined for 1 molar of each of species, any change on concentrations of species for instance using different concentration combinations of $CuCl(aq)$ and $HCl(aq)$ or concentration changes of species through reactions, do not affect the standard properties and standard decomposition potentials, correspondingly.

Table 4.3: Standard thermodynamic properties of $H^+(aq)$ for different temperatures; standard state is temperature of 25℃, pressure of 1bar and concentration of 1 molar.

T (℃)	$\bar{h}^\circ$ J. mol^{-1}	$\bar{s}^\circ$ J. mol^{-1}. K^{-1}	$\bar{g}^\circ$ J. mol^{-1}
15	-288.696	129.704	1301.224
20	-142.256	130.122	652.704
25	0.000	130.541	0.000
30	142.256	130.959	-652.704
35	288.696	131.796	-1309.592
40	430.952	132.214	-1970.664
45	577.392	132.633	-2631.736
50	719.648	133.051	-3296.992
55	866.088	133.470	-3962.248
60	1008.344	133.888	-4631.688
65	1150.600	134.306	-5301.128
70	1297.040	134.725	-5974.752
75	1439.296	135.143	-6648.376
80	1585.736	135.562	-7326.184

4.3: Standard Decomposition Potential

For anode and cathode half-reactions, Table 4.4 shows difference of standard properties of involved electrochemical active species through each half-reaction. It can be seen that standard properties do not change as conversion degree rises, which could be predicted even before running the analysis because standard properties of ions do not relate to activity. Standard decomposition potentials of four predicted anode half-reactions are calculated and

shown by Figure 4.4. The negative sign denotes this fact that the anode half-reaction is not spontaneous.

Table 4.4: Standard thermodynamic properties change through anode and cathode half-reactions for various conversion degrees; standard state is temperature of 25℃, pressure of 1bar and concentration of 1 molar.

Reaction #	$\overline{\Delta g^0}$ J. mol^{-1}	$\overline{\Delta h^0}$ J. mol^{-1}	$\overline{\Delta s^0}$ J. mol^{-1}
0% Conversion			
Reaction1	15585	-5991	-137.700
Reaction2	55802	2891	-242.700
Reaction3	112315	106014	-34.73
Reaction4	68931	-21188	-367.800
HER	0	0	65.27
1% Conversion			
Reaction1	15585	-5991	-137.700
Reaction2	55802	2891	-242.700
Reaction3	112315	106014	-34.73
Reaction4	68931	-21188	-367.800
HER	0	0	65.27
5% Conversion			
Reaction1	15585	-5991	-137.700
Reaction2	55802	2891	-242.700
Reaction3	112315	106014	-34.73
Reaction4	68931	-21188	-367.800
HER	0	0	65.27

Standard decomposition potential of anode half-reactions are calculated. Reaction1 and Reaction3 have the lowest (-0.16V) and the highest (-1.16V) standard decomposition potentials, respectively at 25℃ (Figure 4.4). No doubt, -1.16V is out of range. Therefore, to check if Reaction3 occurs or not, activities are taken into account and decomposition potential at 25℃ is found out of range (-1.10V) as well for Reaction3. In this regard, GEM results (Table 4.1) show that the concentration of $CuCl^0(aq)$ does not change by increasing the conversion degree while the concentration of $CuCl^+(aq)$ rises dramatically to maintain equilibrium. Therefore, it is concluded that oxidation of $CuCl^0(aq)$ is not possible for the

range of voltage needed for a $CuCl/HCl$ electrolysis and should not be considered as a probable anode half-reaction. Note that up to this point I took Reaction3 into account due to the fact that oxidation of $CuCl^0(aq)$ to $CuCl^+(aq)$ looks viable at first glance. Increase in concentration of $CuCl^+(aq)$ can be explained by presence of other mechanisms which are minor and do not affect this study as $CuCl_3^{2-}(aq)$ is the dominating specie for oxidation.

At hypothetical equilibrium condition with a dilute electrolyte, as voltage application starts, first reaction to trigger is Reaction1 then Reaction2 and then Reaction4 up to potential of around 0.8V. In addition, higher temperature of cell results into more potential to maintain equilibrium. At standard state Table 4.4 shows that all anode half-reactions are heat-releasing and non-spontaneous, while the HER is heat-demanding and spontaneous. Standard heat demand of HER is almost one fourth of heat release of Reaction2.

Hydrogen evolution reaction is found to be a spontaneous reaction and heat-demanding in standard situations. It is only at temperatures below room temperature that the HER is not spontaneous. As temperature rises, the standard equilibrium potential of the HER increases. Using equation 3.25, standard decomposition potential of the cell can be determined, and Figure 4.6 reports this value between -0.56V and -0.65V at different temperatures. As it can be seen temperature increases the potential demand of electrolyser at standard condition.

4.4: Standard Gibbs Conversion Coefficient

Following equations 3.26 and 3.27, the Reaction1 is observed to have negative Gibbs conversion coefficient which stems from the fact that the reaction is heat-releasing and non-spontaneous. For this condition, if heat release amount is higher than potential requirement, negative efficiency appears (Figure 4.7).

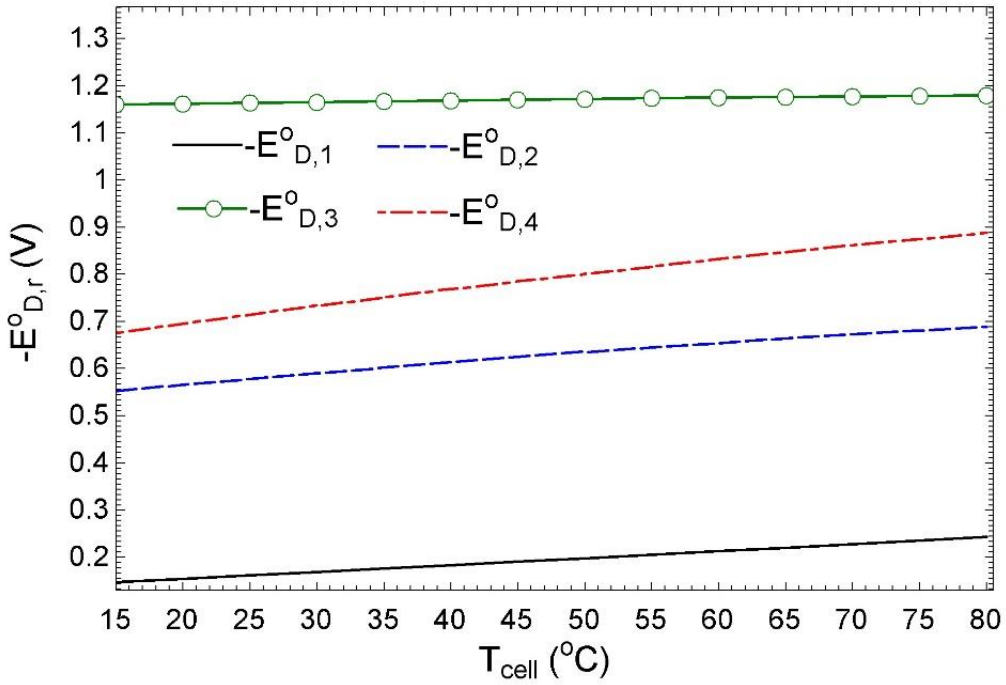

Figure 4.4: Standard decomposition potential of anode half-reactions; standard state is temperature of 25℃, pressure of 1bar and concentration of 1 molar.

Reaction2 leads to standard Gibbs conversion coefficient of zero at around 20℃ (Figure 4.8), due to same amount of required Gibbs energy to run the reaction and amount of heat release. This means that no electron release is possible from the corresponding redox reaction and whatever electricity is applied turns to heat-release. In addition, the standard Gibbs conversion coefficient of negative results same conclusion that electron release is not possible in that standard state for a redox reaction. Therefore, it can be deduced that standard electrochemical analysis does not provide enough results for this study. Temperature rise is found to enhance standard Gibbs conversion coefficient of Reaction2 and one can conclude that, in standard situation at higher temperatures, heat release level drops (which will be studied later to validate this conclusion).

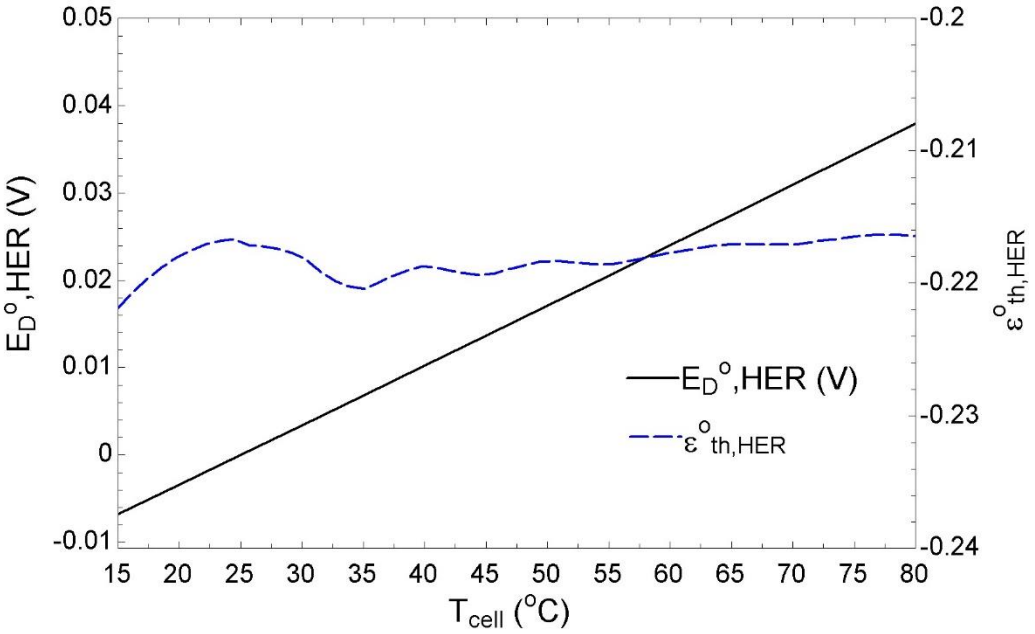

Figure 4.5: Hydrogen evolution standard decomposition potential and standard Gibbs energy conversion coefficient; standard state is temperature of 25℃, pressure of 1bar and concentration of 1 molar.

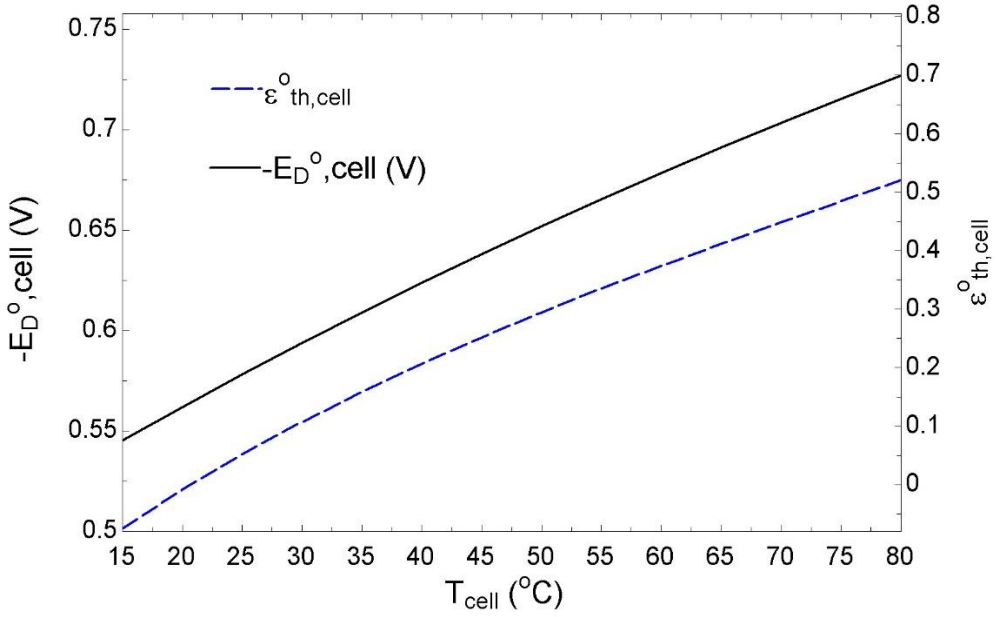

Figure 4.6: Full-cell standard decomposition potential and standard Gibbs conversion coefficient; standard state is temperature of 25℃, pressure of 1bar and concentration of 1 molar.

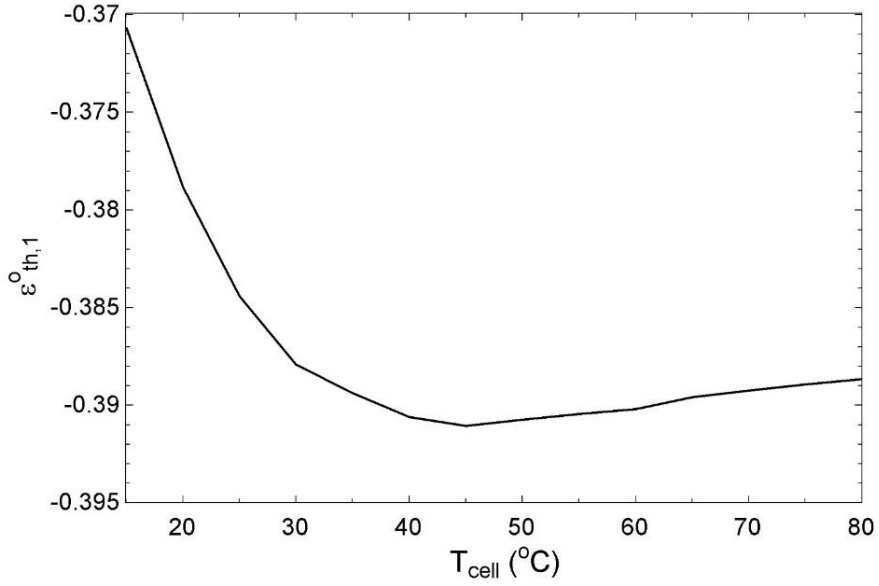

Figure 4.7: Standard Gibbs conversion coefficient of Reaction1; standard state is temperature of 25℃, pressure of 1bar and concentration of 1 molar.

Figure 4.9 presents results of standard Gibbs conversion coefficient of Reaction4. it can be seen that after around 65℃ Reaction4 will demand heat and results positive Gibbs conversion coefficient, while below 65℃ reaction is heat-releasing and results negative efficiency. Negative standard Gibbs conversion coefficient might look incorrect but results of this study are validated by other similar reports in literature such as [59]. Where it is reported that Reaction1 and Reaction4 at 25℃ for certain levels of concentrations are heat-releasing with negative standard Gibbs conversion coefficient, while Reaction2 is reported in other studies to be heat-demanding reaction with positive efficiency. In this study Reaction2 in standard situation is heat-releasing with positive Gibbs conversion coefficient.

The HER is a spontaneous and heat-demanding reaction with negative standard Gibbs conversion coefficient (Figure 4.5).

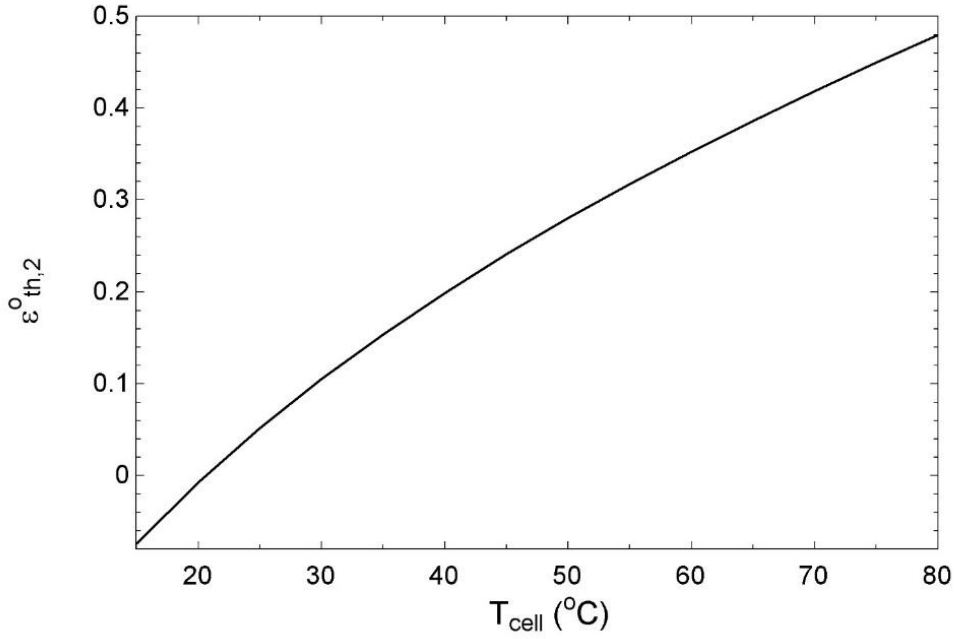

Figure 4.8: Standard Gibbs conversion coefficient of Reaction2; standard state is temperature of 25℃, pressure of 1bar and concentration of 1 molar.

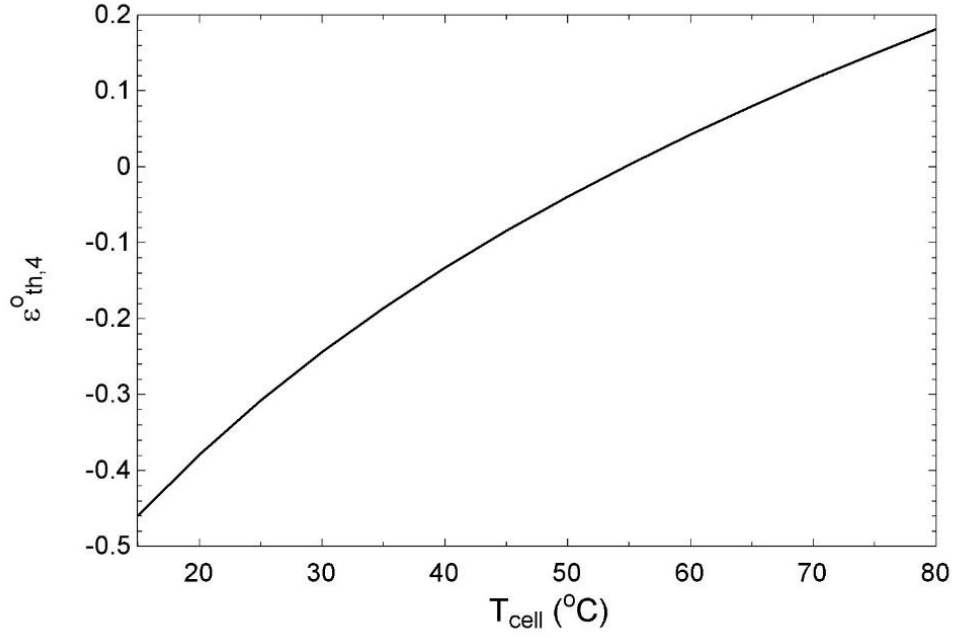

Figure 4.9: Standard Gibbs conversion coefficient of Reaction4; standard state is temperature of 25℃, pressure of 1bar and concentration of 1 molar.

Temperature rise results into decreases of magnitude of standard Gibbs conversion coefficient of the HER. There is no similar data reported in the literature regarding a hydrogen evolution reaction in a concentrated acid solution to compare the results; however, as standard thermodynamic properties are calculated correctly, and standard situation has certain definition, results should be valid.

Figure 4.6 shows the overall standard Gibbs conversion coefficient of cell, which is less than 1 considering Reaction2 as the main anode half-reaction. Hall et al. [61] reported this value to be 5% for their study at 25℃ and certain concentrations, which is almost the same as results of this study for full-cell (Figure 4.6). The temperature rise enhances the standard Gibbs conversion coefficient.

4.5: Decomposition Potential and Gibbs conversion coefficient

Table 4.5 presents results on thermodynamic properties change through half-reactions. Here, unlike the previous section, which was about standard thermodynamic analysis, activities of ions are taken into considerations. Conversion degrees affect thermodynamic properties changes. Therefore, this will be part of the focus in this section to study effects of conversion degrees.

All three thermodynamic properties change of the anode half-reactions are found to be almost the same value, which was first reported by Hall et al. [61] for their studies and validates correct calculation of activity of ions in this study. It means that all three probable anode half-reactions require same amount of potential for their equilibrium. Only Reaction1 doesn't obey this trend for entropy, which would be explained by this observation from the Table 4.1 that $Cu^{2+}(aq)$ is not generated by oxidation of $Cu^{+}(aq)$. As it can be seen,

concentration of $Cu^{+}(aq)$ doesn't change while concentration of $Cu^{2+}(aq)$ increases which would lead to this conclusion that there is another mechanism to generate $Cu^{2+}(aq)$ other than oxidation of $Cu^{+}(aq)$ on the anode surface at low conversion degrees. At 1% and 5% conversion it can be seen that (Table 4.1) $Cu^{2+}(aq)$ is produced at anode by $Cu^{+}(aq)$ and from Table 4.5 it is obvious that thermodynamic properties of Reaction1 gets close to Reaction2 and Reaction4 but not the same. In other words, as potential is hypothetically started to be applied to the anode, all three possible half-reactions trigger but only one of them is dominant, which is Reaction2 due to having the dominant concentrations of active ions. Table 4.5 also reports that anode half-reactions are not spontaneous at 25℃ for studied concentrations while the HER is spontaneous.

Table 4.3: Thermodynamic properties change through half-reactions for various conversion degrees; starting anolyte solution is 2 $mol.l^{-1}$ CuCl(aq) in 10 $mol.l^{-1}$ HCl(aq) and starting catholyte solution is 11 $mol.l^{-1}$ HCl(aq).

Reaction #	$\overline{\Delta g}$ $J.mol^{-1}$	$\overline{\Delta h}$ $J.mol^{-1}$	$\overline{\Delta s}$ $J.mol^{-1}.K^{-1}$
0% Conversion			
Reaction1	16826	19086	7.579
Reaction2	17150	10340	-22.840
Reaction4	16997	10369	-22.230
HER	-11327	0	37.99
1% Conversion			
Reaction1	44605	19086	-85.590
Reaction2	45024	10340	-116.300
Reaction4	44913	10369	-115.900
HER	-11327	0	37.99
5% Conversion			
Reaction1	50040	19086	-103.800
Reaction2	50254	10340	-133.900
Reaction4	50269	10369	-133.800
HER	-11327	0	37.99

Figures 4.13 to 4.17 depict the fact that as conversion degree rises, a higher consequent decomposition potential is required. While Figure 4.15 shows that as reactions start to trigger, decomposition potential requirements rise rapidly and then increases steadily. At 25℃ all probable half-reactions require similar decomposition potential (Figure 4.10-5.18) that are -0.17V at no-conversion mode, -0.46V at 1% conversion, and -0.51V at 5% conversion degree. Naturally, in reality to obtain higher conversion degrees, more voltage is required to be applied. These obtained values are just that amount which is required to maintain the equilibrium and is a hypothetical ideal situation. Accordingly, this can be a basis to conclude that at 25℃ higher than -0.51V should be applied due to presence of series of overpotentials involved with redox reaction. The general observation is increasing in magnitude of both E_D^0 and E_D by rising temperature almost linearly. From Figures 4.13 to 4.17, it is obvious that as temperature elevates from 25℃, potentials vary with regard to each other and they don't stand close anymore. This observation can be explained by the applied assumption which is neglecting the effect of temperature on equilibrium concentrations of species. However, the trend is realistic. This conclusion can literally be validated by results presented by Balashov et al. [55] that in a higher temperature, the conversion of $Cu(I) \rightarrow Cu(II)$ drops for the same applied potential. In other words, at a higher temperature for maintaining a same level of conversion degree, a higher decomposition potential is required.

Figures 4.19-4.21 depict temperature dependency of Gibbs conversion coefficient of anode half-reactions for various conversion degrees. It is shown that at no-conversion, at an elevated temperature Reaction2 and Reaction4 are heat-demanding while Reaction1 shows completely an opposite trend. Since the thermodynamic data are calculated properly and validated by other studies, observations can be accepted as behavior of species. For a higher

conversion degree, the main anode half-reaction (Reaction2) releases heat. Reaction2 has Gibbs conversion coefficient of less than 1. As temperature rises, the amount of heat release from the anode half-reaction decreases. This results into a higher electrochemical thermodynamic efficiency.

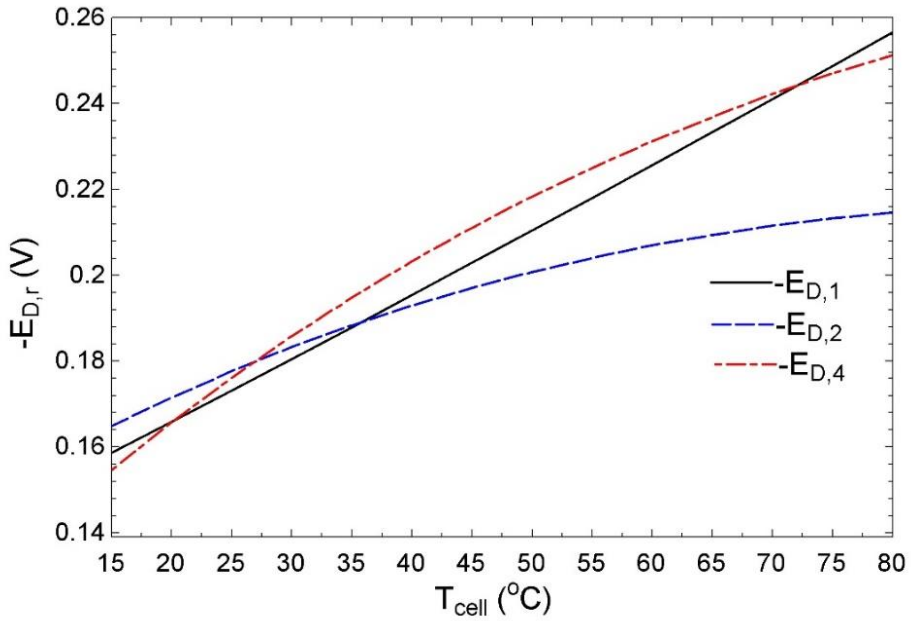

Figure 4.10: Decomposition potential of anode half-reactions at no-conversion; starting anolyte solution is 2 $\mathrm{mol.l^{-1}}$ CuCl(aq) in 10 $\mathrm{mol.l^{-1}}$ HCl(aq).

In order to obtain better results regarding temperature dependency of the anode half-reaction (Reaction2), and correspondingly the full-cell reaction, reported results from Hall et al. [59] are applied to determine concentration change of active species of Reaction2 by temperature around room temperature.

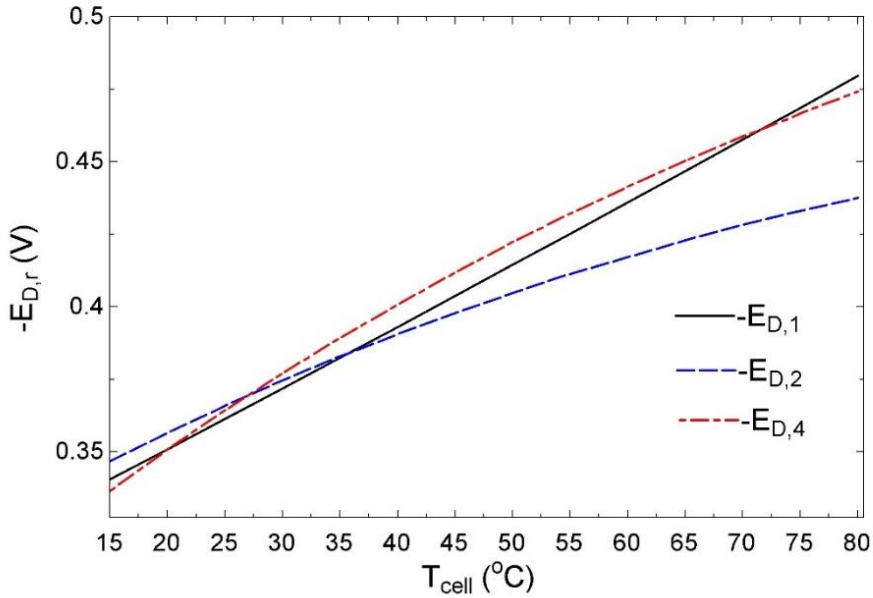

Figure 4.11: Decomposition potential of anode half-reactions at 0.01% conversion; starting anolyte solution is 2 $\mathrm{mol.l^{-1}}$ CuCl(aq) in 10 $\mathrm{mol.l^{-1}}$ HCl(aq).

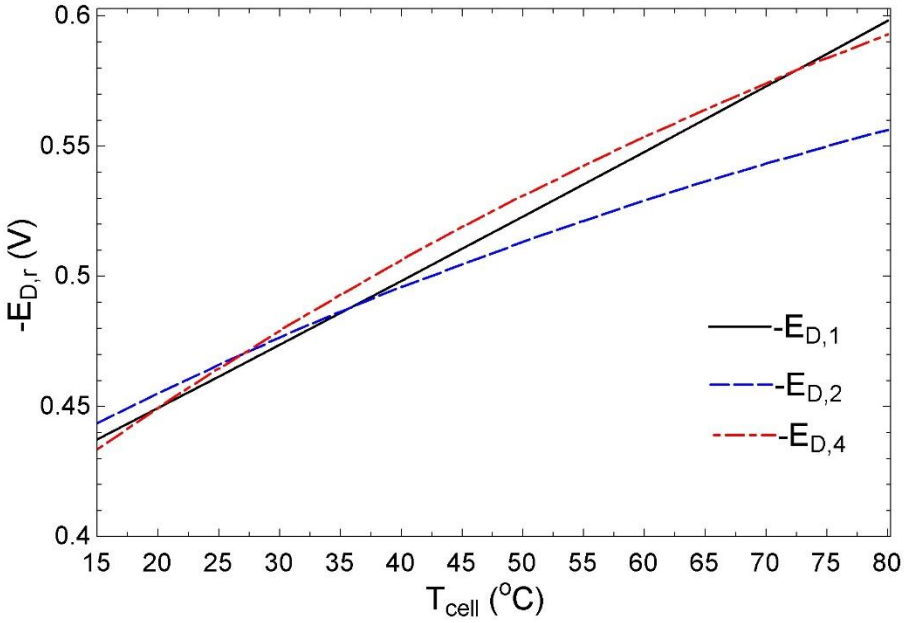

Figure 4.12: Decomposition potential of anode half-reactions at 0.5% conversion; starting anolyte solution is 2 $\mathrm{mol.l^{-1}}$ CuCl(aq) in 10 $\mathrm{mol.l^{-1}}$ HCl(aq).

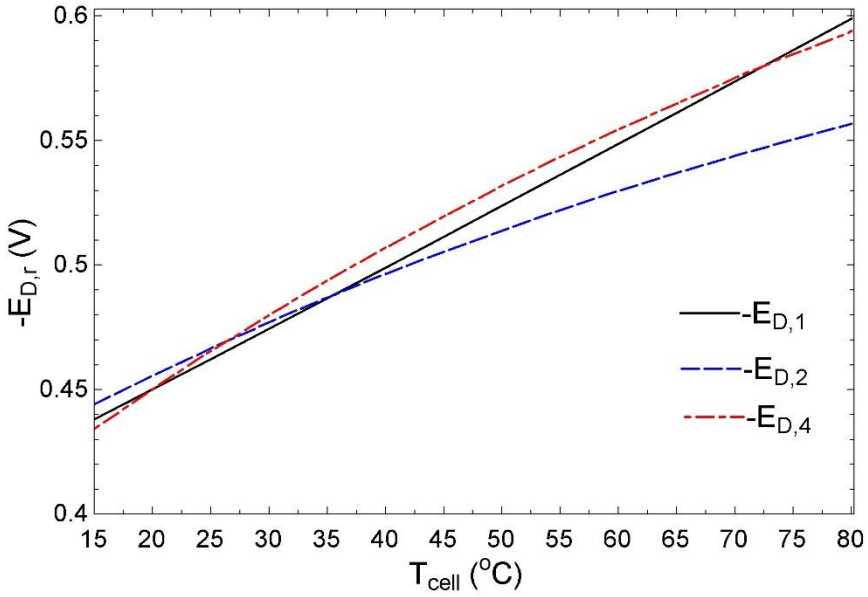

Figure 4.13: Decomposition potential of anode half-reactions at 1% conversion; starting anolyte solution is 2 $\mathrm{mol.l^{-1}}$ CuCl(aq) in 10 $\mathrm{mol.l^{-1}}$ HCl(aq).

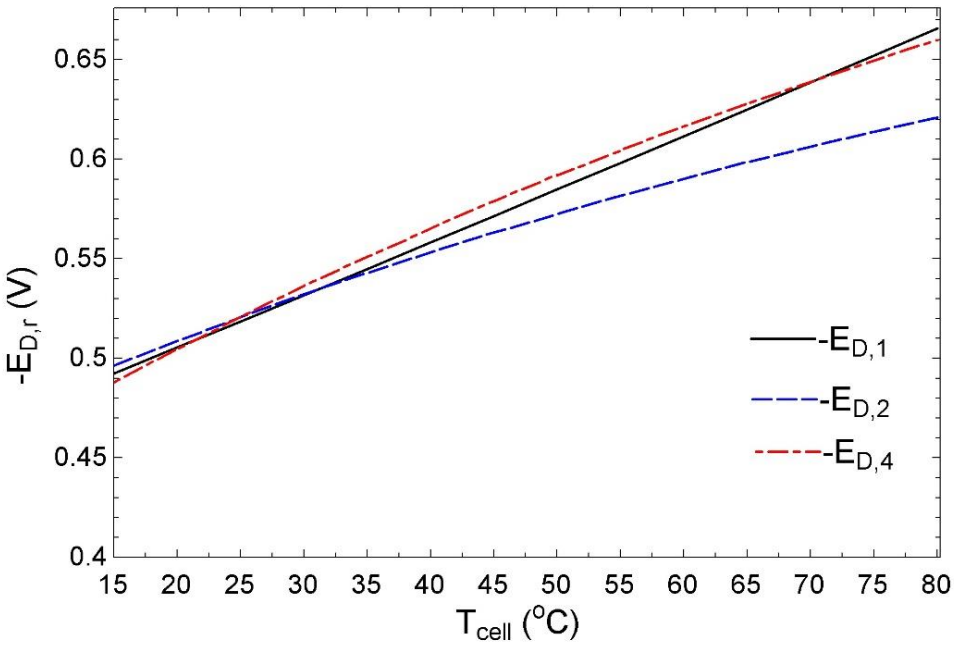

Figure 4.14: Decomposition potential of anode half-reactions at 5% conversion; starting anolyte solution is 2 $\mathrm{mol.l^{-1}}$ CuCl(aq) in 10 $\mathrm{mol.l^{-1}}$ HCl(aq).

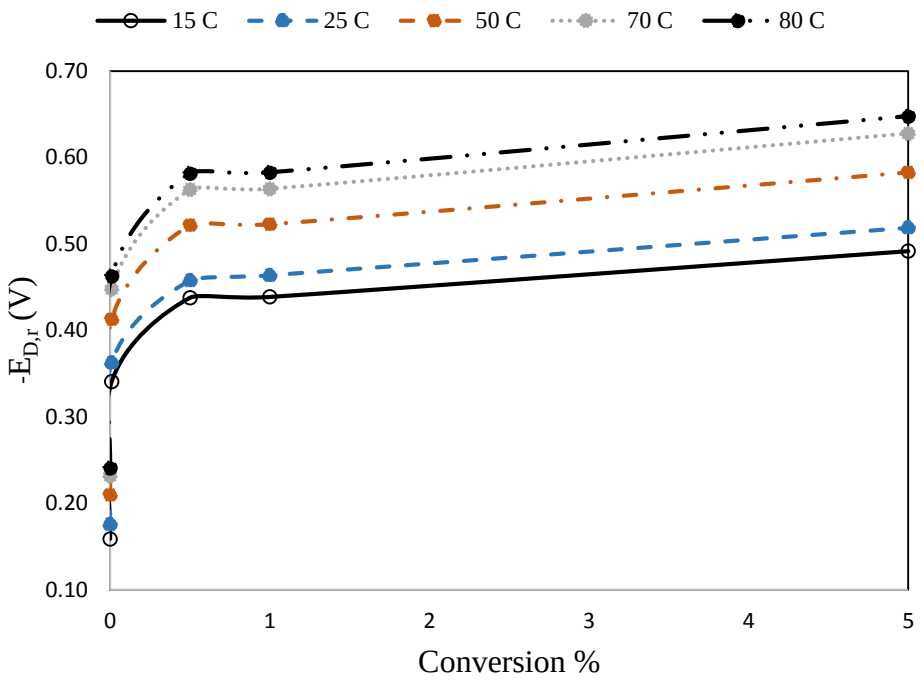

Figure 4.15: Effect of conversion degree on decomposition potential of anode half-reactions for different temperatures; starting anolyte solution is 2 $mol.l^{-1}$ CuCl(aq) in 10 $mol.l^{-1}$ HCl(aq).

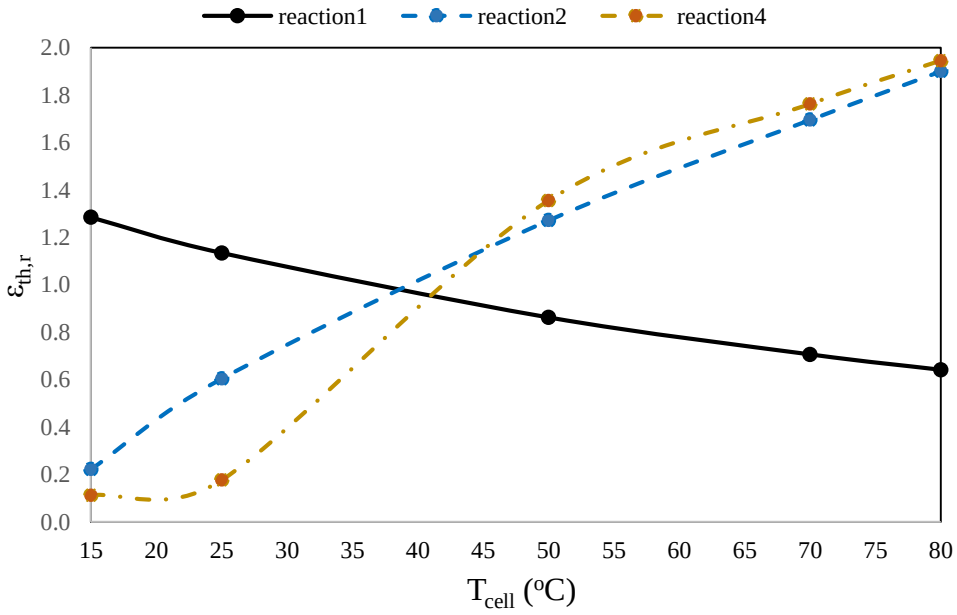

Figure 4.16: Effect of temperature on Gibbs conversion coefficient of anode half-reactions at no-conversion; starting anolyte solution is 2 $mol.l^{-1}$ CuCl(aq) in 10 $mol.l^{-1}$ HCl(aq).

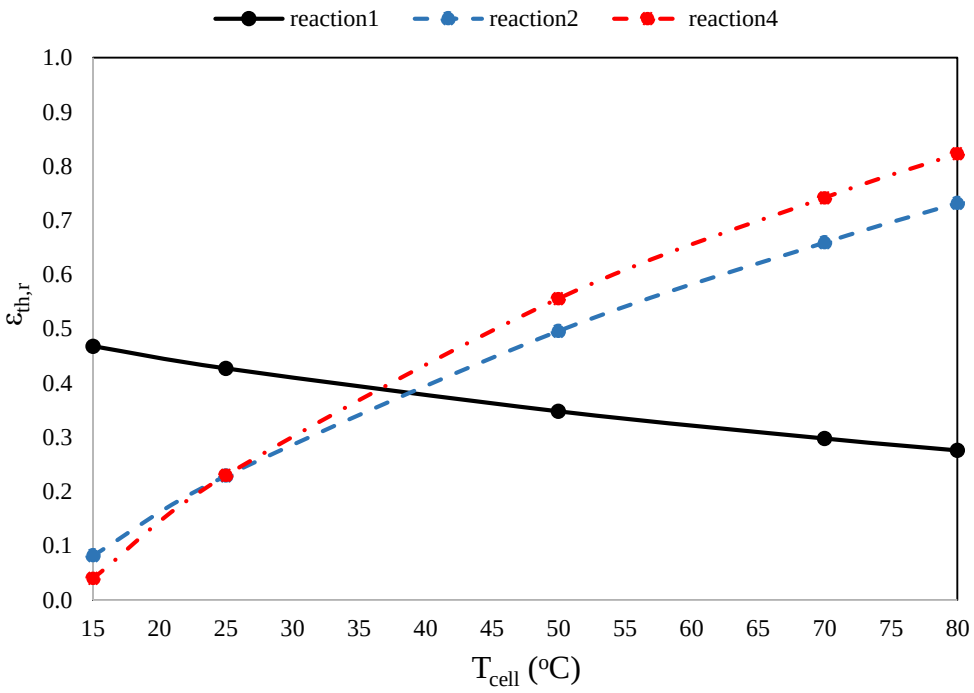

Figure 4.17: Effect of temperature on Gibbs conversion coefficient of anode half-reactions at 1% conversion; starting anolyte solution is 2 mol.l^{-1} CuCl(aq) in 10 mol.l^{-1} HCl(aq).

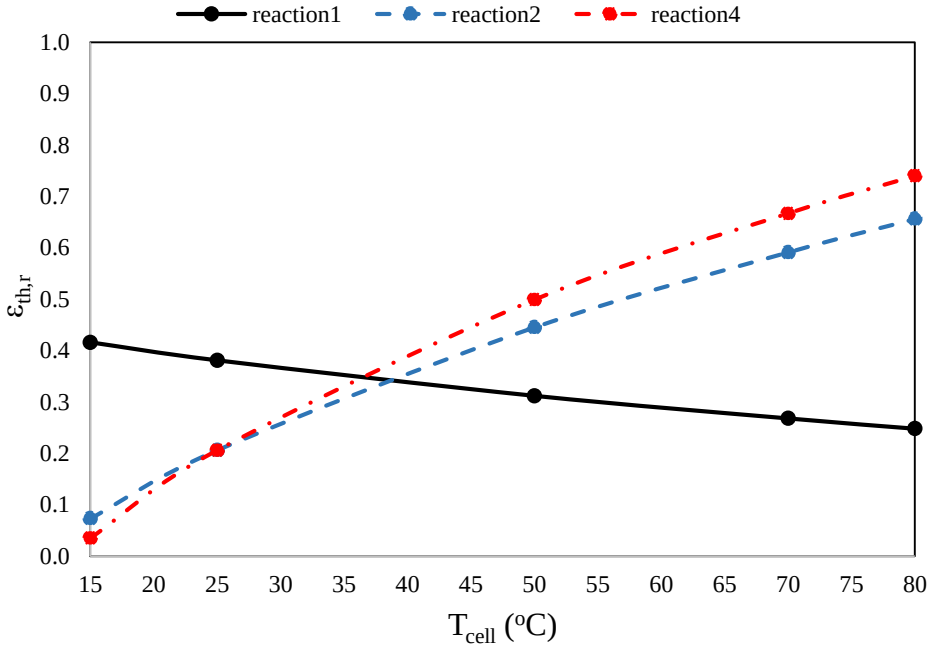

Figure 4.18: Effect of temperature on Gibbs conversion coefficient of anode half-reactions at 5% conversion; starting anolyte solution is 2 mol.l^{-1} CuCl(aq) in 10 mol.l^{-1} HCl(aq).

Figure 4.19 shows that taking concentration variation by temperature into account does not change the overall fact observed from Figure 4.14 (Decomposition potential rises by temperature). This only provides a more precise trend for impact of temperature on decomposition potential. Blue dots in Figures 4.22-4.26 show valid results based on data obtained from [59], while solid black lines show how the trend could be predicted for higher temperatures.

Investigating the playing parameters of presented result in Figure 4.19, effects of temperature on ionic strength of anolyte, activity, and activity coefficient of dominant anode active species (Figures 4.23-4.26) are studied.

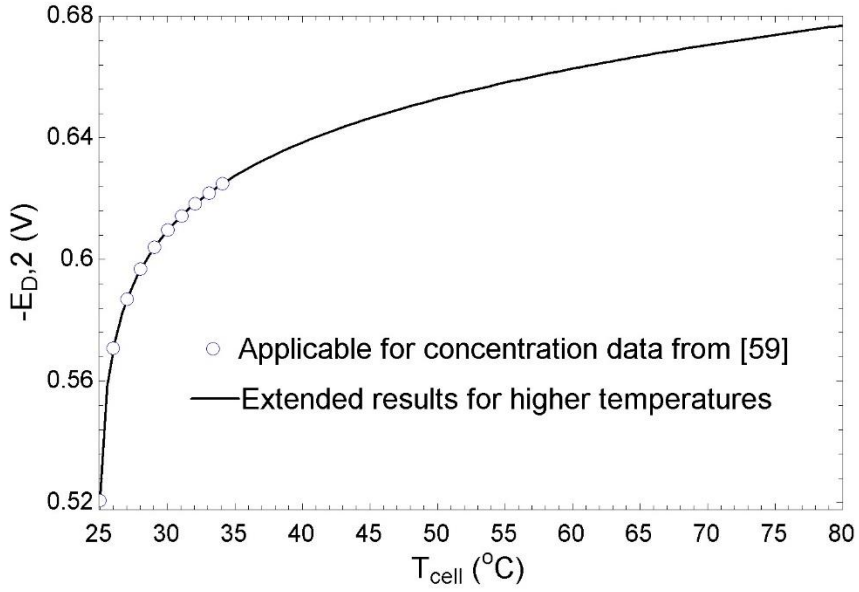

Figure 4.19: Temperature dependency of dominant anode half-reaction considering effect of temperature on ions concentrations; Blue dots are obtained based on concentration data from [59] for temperatures around 25℃; Solid black line is extended results for higher temperatures using linear trend of concentration change by temperature data provided by [59]; this is a non-standard state and activity coefficient of anolyte species are applied in calculations to obtain results.

Figure 4.20 shows that ionic strength of anolyte solution rises linearly by temperature. In addition, value of ionic strength of anolyte is found to be considerably high, which is a fact for a concentrated multicomponent electrolyte. Moreover, both activity values of $CuCl_3^{2-}(aq)$ and $CuCl_3^{1-}(aq)$ increase by temperature rise. For $CuCl_3^{2-}(aq)$ this increase is under the dominance of effect of the activity coefficient, while molarity of the ion decreases by temperature. Accordingly, for $CuCl_3^{1-}(aq)$ both molarity and activity coefficient of ion rise by temperature. Activity of $CuCl_3^{1-}(aq)$ is observed to be significantly higher than activity of $CuCl_3^{2-}(aq)$, which stems from a high activity coefficient. From the equation 3.35, one can notice this is the effect of charges of ions, as $CuCl_3^{2-}(aq)$ and $CuCl_3^{1-}(aq)$ have one electron difference resulting into the huge difference between corresponding activities of ions.

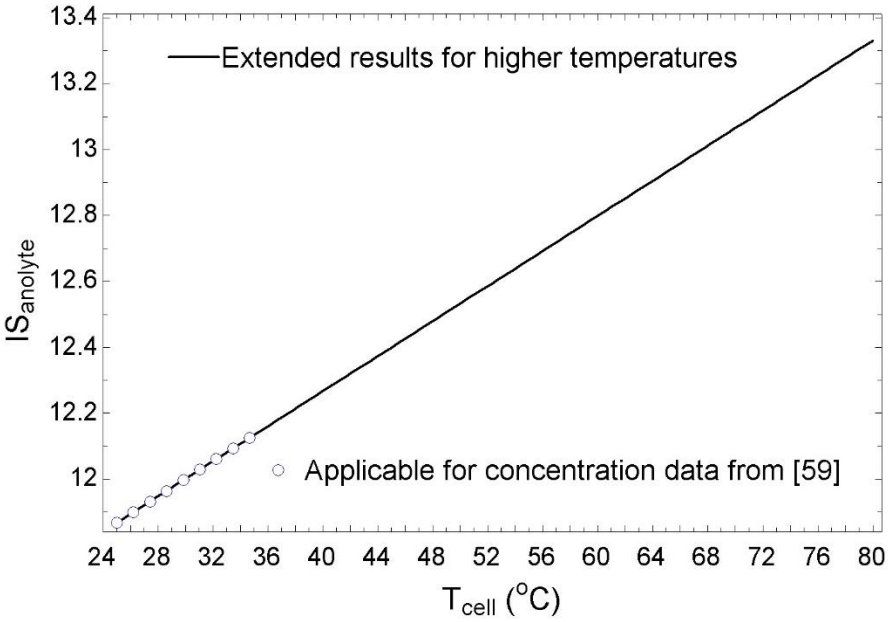

Figure 4.20: Temperature dependency of ionic strength of anolyte considering effect of temperature on concentrations ; Blue dots are obtained based on concentration data from [59] for temperatures around 25℃; Solid black line is extended results for higher temperatures using linear trend of concentration change by temperature data provided by [59].

For the HER, taking activity of the catholyte ions into account, reaction is seen to be spontaneous as well as standard case, but with higher potential (which is a good running force for electrolysis). For instance at 75℃ the standard decomposition potential is 0.03V, while for the same temperature value of corresponding decomposition potential is around 0.16V, which is a significant difference. Catholyte is highly acidic and concentrated. Therefore, large deviations from standard state are observed.

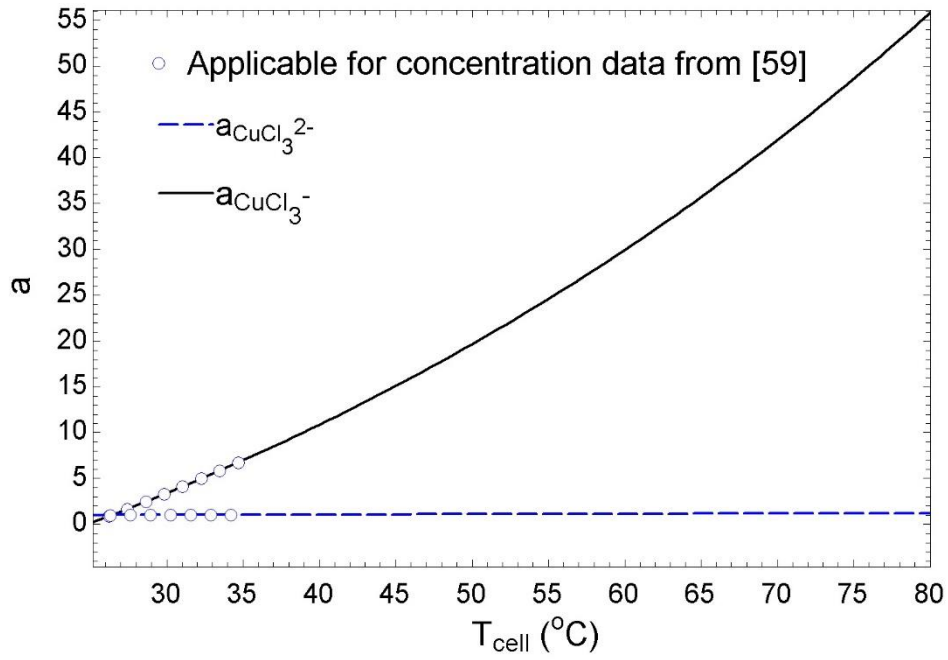

Figure 4.21: Temperature dependency of $CuCl_3^{2-}$(aq) and $CuCl_3^-$(aq) activity considering effect of temperature on concentrations; Blue dots are obtained based on concentration data from [59] for temperatures around 25℃; Solid black and dashed blue line is extended results for higher temperatures using linear trend of concentration change by temperature data provided by [59].

Magnitude of Gibbs conversion coefficient of the HER increases by temperature (Figure 4.24). Actually, the HER is spontaneous with negative Gibbs energy change. On the other hand, the HER is heat-demanding, and the amount of heat demand is higher than Gibbs

energy change through the hydrogen evolution reaction in acidic medium; therefore, negative Gibbs conversion coefficient is resulted.

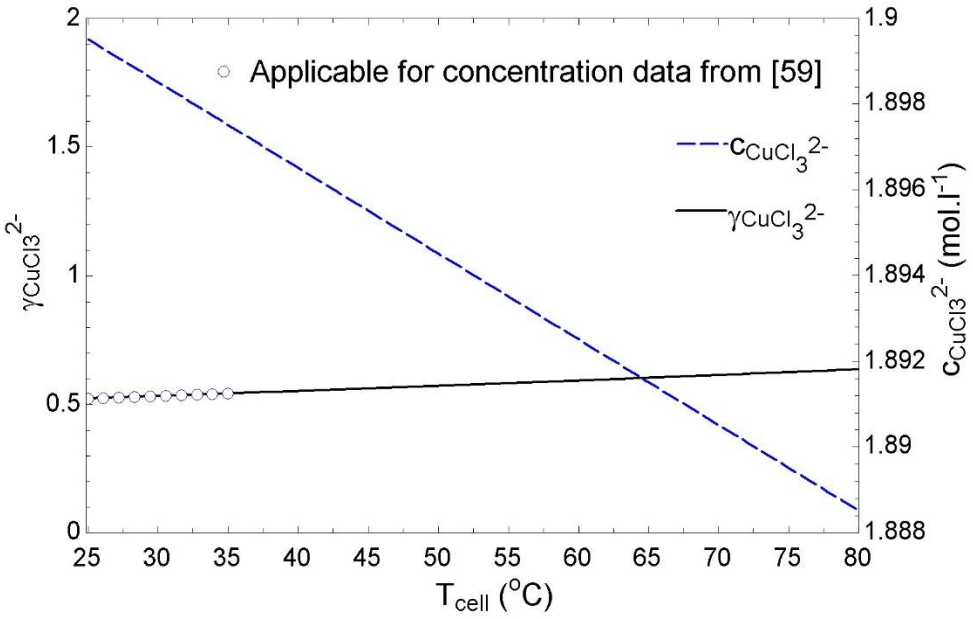

Figure 4.22: Temperature dependency of $CuCl_3^{2-}$(aq) activity parameters considering effect of temperature on concentrations; Blue dots are obtained based on concentration data from [59] for temperatures around 25℃; Solid black line is extended results for higher temperatures using linear trend of concentration change by temperature data provided by [59].

Figure 4.25 and Figure 4.26 provide data presenting overall decomposition potential and Gibbs conversion coefficient of the cell, respectively, by considering the impact of temperature on concentration of active species in anolyte for various conversion degrees. As expected, 5% conversion requires a higher amount of decomposition potential compared to a lower conversion degree. This analysis considers Reaction2 as the dominant anode half-raction. It can be seen that, at 25℃ and 5% conversion, the decomposition potential of the cell is resulted to be around -0.40V. At 80℃ and 5% conversion, the corresponding decomposition

potential of the cell rises from -0.40V to -0.44V. A lower conversion degree requires a less decomposition potential.

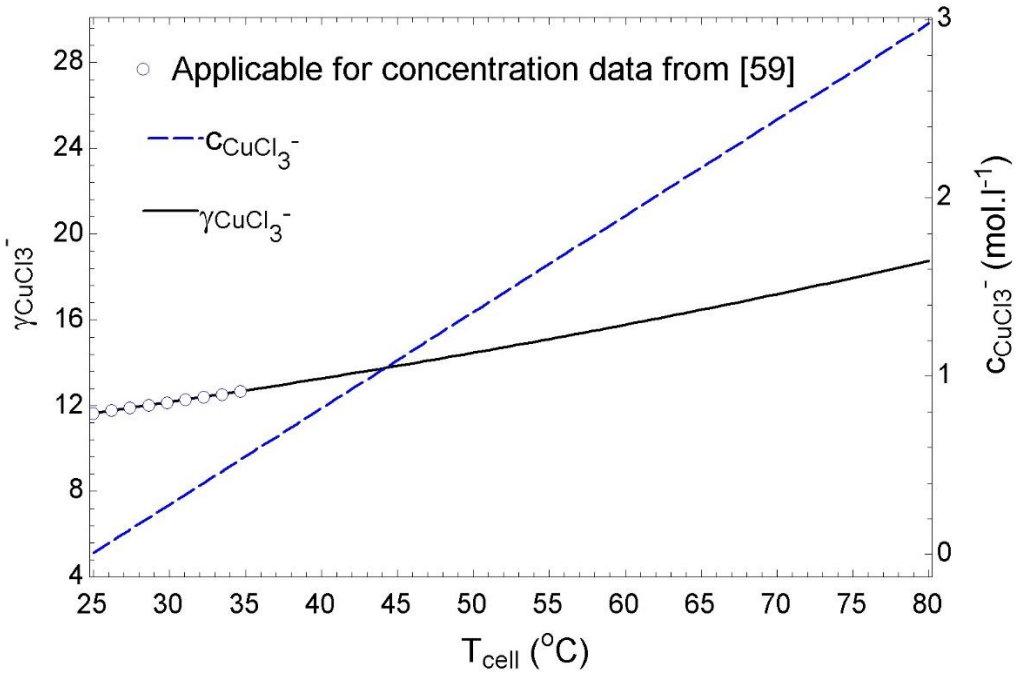

Figure 4.23: Temperature dependency of $CuCl_3^-$(aq) activity parameters considering effect of temperature on concentrations ; Blue dots are obtained based on data from [59] for temperatures around 25℃; Solid black line is extended results for higher temperatures using linear trend of concentration change by temperature data provided by [59].

Note that at zero conversion at anode no electron is sent to cathode for hydrogen evolution and therefore no full-cell reaction is possible to occur. Therefore, no-conversion mode is excluded from full-cell studies. Moreover, full-cell decomposition potential has to be calculated for a dynamic equilibrium condition which means at any conversion degree other than zero.

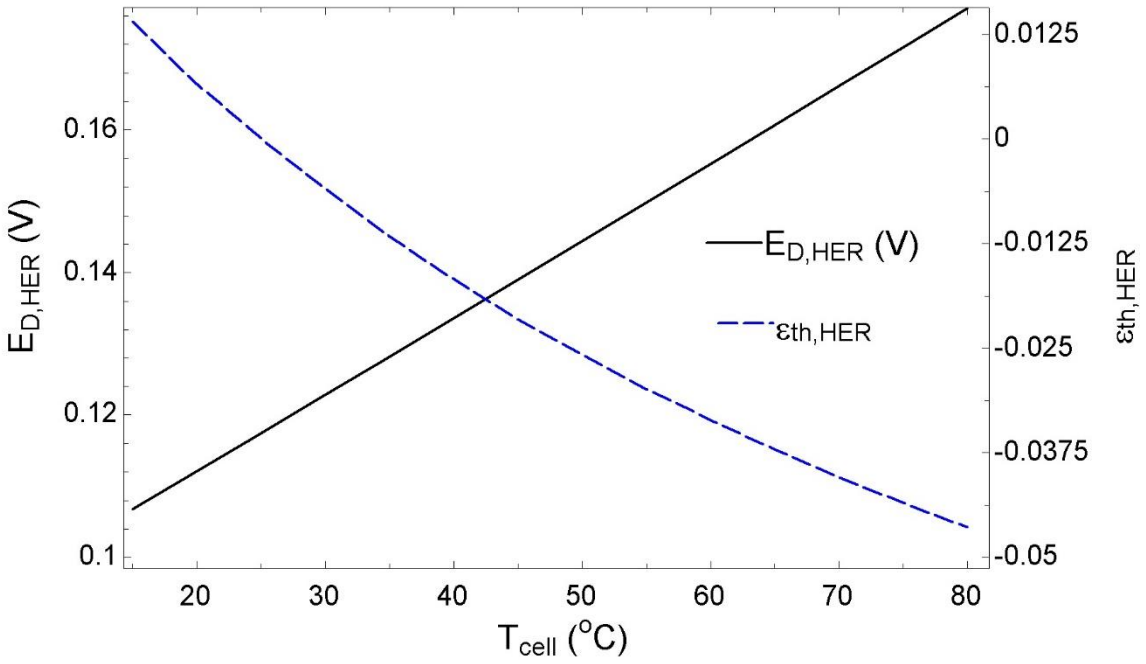

Figure 4.24: Effect of temperature on decomposition potential and Gibbs conversion coefficient of HER; this is a non-standard state and activity coefficient of anolyte species are applied in calculations to obtain results.

Comparison of results of this study with similar data in literature [55, 59] validates the consistency of this theoretical equilibrium study to experimental equilibrium experiments. Balashov et al. [55] reported the cell decomposition potential of between -0.42V and -0.47V for concentrated electrolytes. In addition, Hall et al. through theoretical equilibrium studies on the CuCl/HCl cell, reported that decomposition potential of the cell is less than the corresponding standard decomposition potential that is similar to observations of this study. This observation stems from a huge difference between standard decomposition potential and decomposition potential of the HER at cathode.

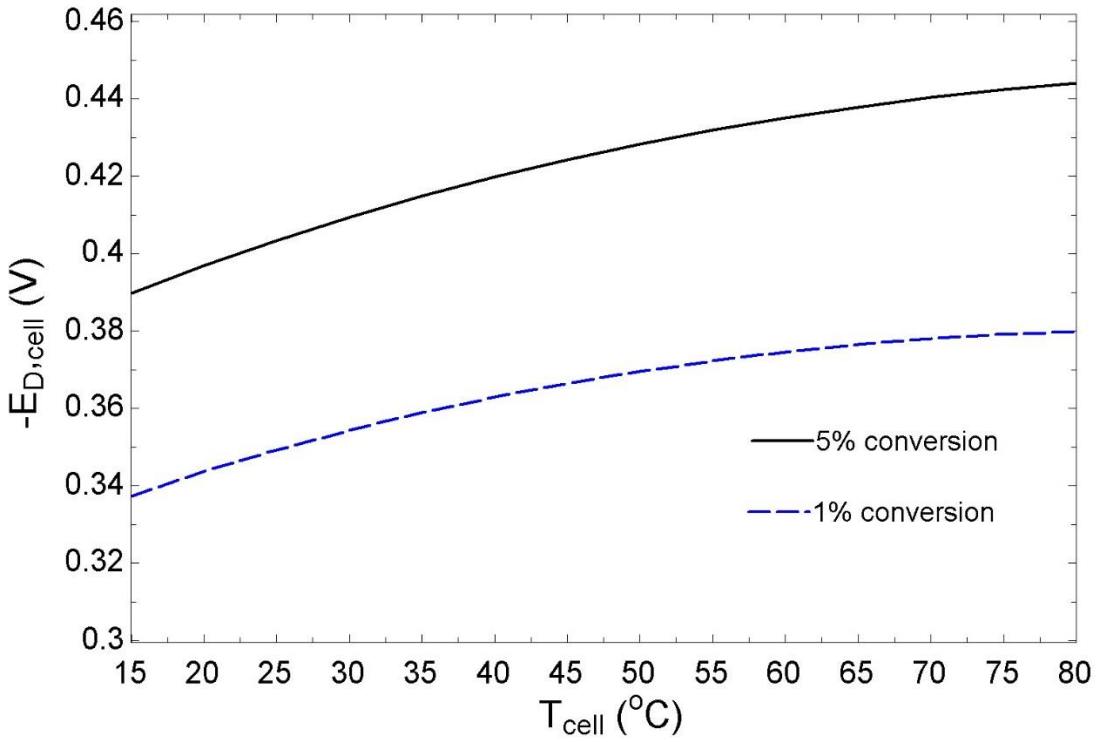

Figure 4.25: Decomposition potential of full-cell for various temperatures and Cu(I) → Cu(II) conversion degrees in anode; Reaction2 is selected as dominating anode half-reaction; effect of temperature on equilibrium concentration of anolyte ions is considered; this is a non-standard state and activity coefficient of anolyte species are applied in calculations to obtain results.

Gibbs conversion coefficient of full-cell increases almost linearly by temperature. A lower conversion degree results a higher level of Gibbs conversion coefficient and this difference between Gibbs conversion coefficient of lower and higher conversion degree increases as temperature increases. At 80℃ and 5% conversion degree Gibbs conversion coefficient of the cell can be estimated around 80%.

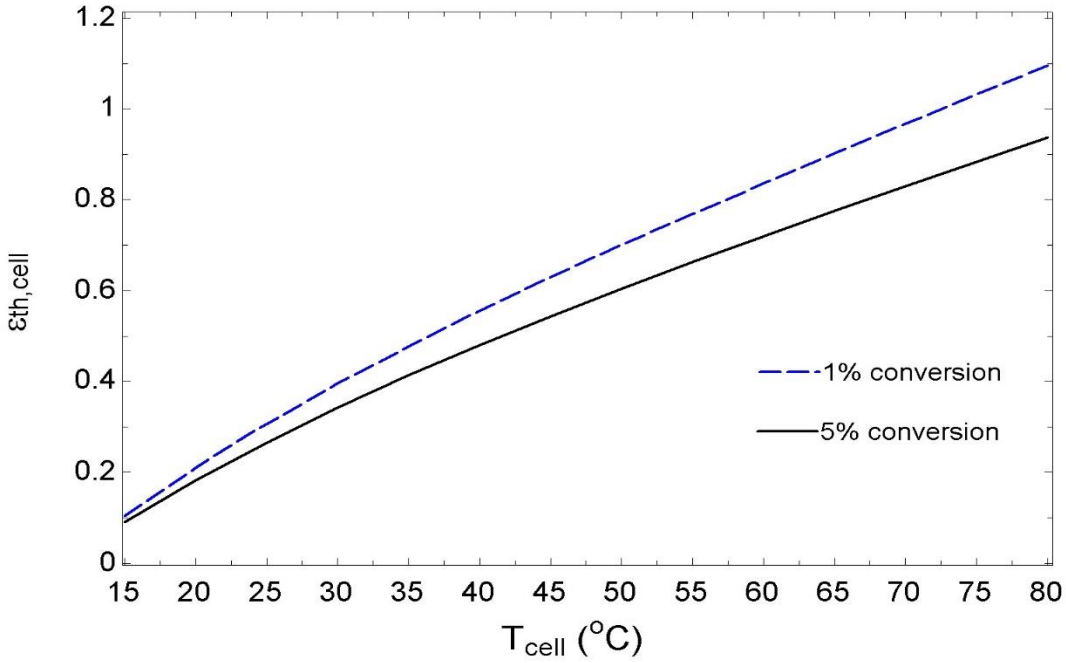

Figure 4.26: Gibbs conversion coefficient of full-cell for various temperatures and Cu(I) → Cu(II) conversion degrees in anode; Reaction2 is selected as dominating anode half-reaction; effect of temperature on equilibrium concentration of anolyte ions is considered; this is a non-standard state and activity coefficient of anolyte species are applied in calculations to obtain results.

4.6: Half-cell and Full-cell Heat Transfer

Anode half-reaction at a conversion mode is heat-releasing and this heat release decreases by temperature rise (Figure 4.27). On the other hand, as conversion degree increases, heat release decreases, which is obtained from entropy change of species through reaction (equations 3.41 and 3.61). The HER is heat-demanding (Figure 4.28) and its heat demand increases as temperature rises. The overall cell is heat-releasing and heat release decreases by temperature (Figure 4.29). But this is from equilibrium point of view, in order to determine whether the cell is heat-releasing or heat-demanding, a Kinetic analysis should be done to investigate heat

generation from irreversibilities within the cell. In some researches [59] the CuCl/HCl electrolyser is reported to be heat-demanding, while in another study the electrolysis step of the Cu-Cl cycle is observed to be heat-releasing [106].

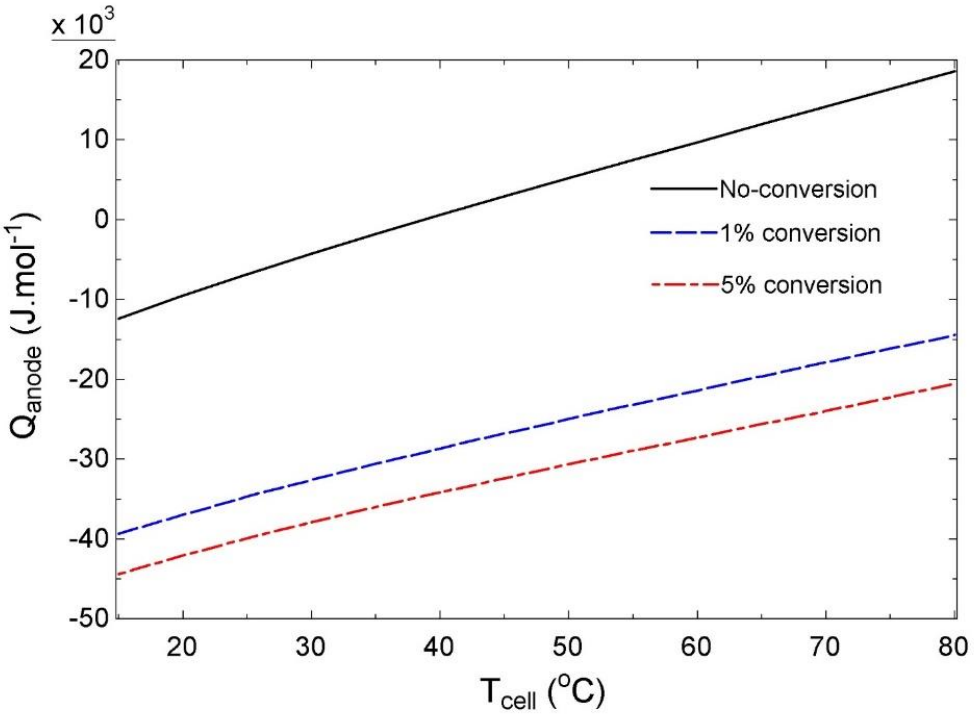

Figure 4.27: Equilibrium heat transfer of anode half-reaction for various temperatures and Cu(I) → Cu(II) conversion degrees in anode; Reaction2 is selected as dominating anode half-reaction; effect of temperature on equilibrium concentration of anolyte ions is considered; negative sign corresponds to an exothermic reaction; this is a non-standard state and activity coefficient of anolyte species are applied in calculations to obtain results.

4.7: Activation Overpotentials

Figure 4.30 shows that considering only electron transfer (blue dashed line) for activation overpotential leads to an incorrect results, as the black solid line can be validated by experimental released reports. Therefore, both electron and mass transfer effects should be taken into account to get close-to-reality results.

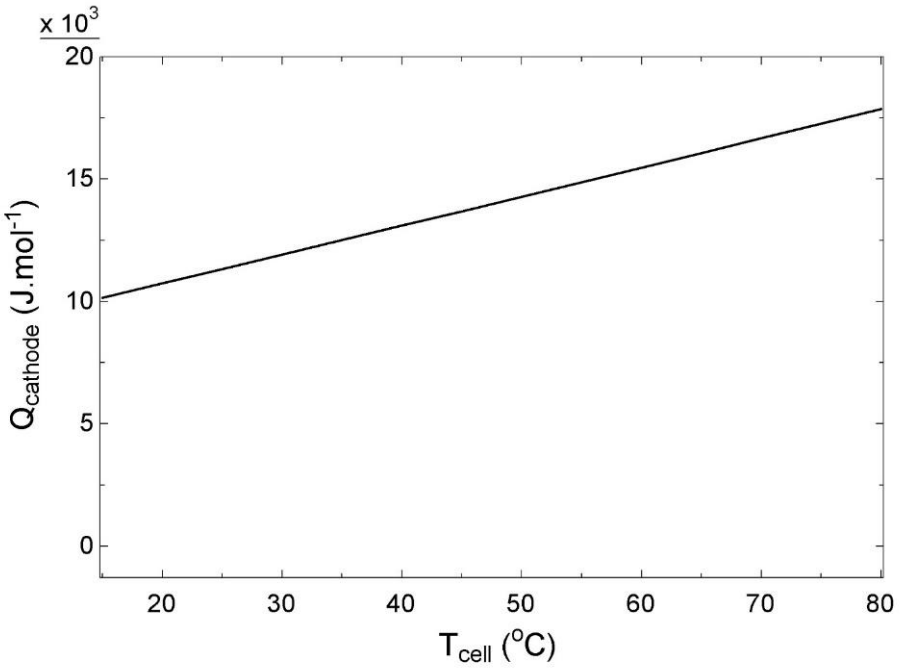

Figure 4.28: Effect of temperature on heat requirement of HER at equilibrium condition; this is a non-standard state and activity coefficient of anolyte species are applied in calculations to obtain results.

At a desired 0.5 A. cm^{-2} current density, the anode activation overpotential is found to be -0.053V. In addition, as Figure 4.31 shows, at a conversion degree other than 5%, overpotential results are not observed to be on a proper trend which is simply due to the fact that the used kinetic parameters are from references corresponding a 5% conversion degree. Comprehensive experiments should be done to investigate effects of temperature and conversion degree on overpotentials.

Since in the literature logarithmic current and activation overpotential is reported for the HER, I initially obtained logarithmic graph to see if the trend is valid. Figure 4.32 shows a proper trend and shape of overpotential for the HER of studied cell. The amount of

activation overpotential of the HER is calculated to be 0.083V to obtain the desired current density of 0.5 $A.cm^{-2}$.

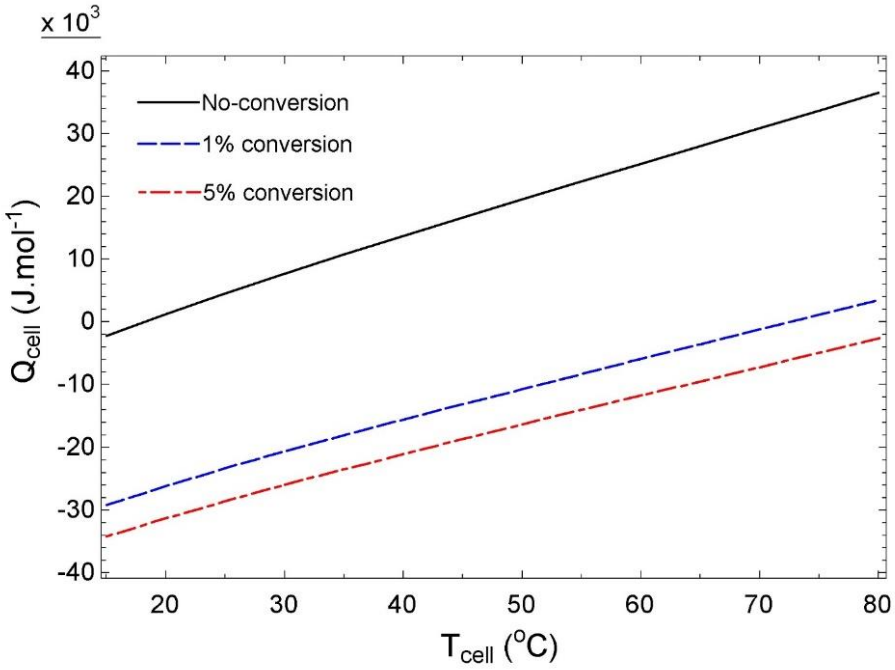

Figure 4.29: Heat transfer of full-cell at various conversion degrees and temperatures; negative sign corresponds to an exothermic reaction; this is a non-standard state and activity coefficient of anolyte species are applied in calculations to obtain results.

In order to investigate the effect of temperature on activation overpotential of the anode half-reaction, exchange current density has to be studied first to observe effects of temperature on it. Fortunately, by having the required transfer coefficient value from [61], this aim could be achieved through using equation 3.47. Figure 4.34 depicts that exchange current density of the anode half-reaction increases for a higher temperature, which can be validated by results presented in [56], as it reports a better (higher) current density for a higher temperature at constant applied potential. Activation overpotential of the anode half-reaction drops under effect of higher exchange current density which can be seen from Figure 4.34.

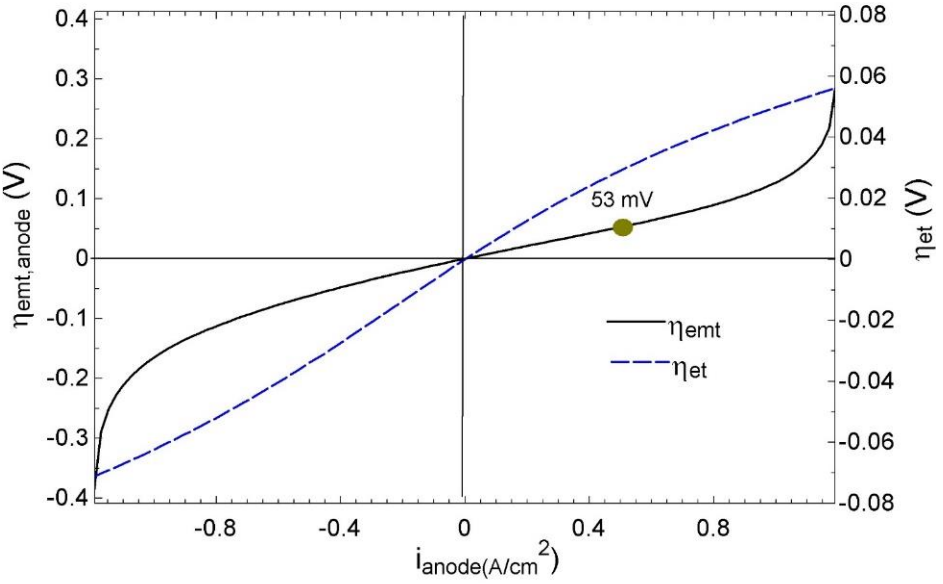

Figure 4.30: Activation overpotential of dominant anode half-reaction; red dot presents corresponding overpotential at cell current density of $0.5A.\,cm^{-1}$; $Cu(I) \rightarrow Cu(II)$ conversion degree is 5%; kinetic data are used considering glassy carbon anode electrode; kinetic data are used from [60].

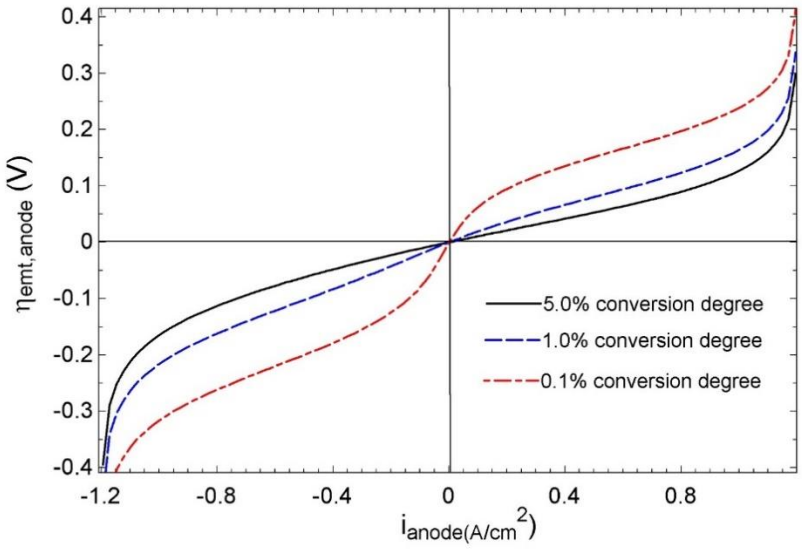

Figure 4.31: Activation overpotential of anode half-reaction for various $Cu(I) \rightarrow Cu(II)$ conversion degree; kinetic data are used considering glassy carbon anode electrode; kinetic data are used from [60].

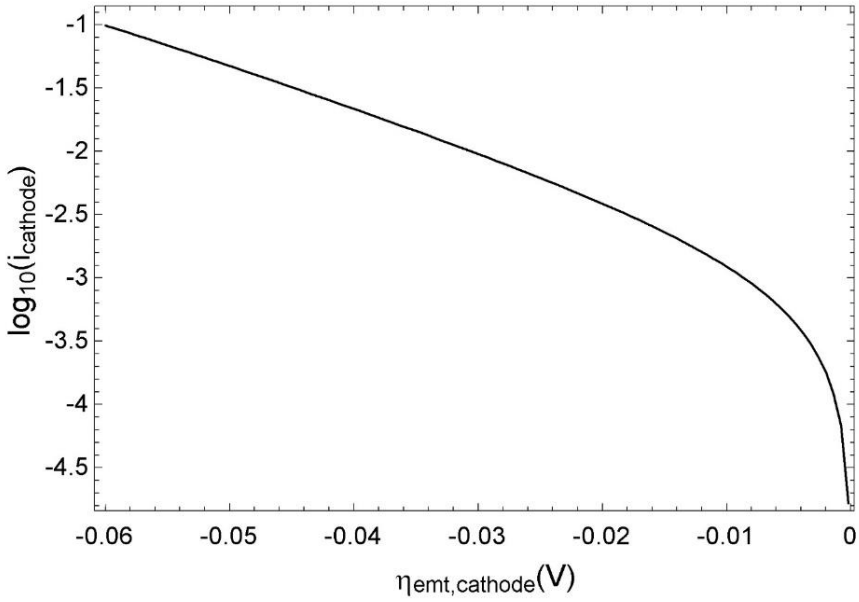

Figure 4.32: Logarithmic current-activation overpotential of HER; kinetic data are used considering Pt cathode electrode; kinetic data are used from [61].

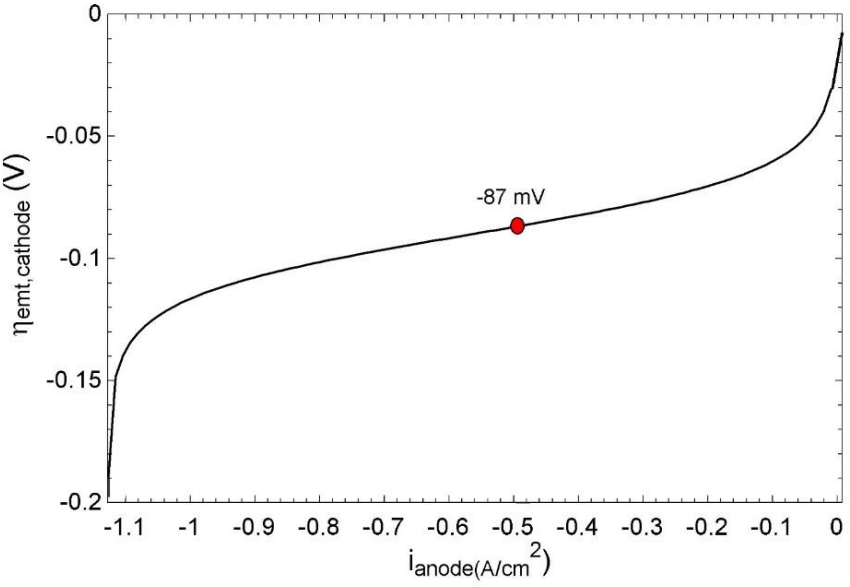

Figure 4.33: Current-activation overpotential of HER; kinetic data are used considering Pt cathode electrode; kinetic data are used from [61]; red dot presents corresponding overpotential at cell current density of $0.5\mathrm{A.\,cm^{-1}}$.

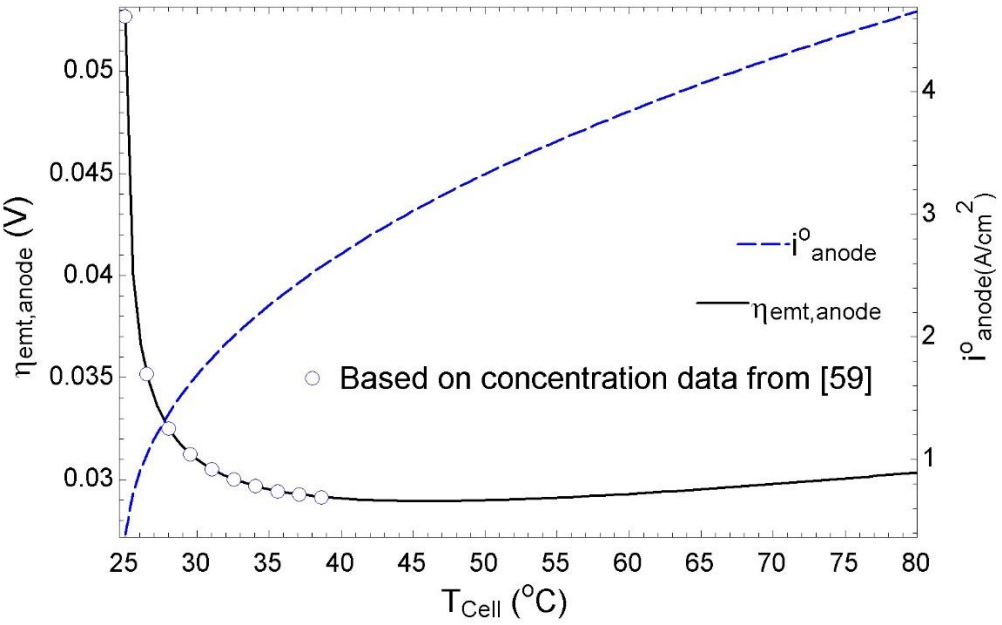

Figure 4.34: Anode half-reaction activation overpotential at current density of $0.5 A.\,cm^{-1}$ and exchange current density as function of temperature with considering concentration changes by temperature; Blue dots are obtained based on data from [59] for temperatures around 25℃.

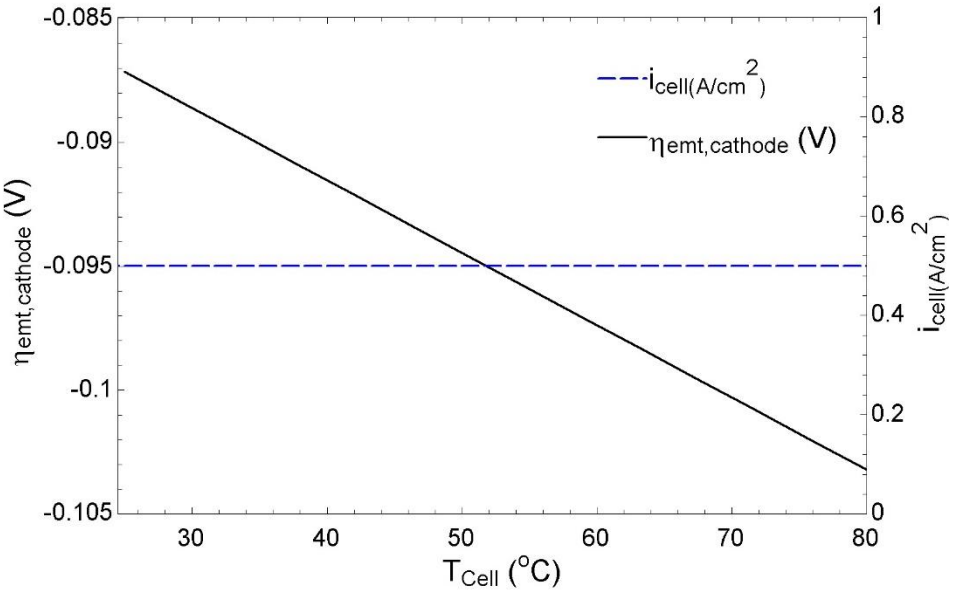

Figure 4.35: Temperature dependency of HER activation overpotential at current density of $0.5\ A.cm^{-2}$.

Activation overpotential of the anode decreases dramatically as temperature rises from room temperature and then plateaus on around 0.030V. In addition, magnitude of activation overpotential of the HER increases by temperature increase (Figure 4.35).

4.8: PEM Ohmic Overpotentials

Ohmic overpotential of the PEM is developed and it has values in order of micro volts which is almost 1000 times smaller than activation overpotentials. For a specific membrane thickness temperature rise decreases the Ohmic overpotential steadily (Figure 4.36), while Figure 4.37 shows that for a certain temperature membrane thickness linearly increases the value of Ohmic overpotential. In addition, after determination of governing overpotentials, internal heat generation can be calculated through equation 3.39. The results show that internal heat generation is around 27000 $\mathrm{J.mol^{-1}}$ and increases linearly with temperature. Overall, the cell is exothermic.

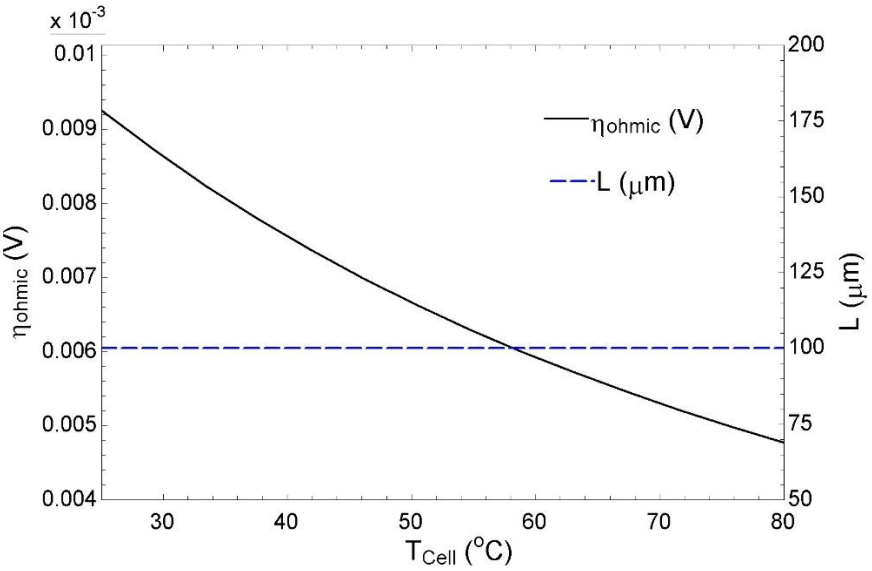

Figure 4.36: Effect of temperature on PEM Ohmic overpotential; membrane thickness is assumed to be $100\mu m$.

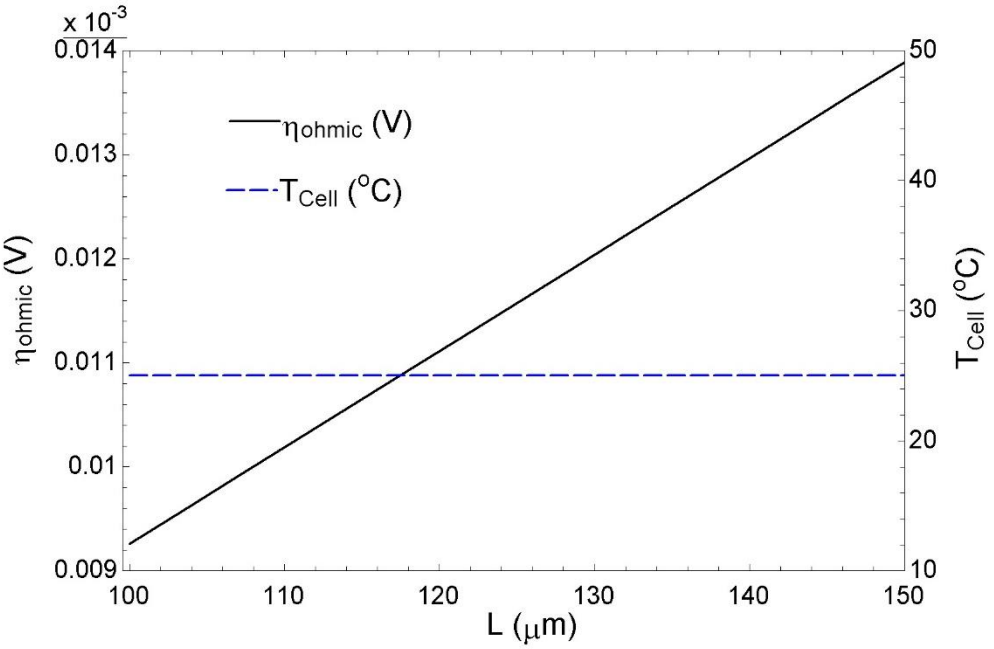

Figure 4.37: Effect of membrane thickness on PEM Ohmic overpotential; temperature is assumed to be 25℃.

4.9: Voltage and Electrochemical Efficiency

The final goal is to determine voltage and overall electrochemical efficiency of the cell. Prior to that, cell potential has to be calculated through equation 3.42 which is adding all overpotentials to the resulted decomposition potential to obtain a final required potential to trigger the electrolysis. Figure 3.45 depicts that cell potential (decomposition potential plus overpotentials) varies between -0.53V to -0.59V at different temperatures. A higher working temperature increases cell potential which means that more electricity should be applied to produce hydrogen. Comparing the CuCl/HCl electrolyser of this study with a water PEM electrolyser working at around 80℃ and current density of 0.5 $A.cm^{-2}$ [101], it can be concluded that voltage requirement of CuCl/HCl electrolyser is almost one third of water PEM electrolyser. Moreover, an equilibrium study on water electrolysis [27] reports

decomposition potential of -1.48V at 25℃ while the corresponding amount for the CuCl/HCl electrolyser of this study is around -0.41V.

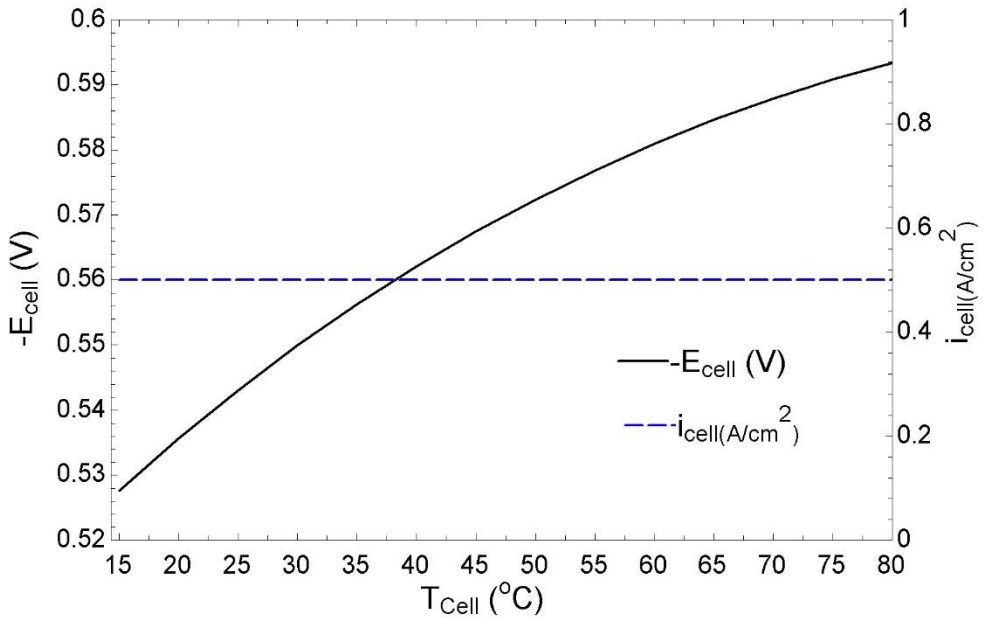

Figure 4.38: Effect of temperature on cell potential at current density of $0.5\mathrm{A.\,cm^{-1}}$ and anode $\mathrm{Cu(I) \rightarrow Cu(II)}$ conversion degree of 5%; activation overpotentials are added to required decomposition potential of electrolysis.

Voltage efficiency of the cell at a 5% conversion degree is found to vary between 73.0% and 74.8% for different temperatures while it peaks at around 60℃. Therefore, in this study based on voltage efficiency, 60℃ is the optimum temperature. Furthermore, electrochemical efficiency of cell which is multiplication of current, voltage, and Gibbs conversion coefficient is found to increase by temperature. As temperature rises from 20℃ to 80℃ electrochemical efficiency of the cell increases from 10% to 70% which clarifies this fact that a high temperature is actually more appropriate for electrolyser. However, this results into a higher potential demands. Which is close to results of previous experimental studies. Temperature

has a positive effect on voltage efficiency as it drops overpotentials. Assuming 100% current efficiency, cell electrochemical efficiency is somehow between 10% and 70% for different temperatures at 5% conversion mode. Hall et al. [59] obtained electrochemical efficiency of between 15% and 95% for their specific study which could validate results of this study.

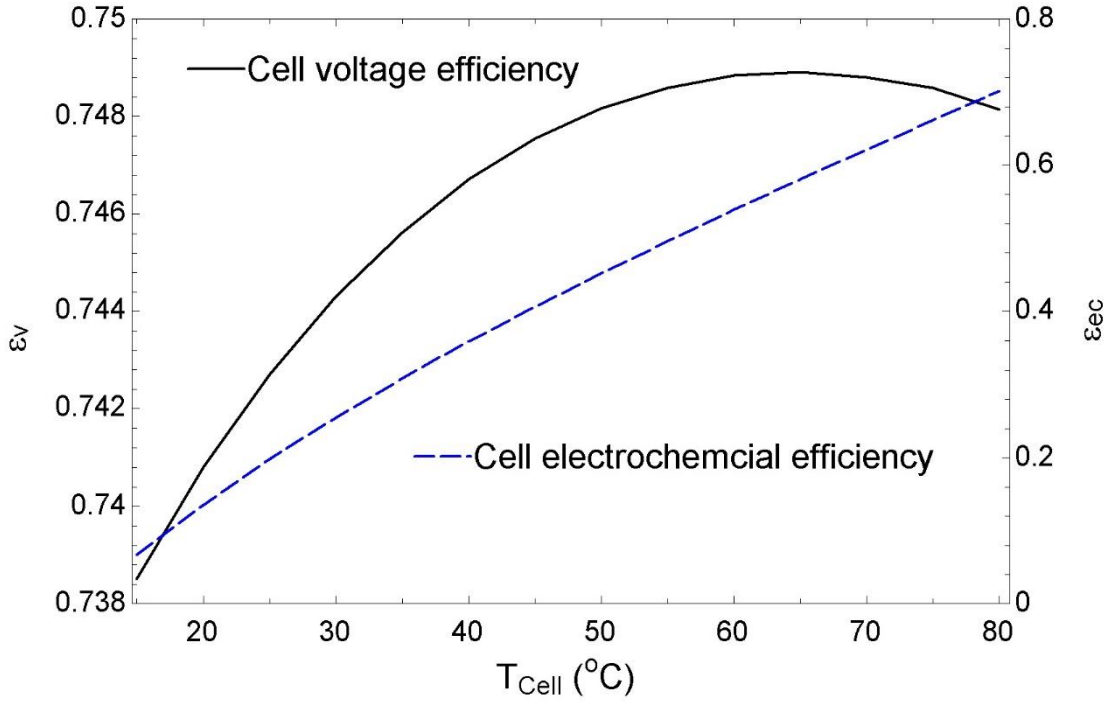

Figure 4.39: Effect of temperature on voltage efficiency and overall electrochemical efficiency of electrolysis at current density of $0.5A.\,cm^{-1}$ and anode $Cu(I) \rightarrow Cu(II)$ conversion degree of 5%; activation overpotentials are added to required decomposition potential of electrolysis.

4.10: Energy and Exergy Conversion Coefficients

Electrochemical efficiency of the cell is found in the previous section. Two new efficiency definitions are used that are from control volume analysis point of view to compare results with electrochemical efficiency. Since the studied cell is heat-releasing, equations 3.65 and

3.66 are applicable to study energy and exergy conversion coefficients, respectively. Results are found interesting that are above 100% i.e. energy and exergy conversion coefficients are close to each other (around 160% at room temperature), due to the fact that exergy input to the system is electricity and on the other hand LHV and chemical exergy values of hydrogen are close in value. Moreover, due to observing value of higher than 100%, energy conversion coefficient (ECC) and exergy conversion coefficient (E_xCC) are used instead of energy and exergy efficiency. Figure 4.40 depicts how temperature has negative effect on corresponding energy and exergy conversion coefficient of electrolysis. Investigating relative results to validate these results, it should be clarified that the only exergy analysis on CuCl/HCl electrolysis is carried out by Orhan et al. [106] which corresponds to a high temperature electrolytic cell with solid copper and gaseous HCl as inerts. Orhan's study resulted into exergy efficiency of almost 100%. However, in that study electricity input is neglected, therefore it would not be a proper validation source for this work.

The electrolysis is heat-releasing, and the amount of heat is low quality, because temperature of heat source is at low temperature. Heat source temperature is assumed to be the same as cell working temperature. Therefore, heat should not be used as output or input. The only inputs are electricity, anolyte, and catholyte solutions. Anolyte and catholyte insert chemical exergy to the system.

For a comprehensive exergy analysis, detail chemical exergy of all present ions in anolyte and catholyte should be calculated and taken into account for a more precise result. Calculation of chemical exergy of ions is out of scope of this research. In addition, in order to employ ion chemical exergies, corresponding mass balance equations have to be developed

for ions which requires a detail mass transfer analysis within the cell as well as through the membrane. Mass transfer analysis is also out of scope if this thesis.

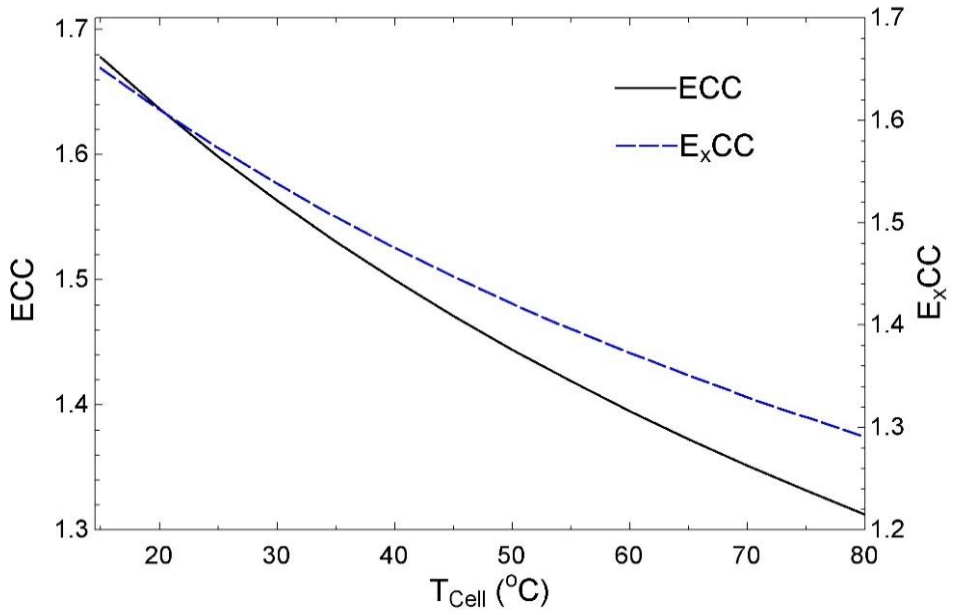

Figure 4.40: Effect of temperature on energy and exergy conversion coefficients of electrolysis at current density of $0.5A.\,cm^{-1}$ and anode $Cu(I) \rightarrow Cu(II)$ conversion degree of 5%; activation overpotentials are added to required decomposition potential of electrolysis.

Therefore, unlike other similar studies on a PEM water electrolysers, chemical exergy on input and output streams of cell have to be determined for all present species to obtain the proper energy and exergy efficiency results. Since the CuCl/HCl electrolyser of this study is found to be heat-releasing, therefore, the following energy and exergy efficiency definitions are proposed for further studies:

$$\psi_{en} = \frac{LHV_{H_2} \times \dot{N}_{H_2}}{P_{electrical} + (\sum \dot{N}_{i,inlet} h_{i,inlet} - \sum \dot{N}_{i,outlet} h_{i,outlet})} \quad (4.1)$$

$$\psi_{ex} = \frac{Ex_{H_2} \times \dot{N}_{H_2}}{\dot{E}x_{electrical} + (\sum \dot{N}_{i,inlet} ex_{i,inlet} - \sum \dot{N}_{i,outlet} ex_{i,outlet})} \quad (4.2)$$

where subscript i denotes present ions in anolyte and catholyte. However, in order to use the above stated proposed equations, molar mass rate of ions have to be determined through mass transfer analysis within the cell.

4.11: Model Validation

Results from this study can be validated by comparison with related experimental or theoretical studies on CuCl/HCl electrolysers, available in literature. It is observed in this study that after consideration of activity coefficients in calculation of thermodynamic properties, all anode half-reactions undergo almost same amount of change of specific molar Gibbs energy change, specific molar enthalpy, and specific molar entropy. While for a dilute standard system, change of standard thermodynamic properties through anode half-reactions are resulted different. The same observation was reported for 25℃ and 1bar by Hall et al. [59] in an experimental/theoretical study. The used anolyte in [59] was 2-2.5 $\mathrm{mol.\,kg^{-1}}$ $\mathrm{CuCl(aq)}$ in 8-9 $\mathrm{mol.\,kg^{-1}}$ $\mathrm{HCl(aq)}$ and catholyte was 8-9 $\mathrm{mol.\,kg^{-1}}$ $\mathrm{HCl(aq)}$.

Balashov et al. [55] analysed a PEM deionized water electrolyser and a CuCl/HCl electrolyser and reported that for hydrogen generation required potential of CuCl/HCl electrolyser is 3 times lower than water electrolyser. Same result is concluded in this study by comparison of required potential of studied CuCl/HCl electrolysis with a PEM water electrolysis at 80℃. In addition, in [55] through a theoretical decomposition potential analysis on an electrolyser with anolyte of 1.17 5 $\mathrm{mol.\,kg^{-1}}$ $\mathrm{CuCl(aq)}$ in 7 $\mathrm{mol.\,kg^{-1}}$ $\mathrm{HCl(aq)}$ and catholyte of 7 $\mathrm{mol.\,kg^{-1}}$ $\mathrm{HCl(aq)}$ at 25℃ and 1bar, the decomposition potential of cell was reported around -0.38V which is comparable to result of this study that is -0.40V at same temperature but different concentrations of electrolytes. In the same study by Balashov et al. [55] on anolyte of 0.2 $\mathrm{mol.\,kg^{-1}}$ $\mathrm{CuCl(aq)}$ in 7 $\mathrm{mol.\,kg^{-1}}$ $\mathrm{HCl(aq)}$, it was resulted that for a same level of $\mathrm{Cu(I)} \rightarrow$

Cu(II) conversion degree at anode, increasing the working temperature results into a consequent higher potential. This validates results of this study regarding increase of potential of cell by temperature rise.

The required voltage to trigger hydrogen production at 80℃ in this study is calculated to be around -0.60V for cell current density of $0.5 A.cm^{-2}$. This result is comparable to corresponding value of almost -0.62V for a same current density and temperature obtained via an experimental study by Hall et al. [60]; the test condition in that study was $0.4\ mg.cm^{-2}$ of Pt catalyst on cathode, $5cm^2$ carbon cloth electrodes, hot-pressed Nafion 117 membrane; and the anolyte was solution of 2 mol CuCl(aq) in $7\ mol.l^{-1}$ HCl(aq), catholyte was $7\ mol.l^{-1}$ HCl(aq), and the flowrate of electrolytes was $400\ ml.min^{-1}$. Note that since the electrolytes concentrations in this study are different from other studies, small differences between results of this study and others are expected.

Chapter 5: Conclusions and Recommendations

5.1: Conclusions

This thesis presents a study on a CuCl/HCl electrolyser from an electrochemical perspective. Due to high ionic strength of multi-component electrolytes, standard thermodynamics was not sufficient for the study. Therefore, the activity of ions had to be taken into consideration. Initially, a number of ions for anolyte were selected. Then, GEM analysis resulted into values of concentration for each of present ions at equilibrium condition which made it possible to carry out equilibrium thermodynamics. The third approximation of Debye-Huckel theory was used to calculate corresponding activity coefficients of electrolyte species. Therefore, thermodynamic properties of ions could be determined from standard values. Decomposition potentials of the anode and cathode half-reactions and corresponding full-cell reaction were calculated. Temperature and the $\mathrm{Cu(I)} \rightarrow \mathrm{Cu(II)}$ conversion degree were used as parametric study variables. Due to this fact that temperature affects ions equilibrium concentrations, corresponding data from references were used to apply this effect in the present analysis. The other parametric study could be consideration of different concentrations for anolyte. The reason why this parametric study is not carried out in this study is that for each of anolyte concentrations GEM analysis should be done which requires lot of time and effort. The equilibrium potential for the cell which is named as decomposition potential in this study was found to be in close agreement with experimental half-cell studies. For the first time, half-cell overpotentials were developed theoretically in close agreement with experimental results available in the literature. The heat transfer analysis of the cell was also investigated by comparing generated heat from irreversibilities within the cell and heat demand/release of

half-cell redox reactions. Energy and exergy conversion coefficients were also determined through energy/exergy analysis. It was concluded that chemical exergy of ions have to be calculated as well as mass balance of ions within cell. Overall, the main findings of this study from equilibrium and kinetic analyses can be listed as follows:

- All anode half-reactions trigger at a same specific potential. However, depending on the concentration of active species, only one reaction is dominant.
- As conversion begins at the anode, decomposition potential increases sharply, then continues to rise steadily at a slower rate.
- At 25℃, magnitude of full-cell electrolysis decomposition potential is 0.40V at full conversion. While at 80℃, correspondingValue rises to 0.44V.
- At no-conversion condition, the anode half-reaction is heat-demanding. As conversion begins, the opposite response is observed with a heat release.
- Hydrogen evolution reaction is spontaneous and heat-demanding, while the anode half-reaction is heat-releasing and non-spontaneous. Considering internal heat generation from irreversibilities (overpotentials), the full-cell is overall heat-releasing.
- A higher temperature results into a higher decomposition potential of the cell.
- At 5% conversion, the anode half-reaction activation overpotential is 53 mV. This value decreases by temperature to around 30mV.
- In term of voltage efficiency, 60℃ is the most suitable working temperature for electrolyser.
- Electrochemical efficiency of the CuCl/HCl electrolysis ranges from 10% to 70% for a temperature range of 25℃ to 80℃.

- Magnitude of overall required potential for electrolysis at full conversion is between 0.53V and 0.59V as temperature rises.
- A Higher temperature results into a higher required potential for electrolysis, but increases electrochemical efficiency of the cell, significantly. Therefore, elevated temperature is believed to be more appropriate for electrolysis.

5.2: Recommendations

Considering all discussion and conclusions of the addressed issues throughout the text, the following recommendations are made for future relative studies:

- The effect of temperature on speciation of various concentrations of electrolytes should be studied in detail: Temperature affects the equilibrium of electrolyte by changing Gibbs energy level of ions. This effect has to be studies in detail. The Hch software can be used to carry out this analysis by defining various temperatures for Gibbs energy minimization of electrolyte.
- Equilibrium and kinetic analyses should be conducted for various anolyte concentrations: For instance varying concentration of $CuCl(aq)$ for certain concentration of $HCl(aq)$ and vice versa. This requires separate speciation and GEM analyses for each step. Hch software can be used for this purpose.
- Comprehensive experiments should be conducted to determine kinetic parameters of anode and cathode half-reactions for various concentration and temperatures: Following the two above-mentioned recommendations, for kinetic study, appropriate kinetic parameters have to determine through experiments for each certain study condition (concentration and temperature).

- Energy and exergy analyses of electrolysis have to be conducted for the CuCl/HCl cell: this involves development of four main thermodynamics balance equations that are mass balance, energy balance, and entropy balance as well as exergy balance equations. Therefore, transport phenomena within the cell has to be modelled first. Then, chemical molar exergy values of each of ions have to be calculated.
- More kinetic parameters have to be determined for the HER in concentrated HCL(aq) solution on Pt electrode: this requires precise half-cell experiments.
- A comprehensive model of the cell (not only from electrochemistry and thermodynamics perspectives) which is a need for future integration of the Cu-Cl hydrogen production cycle has to be developed. In other words, a program can be developed to study performance of electrolyser for various test conditions: one should develop a multiphysics model taking into account heat transfer, mass transfer, and fluid flow as well as electrochemistry. This aim can be achieved by the COMSOL software, however as there in not enough electrochemical data in this software, one should develop his/her own user defined modules.

References

1. Olejarnik, P., World energy outlook. 2010, International Energy Agency: France.
2. Birol, F., Energy and climate change. 2015, International Energy Agency: France.
3. Pachauri, R., Climate change 2007: Synthesis report. 2007, International Energy Agency: France.
4. IEA, Energy technology perspectives: Mobilizing innovation to accelerate climate actions. 2015, International Energy Agency: France.
5. IEA, Key World energy statistics. 2014, International Energy Agency: France.
6. IEA, Tracking clean energy progress 2015. 2015, International Energy Agency: France.
7. Dincer, I., Green methods for hydrogen production. International Journal of Hydrogen Energy, 2012. 37(2): p. 1954-1971.
8. IEA, Technology roadmap: Energy storage. 2014, International Energy Agency: France.
9. Ramachandran, R. and Menon R.K., An overview of industrial uses of hydrogen. International Journal of Hydrogen Energy, 1998. 23(7): p. 593-598.
10. Holladay, J.D., Hu, J., King, DL. and Wang, Y., An overview of hydrogen production technologies. Catalysis Today, 2009. 139(4): p. 244-260.
11. Soltani, R., Rosen, M., and Dincer I., Assessment of CO_2 capture options from various points in steam methane reforming for hydrogen production. International Journal of Hydrogen Energy, 2014. 39(35): p. 20266-20275.
12. Krumpelt, M., Krause, TR., Carter, JD., Kopasz, JP. and Ahmed, S., Fuel processing for fuel cell systems in transportation and portable power applications. Catalysis Today, 2002. 77(1): p. 3-16.
13. McHugh, K., Hydrogen production methods. MPR Associates Inc, 2005. 41.
14. Ding, F. and Y. Yi, Technology of hydrogen production and storage. 2006, Beijing, BJ: Chemical Industry Press.
15. Wilhelm, D., Simbeck, DR., Karp, AD. and Dickenson, RL., Syngas production for gas-to-liquids applications: technologies, issues and outlook. Fuel Processing Technology, 2001. 71(1): p. 139-148.
16. Sadooghi, P. and R. Rauch, Experimental and modeling study of hydrogen production from catalytic steam reforming of methane mixture with hydrogen sulfide. International Journal of Hydrogen Energy, 2015. 40(33): p. 10418-10426.
17. Song, C., Liu, Q., Ji, N., Kansha, Y. and Tsutsumi, A., Optimization of steam methane reforming coupled with pressure swing adsorption hydrogen production process by heat integration. Applied Energy, 2015. 154: p. 392-401.

18. Higman, C. and Tam, S., Advances in coal gasification, hydrogenation, and gas treating for the production of chemicals and fuels. Chemical Reviews, 2013. 114(3): p. 1673-1708.

19. Zwart, R.W. and Boerrigter, H., High efficiency co-production of synthetic natural gas (SNG) and Fischer-Tropsch (FT) transportation fuels from biomass. Energy & Fuels, 2005. 19(2): p. 591-597.

20. Higman, C. andVan der Burgt, M., Gasification. 2011: Gulf professional publishing.

21. Stańczyk, K., kapusta, K., Wiatowski, M., Swiadrowski, J., Smolinski, A., Rogut, J. and Kotyrba, A., Experimental simulation of hard coal underground gasification for hydrogen production. Fuel, 2012. 91(1): p. 40-50.

22. Levin, D.B. and R. Chahine, Challenges for renewable hydrogen production from biomass. International Journal of Hydrogen Energy, 2010. 35(10): p. 4962-4969.

23. Dincer, I. and Zamfirescu C., Sustainable hydrogen production options and the role of IAHE. International Journal of Hydrogen Energy, 2012. 37(21): p. 16266-16286.

24. Serban, M., Lewis M., and Basco J., Kinetic study of the hydrogen and oxygen production reactions in the copper-chloride thermochemical cycle. in AIChE 2004 spring national meeting, New Orleans, LA. 2004.

25. Naterer, G., Suppiah, S., Lewis, M., Gabriel, K., Dincer, I., Rosen, M., Fowler, M., Risvi, G., Easton, EB. and Ikeda, BM., Recent Canadian advances in nuclear-based hydrogen production and the thermochemical Cu–Cl cycle. International Journal of Hydrogen Energy, 2009. 34(7): p. 2901-2917.

26. Naterer, G., Suppiah, S., Stolberg, L., Lewis, M., Ahmed, S., Wang, Z., Rosen, M., Dincer, I., Gabriel, K. and Secnik, E., Progress of international program on hydrogen production with the copper–chlorine cycle. International Journal of Hydrogen Energy, 2014. 39(6): p. 2431-2445.

27. Naterer, G.F., Dincer, I. and Zamfirescu, C., Hydrogen production from nuclear energy. 2013: Springer.

28. Acar, C. and Dincer, I., Comparative assessment of hydrogen production methods from renewable and non-renewable sources. International Journal of Hydrogen Energy, 2014. 39(1): p. 1-12.

29. Garland, N., Milliken, J., Satyapal, S., Munetz, L. and McMurphy, K., Recent advances in hydrogen and fuel cell technology. ECS Transactions, 2009. 17(1): p. 223-232.

30. Suleman, F., Comparative study of various hydrogen production methods for vehicles. 2014, MASc. Thesis, University of Ontario Institute of Technology.

31. Arcotumapathy,V.,Vo, D., Chesterfield, D., Tin, C., Siahvashi, A., Lucien, FP. and Adesina, AA., Catalyst design for methane steam reforming. Applied Catalysis A: General, 2014. 479: p. 87-102.

32. Gholinezhad, J., Chapoy, A., and Tohidi, B., Separation and capture of carbon dioxide from CO_2/H_2 syngas mixture using semi-clathrate hydrates. Chemical Engineering Research and Design, 2011. 89(9): p. 1747-1751.

33. Abuadala, A., Dincer, I., and Naterer, G., Exergy analysis of hydrogen production from biomass gasification. International Journal of Hydrogen Energy, 2010. 35(10): p. 4981-4990.

34. Rao, MS., Singh, SP., Sodha, MS., Dubey, AK. and Shyam, M., Stoichiometric, mass, energy and exergy balance analysis of countercurrent fixed-bed gasification of post-consumer residues. Biomass and Bioenergy, 2004. 27(2): p. 155-171.

35. Herdem, MS., Farhad, S., Dincer, I. and Hamdullahpur, F., Thermodynamic modeling and assessment of a combined coal gasification and alkaline water electrolysis system for hydrogen production. International Journal of Hydrogen Energy, 2014. 39(7): p. 3061-3071.

36. Olateju, B. and Kumar, A., Techno-economic assessment of hydrogen production from underground coal gasification (UCG) in Western Canada with carbon capture and sequestration (CCS) for upgrading bitumen from oil sands. Applied Energy, 2013. 111: p. 428-440.

37. Friedmann, SJ., Upadhye, R., and Kong, FM., Prospects for underground coal gasification in carbon-constrained world. Energy Procedia, 2009. 1(1): p. 4551-4557.

38. Prabu,V. and Jayanti, S., Underground coal-air gasification based solid oxide fuel cell system. Applied Energy, 2012. 94: p. 406-414.

39. Kothari, R., Buddhi, D., and Sawhney, R., Comparison of environmental and economic aspects of various hydrogen production methods. Renewable and Sustainable Energy Reviews, 2008. 12(2): p. 553-563.

40. Möller, S., Kaucic, D., and Sattler, C., Hydrogen production by solar reforming of natural gas: a comparison study of two possible process configurations. Journal of Solar Energy Engineering, 2006. 128(1): p. 16-23.

41. Baykara, S., and Bilgen, E., An overall assessment of hydrogen production by solar water thermolysis. International Journal of Hydrogen Energy, 1989. 14(12): p. 881-891.

42. Rehman, F., Abdul Majeed WS., and Zimmerman, WB., Hydrogen production from water vapor plasmolysis using DBD-Corona hybrid reactor. Energy & Fuels, 2013. 27(5): p. 2748-2761.

43. Bockris, J., Bonciocat, N., and Gutmann, F., An introduction to electrochemical science.Vol. 29. 1974: Wykeham Publications.

44. Wang, ZL., Naterer, GF., Gabriel, KS., Gravelsins, R., and Daggupati,VN., Comparison of sulfur–iodine and copper–chlorine thermochemical hydrogen production cycles. International Journal of Hydrogen Energy, 2010. 35(10): p. 4820-4830.

45. Naterer, G., Suppiah, S., Stolberg, L., Lewis, M., Wang, ZL., Daggupati,V., Gabriel, K., Dincer, I., Rosen, M., and Spekkens, P., Canada's program on nuclear hydrogen

production and the thermochemical Cu–Cl cycle. International Journal of Hydrogen Energy, 2010. 35(20): p. 10905-10926.

46. Naterer, G., Suppiah, S., Stolberg, L., Lewis, M., Ferrandon, M., Wang, ZL., Dincer, I., Gabriel, K., Rosen, M., and Secnik, E., Clean hydrogen production with the Cu–Cl cycle–progress of international consortium, I: experimental unit operations. International Journal of Hydrogen Energy, 2011. 36(24): p. 15472-15485.

47. Naterer, G., Suppiah, S., Stolberg, L., Lewis, M., Ferrandon, M., Wang, ZL., Dincer, I., Gabriel, K., Rosen, M., and Secnik, E., Clean hydrogen production with the Cu–Cl cycle–progress of international consortium, II: Simulations, thermochemical data and materials. International Journal of Hydrogen Energy, 2011. 36(24): p. 15486-15501.

48. Naterer, G., Suppiah, S., Stolberg, L., Lewis, M., Wang, ZL., Dincer, I., Rosen, M., Gabriel, K., Secnik., E., and Easton, EB., Progress of international hydrogen production network for the thermochemical Cu–Cl cycle. International Journal of Hydrogen Energy, 2013. 38(2): p. 740-759.

49. Naterer, G., Suppiah, S., Stolberg, L., Lewis, M., Wang, ZL., Rosen, M., Dincer, I., Gabriel, K., Odukoya, A., and Secnik, E., Progress in thermochemical hydrogen production with the copper–chlorine cycle. International Journal of Hydrogen Energy, 2015. 40(19): p. 6283-6295.

50. Stolberg, L., Electrolysis cell for the conversion of cuprous chloride in hydrochloric acid to cupric chloride and hydrogen gas. 2014, Google Patents.

51. Kettner, A., Stolberg, L., Li, H., Shkarupin, A., and Suppiah, S., Electrolysis cell with multiple membranes for CuCI/HCI electrolysis in hydrogen production. 2013, Google Patents.

52. Suppiah, S., Naterer, GF., Lewis, M., Lvov, S., Easton, B., and Dincer, I., Thermo-mechanical design of nuclear-based hydrogen production. in ORF Workshops on Nuclear-Based Thermochemical Hydrogen Production. 2010.

53. Gong, Y., Chalkova, E., Akinfiev, NN., Balashov,V., Fedkin, M., and Lvov, S., CuCl-HCl electrolyser for hydrogen productionVia Cu-Cl thermochemical cycle. ECS Transactions, 2009. 19(10): p. 21-32.

54. Stolberg, L., Boniface, HA., McMohan, S., Suppiah, S., York, S., Electrolysis of the CuCl/HCl aqueous system for the production of nuclear hydrogen. In fourth international topical meeting on high temperature reactor technology. 2008. American Society of Mechanical Engineers.

55. Balashov,V., Schatz, RS., Chalkova, E., Akinfiev, NN., Fedkin, MV., and Lvov, S., CuCl electrolysis for hydrogen production in the Cu–Cl thermochemical cycle. Journal of The Electrochemical Society, 2011. 158(3): p. B266-B275.

56. Khurana, S., Hall, D., Schatz, R., and Lvov, S., Diagnosis and modeling of the CuCl electrolyser using electrochemical impedance spectroscopy. ECS Transactions, 2013. 53(9): p. 41-50.

57. Schatz, R., Kim, S., Khurana, S., fedkin, M., and Lvov, S., High efficiency cucl electrolyser for Cu-Cl thermochemical cycle. ECS Transactions, 2013. 50(49): p. 153-164.

58. Hall, DM., Schatz, RS., LaRow, EG., and Lvov, S., CuCl/HCl electrolyser kinetics for hydrogen productionVia Cu-Cl thermochemical cycle. ECS Transactions, 2013. 58(2): p. 15-25.

59. Hall, DM., Akinfiev NN., LaRow, EG., Schatz, RS., and Lvov, S., Thermodynamics and Efficiency of a CuCl(aq)/HCl(aq) Electrolyser. Electrochimica Acta, 2014. 143: p. 70-82.

60. Hall, DM., LaRow, EG., Schatz, RS., Beck, JR., and Lvov, S., Electrochemical kinetics of CuCl(aq)/HCl(aq) electrolyser for hydrogen production via a Cu-Cl thermochemical cycle. Journal of The Electrochemical Society, 2015. 162(1): p. F108-F114.

61. Hall, D.M., Beck, JR, and Lvov, S., Electrochemical kinetics of the hydrogen reaction on platinum in concentrated HCl(aq). Electrochemistry Communications, 2015.

62. Hall, DM., Lotfi, R., Kim, S., and Lvov, S., Membrane transport in a CuCl(aq)/HCl(aq) electrolytic cell. ECS Transactions, 2015. 66(24): p. 103-119.

63. Khurana, S., Hall, DM., Schatz, RS., Fedkin, MV., and Lvov, S., State-of-health of a CuCl electrolyser during a 168-h test. International Journal of Hydrogen Energy, 2015. 40(1): p. 62-69.

64. Ranganathan, S. and Easton, EB., High performance ceramic carbon electrode-based anodes for use in the Cu–Cl thermochemical cycle for hydrogen production. International Journal of Hydrogen Energy, 2010. 35(3): p. 1001-1007.

65. Pauric, AD., Pedersen, AW., Andrusiak, T., and Easton, EB., A surface modification route to nonprecious metal fuel cell catalysts. Journal of the Electrochemical Society, 2010. 157(3): p. B370-B375.

66. Ranganathan, S., Edge, PS., and Easton, EB., Evaluation of anode electrode materials for Cu-Cl/HCl electrolysers for hydrogen production. ECS Transactions, 2012. 41(31): p. 111-120.

67. Aghahosseini, S., System integration and optimization of copper-chlorine thermochemical cycle with various options for hydrogen production. 2013, University of Ontario Institute of Technology.

68. T-Raissi, A., Analysis of solar thermochemical water splitting cycles for hydrogen production. Hydrogen, Fuel Cells, and Infrastructure Technologies, FY, 2003.

69. Zhou, J., Zhang, Y., Wang., Z., Yang, W., Zhou, Z., Liu, J., and Cen, K., Thermal evaluation of open-loop SI thermochemical cycle for the production of hydrogen, sulfuric acid and electric power. International Journal of Hydrogen Energy, 2007. 32(5): p. 567-575.

70. Kubo, S., Kasahara, S., Okuda, H., Terada, A., Tanaka, N., Inaba, Y., Ohashi, H., Inagak, Y., Onuki, K., and Hino, R., A pilot test plan of the thermochemical water

splitting iodine–sulfur process. Nuclear Engineering and Design, 2004. 233(1): p. 355-362.

71. Schultz, K., Thermochemical production of hydrogen from solar and nuclear energy. Presentation to the Stanford Global Climate and Energy Project, 2003. 14.

72. Anzieu, P., Carles, Ph., Duigou, A.,Vitart, X., and Lemort, F., The sulphur–iodine and other thermochemical process studies at CEA. International Journal of Nuclear Hydrogen Production and Applications, 2006. 1(2): p. 144-153.

73. Moore, RC., Gelbard, F., Parma, EJ.,Vernon, ME., Lenard, RX., and Pickard, PS., A Laboratory-Scale sulfuric acid decomposition apparatus for use in hydrogen production Cycles. 2007, Sandia National Laboratories (SNL-NM), Albuquerque, NM (United States).

74. Lewis, MA., Masin, JG., and O'Hare, PA., Evaluation of alternative thermochemical cycles, Part I: the methodology. International Journal of Hydrogen Energy, 2009. 34(9): p. 4115-4124.

75. Sadhankar, RR., Li, J., Li, H., Ryland, DK., and Suppiah, S., Future hydrogen production using nuclear reactors. in EIC Climate Change Technology, 2006 IEEE. 2006. IEEE.

76. Pettersson, J., Ramsey, B., and Harrison, D., A review of the latest developments in electrodes for unitised regenerative polymer electrolyte fuel cells. Journal of Power Sources, 2006. 157(1): p. 28-34.

77. Zeng, K., Zhang, D., Recent progress in alkaline water electrolysis for hydrogen production and applications. Progress in Energy and Combustion Science, vol. 36, pp. 307-326, 2010.

78. Hamann, CH., Hamnett, A., andVielstich, W., Electrochemistry. 1998. 1998, Wiley-VCH.

79. Bagotsky,VS., Fundamentals of electrochemistry.Vol. 44. 2005: John Wiley & Sons.

80. Lvov, S., Introduction to Electrochemical Science and Engineering. 1 ed. 2014, Boca Raton: CRC Press.

81. Sverjensky, D., Shock, E., and Helgeson, H., Prediction of the thermodynamic properties of aqueous metal complexes to 1000℃ and 5 kb. Geochimica et Cosmochimica Acta, 1997. 61(7): p. 1359-1412.

82. Brugger, J., Etschmann, B., Liu, W., Testemale, D., Hazemann, JL., Emerich, H.,Van Beek, W., and Proux, O., An XAS study of the structure and thermodynamics of Cu (I) chloride complexes in brines up to high temperature (400℃, 600bar). Geochimica et Cosmochimica Acta, 2007. 71(20): p. 4920-4941.

83. Haghtalab, A., Papangelakis,VG., and Zhu, X., The electrolyte NRTL model and speciation approach as applied to multicomponent aqueous solutions of H_2SO_4, $Fe_2(SO_4)3$, $MgSO_4$ and $Al_2(SO_4)_3$ at 230–270℃. Fluid Phase Equilibria, 2004. 220(2): p. 199-209.

84. Koukkari, P., and Pajarre, R., Calculation of constrained equilibria by Gibbs energy minimization. Calphad, 2006. 30(1): p. 18-26.

85. Shvarov, YV., HCh: New potentialities for the thermodynamic simulation of geochemical systems offered by Windows. Geochemistry International, 2008. 46(8): p. 834-839.

86. Eriksson, G., and Hack, K., ChemSage—a computer program for the calculation of complex chemical equilibria. Metallurgical Transactions B, 1990. 21(6): p. 1013-1023.

87. Bale, C., Chartrand, P., Degterov, SA., Eriksson, G., Hack, K., Mahfoud, RB., Melancon, J., Pelton, AD., and Petersen, S., FactSage thermochemical software and databases. Calphad, 2002. 26(2): p. 189-228.

88. Kulik, D., Berner, U., and Curti, E., Modelling chemical equilibrium partitioning with the GEMS-PSI code. PSI Scientific Report, 2003. 4: p. 109-122.

89. Shvarov, YV., Algorithmization of the numeric equilibrium modeling of dynamic geochemical processes. Geochemistry International, 1999. 37(6): p. 571-576.

90. Helgeson, HC., Kirkham, DH., and Flowers, GC., Theoretical prediction of the thermodynamic behavior of aqueous electrolytes by high pressures and temperatures; IV, Calculation of activity coefficients, osmotic coefficients, and apparent molal and standard and relative partial molal properties to 600℃ and 5kb. American Journal of Science, 1981. 281(10): p. 1249-1516.

91. Soltani, R., Dincer, I., Rosen, M., Hall, DM, and Lvov, S., Electrochemical analysis of a HCl(aq)/CuCl(aq) electrolyser. International Journal of Hydrogen Energy,2015 (under review)

92. Lvov, S., Personal technical communication. 2015.

93. Tanger, JC., and Helgeson, HC., Calculation of the thermodynamic and transport properties of aqueous species at high pressures and temperatures; revised equaitons of state for the standard partial molal properties of ions and electrolytes. American Journal of Science, 1988. 288(1): p. 19-98.

94. Helgeson, HC., and Kirkham, DH., Theoretical prediction of the thermodynamic behavior of aqueous electrolytes at high pressures and temperatures; I, Summary of the thermodynamic/electrostatic properties of the solvent. American Journal of Science, 1974. 274(10): p. 1089-1198.

95. Johnson, JW., Oelkers, EH., and Helgeson, HC., SUPCRT92: A software package for calculating the standard molal thermodynamic properties of minerals, gases, aqueous species, and reactions from 1 to 5000 bar and 0 to 1000℃. Computers & Geosciences, 1992. 18(7): p. 899-947.

96. Shock, EL., Sassani, DC., Willis, M., and Sverjensky, DA., Inorganic species in geologic fluids: correlations among standard molal thermodynamic properties of aqueous ions and hydroxide complexes. Geochimica et Cosmochimica Acta, 1997. 61(5): p. 907-950.

97. Pokrovskii,VA., Calculation of the standard partial molal thermodynamic properties and dissociation constants of aqueous HCl^o and HBr^o at temperatures to 1000° C and pressures to 5 kbar. Geochimica et Cosmochimica Acta, 1999. 63(7): p. 1107-1115.

98. Shock, EL., and Helgeson, HC., Calculation of the thermodynamic and transport properties of aqueous species at high pressures and temperatures: Correlation algorithms for ionic species and equation of state predictions to 5 kb and 1000 C. Geochimica et Cosmochimica Acta, 1988. 52(8): p. 2009-2036.

99. Treimer, S., Tang, A., and Johnson, DC., A Consideration of the application of Koutecký-Levich plots in the diagnoses of charge-transfer mechanisms at rotated disk electrodes. Electroanalysis, 2002. 14(3): p. 165-171.

100. Esmaili, P., Thermodynamic analysis of an integrated photovoltaic system for hydrogen and methanol production. 2012, University of Ontario Institute of Technology.

101. Ni, M., Leung, MK., and Leung, DY., Energy and exergy analysis of hydrogen production by solid oxide steam electrolyser plant. International Journal of Hydrogen Energy, 2007. 32(18): p. 4648-4660.

102. Springer, TE., Zawodzinski, T., and Gottesfeld, S., Polymer electrolyte fuel cell model. Journal of the Electrochemical Society, 1991. 138(8): p. 2334-2342.

103. Gurau,V., Barbir, F., and Liu, H., An analytical solution of a half-cell Model for PEM fuel cells. Journal of The Electrochemical Society, 2000. 147(7): p. 2468-2477.

104. Szargut, J., Morris, DR., and Steward, FR., Exergy analysis of thermal, chemical, and metallurgical processes. 1987.

105. Hall, DM., Technical communication via email. 2015.

106. Orhan, MF., Energy, exergy and cost analyses of nuclear-based hydrogen productionVia thermochemical water decomposition using a Copper-Chlorine (Cu-Cl) cycle. 2008, University of Ontario Institute of Technology.